

AN ABSTRACT OF THE THESIS OF

Mohammed Jahangir Alam Chowdhury for the degree of Doctor of Philosophy in Forest Products presented on September 13, 1999.

Title: Sealed Consolidation of Natural Fiber Composites with Chemical Reactant Injection and Removal

Redacted for privacy

Abstract approved:

Philip E. Humphrey



High performance composite materials may be formed from natural fiber networks by controlling internal environments within them during their consolidation. By doing so, it may be possible to affect control over the spatial distribution of internal structure and consequent bulk properties. Consolidation of pre-formed fiber networks in a sealed pressing system and manipulation of thermodynamic and chemical environments inside such pre-forms is therefore an objective of this research.

The research involves the development and use of an automated system for sealed pressing of pre-formed natural fiber networks. The system is used to evaluate the effects of highly controlled chemical, thermal, and mechanical conditions on the networks. The sealed pressing system effectively behaves as a chemical treatment chamber since it has provision for sequential injection and removal of chemicals in the vapor phase. A wide range of chemical treatment methods for fiber modification is reviewed. Chemicals have been selected to sequentially stimulate fiber softening and adhesion in the pressing system.

## AN ABSTRACT OF THE THESIS (Continued)

The softening action of gaseous ammonia has been explored in terms of treatment time, temperature and vapor pressure. It was found that moderate vapor pressures of ammonia rapidly soften fiber networks at room temperature.

For adhesion, the feasibility of using resole phenol-formaldehyde (PF) adhesives with methyl formate vapor as catalyst was explored. Trial samples were formed by treating the fiber-PF mix first with gaseous ammonia (to affect softening) and then curing the resin by injecting methyl formate vapor at 40<sup>0</sup>C. For comparison, samples were also formed in the conventional hot press. The physical and mechanical properties of the samples are reported and the results were found very encouraging; stable and strong material was rapidly formed.

Adhesion kinetics in the presence of the chemicals was also explored. Miniature adhesive bonds were formed and tested by sequentially injecting gaseous ammonia followed by liquid methyl formate into test bonds. Such tests were conducted with a specially modified Automated Bonding Evaluation System. The results showed that ammonia did not significantly stimulate curing, but that subsequent addition of methyl formate stimulated rapid cure. These results aided in the development of the sealed pressing sequence for fiber pre-forms.

Sealed Consolidation of Natural Fiber Composites with  
Chemical Reactant Injection and Removal

By

Mohammed Jahangir Alam Chowdhury

A THESIS

submitted to

Oregon State University

in partial fulfillment of  
the requirements for the  
degree of

Doctor of Philosophy

Presented September 13, 1999  
Commencement June 2000

Doctor of Philosophy thesis of Mohammed Jahangir Alam Chowdhury presented on September 13, 1999

APPROVED:

Redacted for privacy

Major Professor, ~~representing Forest Products~~

---

Redacted for privacy

Head of Department of Forest Products

---

Redacted for privacy

Dean of Graduate School

---

I understand that my thesis will become part of the permanent collection of Oregon State University libraries. My signature below authorizes release of my thesis to any reader upon request.

Redacted for privacy

---

Mohammed Jahangir Alam Chowdhury, Author

## ACKNOWLEDGMENT

First of all I have to thank the Almighty Allah who gave me the talent and opportunity to do this research project.

I would like to express my sincere gratitude and appreciation to Dr. Philip E. Humphrey, my advisor. Without his guidance, encouragement, enthusiasm and support this project wouldn't be accomplished.

I would also like to thank Dr. Joseph J. Karchesy for sharing his expertise in this project. My appreciation is also extended to Dr. Charles C. Brunner, Dr. William H. Warnes and Dr. Douglas Brodie for their encouragement and help as my committee members.

My special thanks are extended to Milo Clauson who always spent his time to discuss electronics and other matters with me.

I wish to thank the Forest Resources Management Project (Institute of Forestry and Environmental Sciences, Chittagong University Component), Bangladesh, and the Department of Forest Products, Oregon State University, USA for their financial support of this research.

I also want to thank my teachers, friends, colleagues and well-wishers both in Bangladesh and USA who have done so many kind things for me.

Finally, I would like to thank my wife Rahima and my two kids Tanzina and Mohsen for their support, encouragement, and inspiration.

## TABLE OF CONTENTS

	Page
CHAPTER 1. INTRODUCTION	1
1.1. Introduction to the field of wood-based composites	1
1.2. Needs for future development in the field of wood-based composites	2
1.3. Basic objectives of this research	4
CHAPTER 2. LITERATURE REVIEW	6
2.1. Brief discussion about existing wood-based composites	6
2.2. Brief review of adhesives presently used in wood-based composites	9
2.2.1. Phenolic resins	10
2.2.2. Amino resins	14
2.2.3. Isocyanate adhesives	17
2.3. Overview of the internal behavior of fiber mats during hot pressing	17
2.4. Chemistry, reactivity and accessibility of wood cell wall components	19
2.4.1. Wood cellulose	20
2.4.2. Wood hemicelluloses	21
2.4.3. Wood lignins	22
2.5. Brief review of chemical modification options for wood	23
2.5.1. Esterification	25
2.5.1.1. Acetylation	25
2.5.1.2. Reaction with dicarboxylic acid anhydrides	29
2.5.1.3. Oligoesterification	32
2.5.1.4. Reaction with isocyanates	34

## TABLE OF CONTENTS (Continued)

2.5.2. Etherification	35
2.5.2.1. Epoxidation	36
2.5.2.2. Benzylation	37
2.5.2.3. Allylation	40
2.5.2.4. Cyanoethylation	41
2.5.2.5. Modification with maleic acid-glycerol mixture	42
2.5.2.6. Methylation	43
2.5.3. Acetyls formation	44
2.5.3.1. Formalization	44
2.5.3.2. Non-formaldehyde cross-linking	45
2.5.4. Treatment of wood with ammonia	46
2.5.4.1. Introduction	46
2.5.4.2. Effect of ammonia on wood	47
2.5.4.2.1. Chemical changes	47
2.5.4.2.2. Morphological changes	50
2.5.4.2.3. Physical and mechanical property changes	51
2.5.4.3. Application of ammonia in wood-based composites manufacture	52
2.5.5. Selection of candidate chemical treatment methods for the sealed pressing system	52
2.6. Curing behavior of alkaline catalyzed phenol-formaldehyde (PF) adhesives	55
2.6.1. Curing behavior of PF resin under very alkaline conditions	57
2.6.2. Acceleration of the curing of alkaline catalyzed PF (resole) adhesive	58
2.7. Sealed pressing system	61
CHAPTER 3. EXPERIMENTAL OBJECTIVES OF THIS RESEARCH	63
CHAPTER 4. MATERIALS AND METHODS	67
4.1. Introduction	67
4.2. Materials	67
4.2.1. Mats from dried fibers	68
4.2.1.1. Mat formation for ammonia softening studies	69
4.2.1.2. Mat formation for sample formation trials	69

## TABLE OF CONTENTS (Continued)

4.2.2. Fiber mat material for preliminary ammonia softening studies	71
4.2.3. Wood strips for adhesion studies	72
4.2.4. Adhesive	73
4.3. Experimental methods	73
4.3.1. Evaluation of strength development of miniature test bonds	73
4.3.1.1. The automated bonding evaluation system (ABES)	73
4.3.1.2. Refinement of ABES	78
4.3.1.3. Bond pressing and testing sequence	80
4.3.2. A sealed pressing device	82
4.3.2.1. Performance needs and design strategy	83
4.3.2.2. Mechanical design	84
4.3.2.2.1. Porous plate	87
4.3.2.2.2. Back plate	88
4.3.2.2.3. Gas supply block	89
4.3.2.2.4. Heating block	90
4.3.2.2.5. Thermal barrier	90
4.3.2.2.6. Connecting column	91
4.3.2.2.7. Collar	91
4.3.2.2.8. Safety stop	92
4.3.2.3. External gas supply and removal system	92
4.3.2.4. Platen position control and load measurement	95
4.3.2.5. Temperature control and measurement	97
4.3.2.6. Gas pressure measurement	98
4.3.2.7. Computer control and data acquisition system	99
4.3.3. Chemical treatment and pressing sequence	100
4.3.3.1. Softening action of gaseous ammonia	101
4.3.3.1.1. Treatment time effects	102
4.3.3.1.2. Treatment temperature effects	104
4.3.3.1.3. Ammonia vapor pressure effects	107
4.3.3.2. Composite sample formation trials	110
4.3.4. Characterization of trial fiber disks	114
4.3.4.1. Static bending tests	114
4.3.4.2. Tensile strength	117
4.3.4.3. Thickness swelling test	118
CHAPTER 5. RESULTS AND DISCUSSION	119
5.1. The sealed pressing system	119



## TABLE OF CONTENTS (Continued)

5.1.1. Pressure cross-check, and dead volume and flow resistance measurements	119
5.1.2. Position cross-check	123
5.1.3. Calibration of proportionally opening electronic servo-valve control system	124
5.2. Softening action of gaseous ammonia	126
5.2.1. Ammonia treatment time and temperature effects	126
5.2.2. Ammonia treatment vapor pressure effects	130
5.3. Bond strength development studies	136
5.4. Characterization of trial fiber disks	141
5.4.1. Thickness swelling	141
5.4.2. Tensile strength	143
5.4.3. Bending strength	145
CHAPTER 6. CONCLUSIONS AND POSSIBLE FUTURE RESEARCH	148
6.1. Conclusions of the current research	148
6.2. Possible future research	149
BIBLIOGRAPHY	151
APPENDICES	164
APPENDIX A Engineering drawing of each part of the upper/lower portion of the sealed pressing device	165
APPENDIX B Strawberry Tree <sup>®</sup> Program	173
APPENDIX C Fluid pressures at the center of trial samples during pressing	177

## LIST OF FIGURES

Figure		Page
2.1	Addition, condensations, and cross-linking reactions of phenol-formaldehyde (resole) (from Marra, 1992)	10
2.2	Addition, condensation, and linear growth of novolak molecule (from Marra, 1992)	12
2.3	Addition and condensation reactions of resorcinol-formaldehyde (from Marra, 1992)	13
2.4	Addition, condensation, and cross-linking reactions of urea-formaldehyde (from Marra, 1992)	15
2.5	Reaction of melamine and formaldehyde (from Marra, 1992)	16
2.6	Ionization of the phenol to form phenate ions	56
2.7	Gel time versus pH curve of PF resin. The dashed line indicates extrapolated assumed of behavior (from Pizzi and Stephanou 1994a)	56
2.8	Experimentally derived gel time versus pH curve of a PF resin over a very wide pH range (from Pizzi and Stephanou, 1994a)	57
2.9	Dependence of gel time of a PF resin at pH 11.26 on percentage and type of ester added (from Pizzi and Stephanou, 1994b)	59
2.10	Reaction between ester and phenolic nucleus shows ester acts as a reagent	60
2.11	Sealed steam press (from Shen, 1973)	61
4.1	Adhesive spraying system	71
4.2	Schematic showing principle functions of ABES (from Chowdhury and Humphrey, 1999)	74

## LIST OF FIGURES (Continued)

4.3	An overview of the main bond forming and testing module of ABES	75
4.4	A close-up of the bond-pressing zone with bond cooling-head in the elevated position	77
4.5	Basic principle of bond formation with chemicals injection	77
4.6	Vertical cross-section of the modified pressing heads of ABES	78
4.7	A close-up of the bond-pressing zone with sample being injected with chemicals	79
4.8	Bonds formed and tested for different types of treatment	81
4.9	Basic principle of the sealed press	83
4.10	Schematic showing the upper and lower portions of the sealed pressing system	86
4.11	An overview of the upper portion (A) and the lower portion (B) of the pressing system	87
4.12	Schematic representation of the external gas supply and removal system	94
4.13	An overview of the complete test system	96
4.14	Gas pressure measurement arrangement	98
4.15	A schematic of the computer control and data acquisition system	100
4.16	Sequence for the NH <sub>3</sub> treatment time experiments	103
4.17	100% saturated and 11% saturated vapor pressure of ammonia with temperature (derived from Braker and Mossman, 1971)	106
4.18	Sequence for the NH <sub>3</sub> treatment temperature experiments	107
4.19	Sequence for the NH <sub>3</sub> treatment vapor pressure experiments	109

## LIST OF FIGURES (Continued)

4.20	Sequence for the NH <sub>3</sub> and MeF treatment during sample formation trials	112
4.21	Sequence for the NH <sub>3</sub> treatment during sample formation trials	113
4.22	Sequence for the MeF treatment during sample formation trials	113
4.23	Tests performed on each set of samples (number indicate replications)	114
4.24	Cutting patterns for the specimens	115
4.25	Bending tests arrangement	116
5.1	Pressure cross-check of the sealed pressing system	120
5.2	Flow resistance versus flow rate in the pressing system	123
5.3	Position cross-check of the sealed pressing system	124
5.4	Calibration of the proportionally opening electronic servo-valve control system	125
5.5	A typical plot of mat thickness variation with pressing time (in this case following 300 seconds ammonia treatment)	127
5.6	Effect of ammonia treatment time on density development (30 seconds after the platens reached a target pressing pressure of 8.4 MPa)	128
5.7	Effect of ammonia treatment temperature on density development (after 30 seconds of pressing with constant pressure of 8.4 MPa)	129
5.8	Stress relaxation with ammonia injection after press closure (with ammonia vapor pressure of 0.42 MPa)	131
5.9	A typical close-up of the compressive pressure drop curve upon NH <sub>3</sub> injection (with NH <sub>3</sub> vapor pressure of 0.42 MPa)	132

## LIST OF FIGURES (Continued)

5.10	Quotient of counterpressure over ammonia pressure versus elapsed time	133
5.11	Effect of ammonia partial pressure on its softening action on fiber networks	135
5.12	A typical set of bond strength development data at room temperature (in this case for PF adhesive-to-maple bonds)	137
5.13	Accumulated shear strength values for bonds formed at room temperature, at various bonds forming times and at various chemical treatments	138
5.14	Bond strength in delayed (after 400 seconds) injection of methyl formate	140
5.15	Thickness swelling of the different types of samples as a result of water soaking	142
5.16	Thickness swelling of different types of samples after 24 hours water soaking	143
5.17	Tensile strength of the different types of samples	144
5.18	Modulus of rupture (MOR) of the different types of samples	146
5.19	Modulus of elasticity (MOE) of the different types of samples	147

## LIST OF APPENDIX FIGURES

Figure		Page
A1	Porous plate	165
A2	Back plate	166
A3	Gas supply block	167
A4	Heating block	168
A5	Thermal barrier	169
A6	Connecting column	170
A7	Collar	171
A8	Safety stop	172
C1	Fluid pressures at the center of trial sample during pressing	177

## DEDICATION

This thesis is dedicated to my late father, Md. Ibrahim Chowdhury, and my mother, Rezia Begum.

# Sealed Consolidation of Natural Fiber Composites with Chemical Reactant Injection and Removal

## CHAPTER 1. INTRODUCTION

### **1.1. Introduction to the field of wood-based composites**

“Wood-based composite” is a term which is used to describe any wood material made of small pieces glued together. The wood component may range in size from lumber, to veneer, to wafers to flakes and particles, and fiber bundles and individual fibers. The adhesive may be selected from a wide range of possible types. Thermosetting adhesives are predominantly used to achieve the rapid cure necessary to make industrial manufacture economically viable on a large scale. Wood-based composites found in today’s market include panel products (plywood, blackboard, fiberboard, medium density fiberboard, particleboard, waferboard, oriented strandboard, COM-PLY<sup>R</sup> panels etc.), molded products (automobile panels, door skins etc.), lumber and timber products (laminated veneer lumber, parallel strand lumber- Parallam<sup>TM</sup>, oriented strand lumber- Scrimber<sup>TM</sup> or TimberStrand<sup>TM</sup>, railroad ties etc.), and other products produced by combinations of wood and other materials (e.g., plastic fiber, inorganic materials, or agricultural residues).



## **1.2. Needs for future development in the field of wood-based composites**

Conventional hot pressing methods for wood-based composites yield products with internal structures and consequent properties which are largely dictated by the nature of the pressing process. During the consolidation of conventional wood-based composites, unsteady-state heat and moisture transfer and phase change affects spatial variation in densification in the consolidation direction (Humphrey, 1994); this is due to the hygro-thermo-viscoelastic properties of the wood cell wall. Cross-sectional density profiles effect the flexural properties of the composites. Furthermore, inter-fiber bonding characteristics and residual stress within the micro-structures also differ throughout the composite as consolidation progresses. Manufacturers of conventional wood-based composites (mainly panels) have little control over these mechanisms however, and the products are generally quite primitive when compared to the fine structure of the fibers from which they are made.

In addition to being rather weak compared to their constituent fibers, conventional wood-based composite panels are subject to high irreversible swelling due to the spring-back of compressed (densified) wood i.e. relaxation of residual stress and the breakage of adhesive bonds between wood particles. The reversible swelling is a secondary consequence of the hygroscopic nature of the wood cell wall.

A long-term goal of the research of which the present thesis is a part is to control the distribution of internal structure within composites and, thereby, affect

control of spatial property distribution. It is believed that high performance composite materials and objects can be produced by using natural fibers, high performance adhesives, fiber chemical treatment and modification, and orientation of fibers in the pre-formed fiber network. The properties that we desire to control include spatial density distribution, dimensional stability, bulk strength and durability in adverse environments. Emphasis in the present work is placed on all but the latter.

Using flexible fiber mats and appropriate pressing devices, one can also produce products with complex shapes. By controlling internal structure together with external shape, it may be possible to produce a new generation of high performance engineering composite components. These may resemble in structure and function objects such as mammalian bones found in nature (Humphrey, 1994). The work represented in this thesis will, it is hoped, lay some of the groundwork for such innovations.

One important aspect of our objective of forming high performance molded natural fiber objects is to control internal environments within fiber mats during their consolidation. Consolidation of pre-formed fiber networks in a sealed pressing system may enable us to manipulate the thermodynamic and chemical environments inside them in hitherto unattainable ways. This may offer opportunities to create superior products with structures which are highly tailored to end-use requirements. The development of a sealed pressing approach with chemical reactant injection and removal is therefore the primary concern of this

research. Pre-formed thermomechanical pulp (TMP) mats pre-treated with adhesive are so compressed. In this way, localized plasticisation, adhesion, and dimensional stabilization of the fiber networks may be affected *in situ*. This approach offers the potential of creating mechanical components which may perform in service better than existing products made from natural fibers and metal objects of complex shape but homogeneous internal structure. The approach may also enable toxic chemicals to be used since it will be a sealed system. The consequent objectives of the research are summarized below.

### **1.3. Basic objectives of this research**

The overall and long term objective of the program into which the present thesis falls is to develop ways of creating new molded composites of controlled shape, which have spatially controlled mass distribution, adhesion characteristics, and fiber wall modification to suite specific and demanding service requirements.

The specific objectives of this research are to:

- I. Design and construct a laboratory trial sealed pressing system capable of affecting the following basic functions: (i) controlled application of uniaxial compressive stress, (ii) sequential injection and removal of chemical reactants, (iii) controlled heating, (iv) peripheral sealing, and (v) internal sensing of material conditions. This system will be used to perform

chemical vapor treatment and pressing of pre-formed fiber networks *in situ* under highly controlled chemical and thermodynamic environments;

- II. Provide a substantive literature review regarding chemical treatment and modification of wood materials for property enhancement and go on to select viable and mutually compatible chemical reactants which will stimulate desirable transformations of fibers within a network;
- III. Conduct studies of the action of any one or more of the above selected chemical reactants on pre-formed fiber networks;
- IV. Evaluate the likely response of adhesive bonds to the selected reactants;
- V. Perform consolidation trials involving natural fiber networks (mixed with adhesive) with the above selected chemical reactants;
- VI. Evaluate the properties of trial samples produced in the laboratory sealed pressing system.

## CHAPTER 2. LITERATURE REVIEW

### 2.1. Brief discussion about existing wood-based composites

The word composite means materials that are composed of more than a single base material i.e. any combination of two or more materials. Wood-based composites can be divided into three main groups depending on the size of the wood constituents: veneer-based, particle or flake-based and fiber-based products.

Veneer-based products include plywood, laminated veneer lumber (LVL), parallel strand lumber (Parallam<sup>TM</sup>) etc. Plywoods are glued wood panel products made up of thin veneers in such an arrangement that the grain of each veneer is at right angles to that of the adjacent veneer in the assembly (Anon., 1970). Usually, plywood consists of odd numbers of plies to produce a structurally balanced construction. Compared to solid wood, the most significant advantages of plywood are (i) its higher in-plane dimensional stability, (ii) nearly equal strength properties in both in-plane directions (length and width), (iii) little or no tendency to split, and (iv) can be made in large sizes. In laminated veneer lumber (LVL), the veneers are assembled with their grain running parallel to one another. LVL represents a relatively new lumber construction material; it is usually made in billets 0.6 to 1.2 m wide, 38 to 44 mm thick, and 2 to 18 m long and then cut into required sizes. LVL needs long press (hot) times to cure the phenol-formaldehyde (PF) adhesive sufficiently to overcome internal vapor pressures either in platen or continuous presses (Zavala and Humphrey, 1996; Theomen and Humphrey, 1999). Radio-

frequency curing of the gluelines is sometimes used to reduce press times. LVL is primarily used for structural applications, particularly as flanges (top and bottom portions) in I-section beams (plywood or OSB is often used for webs).

Another structural material having similar properties to LVL, called parallel strand lumber (Parallam™), is made from long strands of veneer 12.5 mm wide and up to about 0.91 m long which are oriented in the lengthwise direction and laid-up into a mat. PF is predominantly used as adhesive and a microwave-type of heating is used in a continuous press. The size of the billets are usually 280 by 460 mm or 280 by 355 mm. Another interesting material, called Com-ply lumber®, is made of random or oriented wood flakes or particles sandwiched between one or more layers of veneer.

Particle-based products include particleboard, flakeboard, waferboard and oriented strandboard (OSB). Particleboard is a generic name for boards made from any discrete pieces or small particles of wood. Mainly it refers to those boards composed of the more granular or sliver-type elements. Phenol-formaldehyde, urea-formaldehyde (UF) and melamine urea formaldehyde (MUF) are usually used as binders in particleboard depending on its end-use. Conventional, continuous, and gas injection hot pressing methods are used to cure the adhesive and to consolidate the mat. Particleboard remains the world's dominant furniture panel, although it is still also used for structural applications such as manufactured home floors, roof sheathing, wall panels etc. Flakeboard is made up of flakes, small pieces of veneer, 50 to 75 mm square, and usually 0.6 mm thick. Flakes are laid-up randomly before

pressing and tend to restrain and complement each other in the product in a similar way to the cross-plyies in plywood. The board is usually bonded with an exterior-type resin. When the thickness of flakes are about 1.3 mm or so, then the products are known as waferboard (Marra, 1992). Waferboard has been well accepted in several sheathing applications in North America, although it has now been largely replaced in the marketplace by another kind of product called oriented strandboard (OSB). Due to their geometry, strands (typically measuring 12.7 mm wide and 38 to 76 mm long) can be partially aligned by dropping them through narrow slots. OSB typically has 3 or 5 layers and the strands in each layer are, on an average basis, aligned  $90^{\circ}$  from the adjacent layer. When consolidated, OSB has directional properties somewhat similar to those of plywood, and the properties of OSB make it suitable for many applications traditionally dominated by plywood.

Fiber-based products include hardboard, medium-density fiberboard (MDF) and insulation board. Hardboard is a generic name for a panel which is manufactured primarily from inter-felted fiber mats formed by wet- or dry-processes and consolidated by pressure and heat to a density near to  $1000 \text{ Kg/m}^3$  (within the range of 500 to  $1450 \text{ Kg/m}^3$ ) (Haygreen and Bowyer, 1989). Bonding agents and other additives may be added at the felting stage to improve certain properties. Hardboard is usually used for construction, furniture and furnishings, cabinet and store fixture work appliances and automotive stock. A more recently developed type of fiber-based product called medium-density fiberboard (MDF) is dry-formed and made from wood fibers usually combined with a synthetic resin or

other suitable bonding agent. The density of MDF usually ranges from 500-800 Kg/m<sup>3</sup> (Haygreen and Bowyer, 1989). Like particleboard, inter-fiber bonding in MDF is created by the added synthetic resin rather than ligneous bonds that are possible in hardboard. MDF has very smooth surfaces which helps in wood-grain printing, overlaying, and veneering. It has also tight edges which do not require any banding. In the furniture industry, MDF often now takes the place of solid wood, plywood, and particleboard. Another type of fiber-product called insulation board is manufacture from wet-formed, inter-felted wood fibers by heat and pressure to a density of 160 to 500 Kg/m<sup>3</sup>.

Some other different types of wood-based composites available in today's market include inorganic-bonded wood and fiber composites (cement-bonded and gypsum-bonded boards) and wood-plastic composites.

## **2.2. Brief review of adhesives presently used in wood-based composites**

Adhesives are often an expensive component in the manufacture of wood-based composites. A great variety of adhesives have been used and the following are the most common:

- Phenolic resins
- Amino resins
- Isocyanate resin

Each of them will be considered in turn.



### 2.2.1. Phenolic resins

Phenolic resin is the reaction product of phenolic or phenol derivative monomer with a cross-linking agent, formaldehyde. The reaction proceeds in two discrete steps. The first step is called addition or methylation, in which formaldehyde adds itself onto the active ortho- or para- positions of the phenol

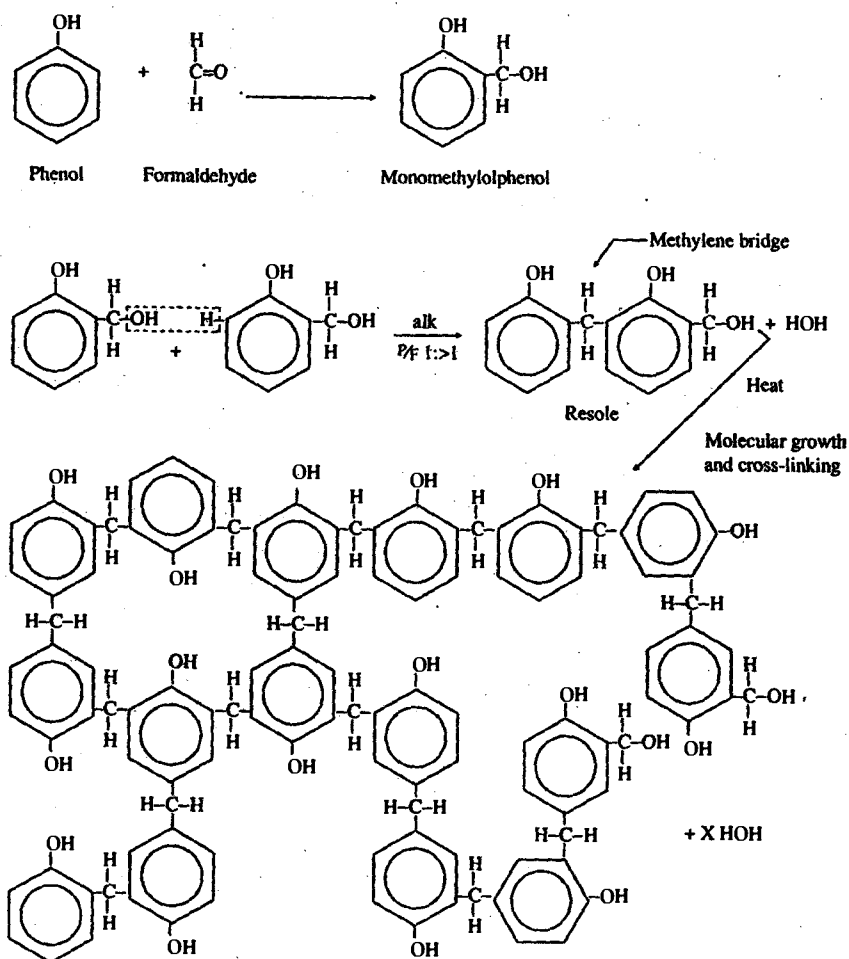


Figure 2.1 Addition, condensations, and cross-linking reactions of phenol-formaldehyde (resole) (from Marra, 1992).

molecule without losing any atoms to form methylolated phenolic product such as mono-, di- and tri- methylol derivatives. The second step of the reaction is of the condensation type in which the methylol phenol reacts with itself or with another phenol (condenses). Under proper conditions of temperature and pH very large molecules are formed through "methylene (-CH<sub>2</sub>-) bridging". The methylol (-CH<sub>2</sub>OH) group of one methylol phenol reacts with the hydrogen of another to form a methylene bridge and generate water as a condensation by-product. The reactions first form linear polymers and are followed by highly branched three dimensional structures (Pizzi, 1983).

Phenolic resins generally are phenol-formaldehyde (PF), resorcinol-formaldehyde (RF) (resorcinol is a derivative of phenol, having an additional hydroxyl group in the benzene ring) and phenol-resorcinol-formaldehyde (PRF). There are two types of PF resins depending on the molar ratio of phenol to formaldehyde. When the molar ratio is less than 1 (molar ratio of phenol to formaldehyde of 1:1.8 to 1:2.2) then it is called resole, and when the ratio is greater than 1 (molar ratio of phenol to formaldehyde of 0.8:1 to 1:1) then it is called novolak.

Resols are produced with alkaline catalyzed processes and an excess of formaldehyde. Resole is rich in methylol groups and capable of polymerizing under heat and pressure without the addition of other ingredients. Novolak is produced with acid catalysis and a deficiency of formaldehyde. It has no reactive methylol groups so is unable to polymerize on its own. Novolak needs a source of

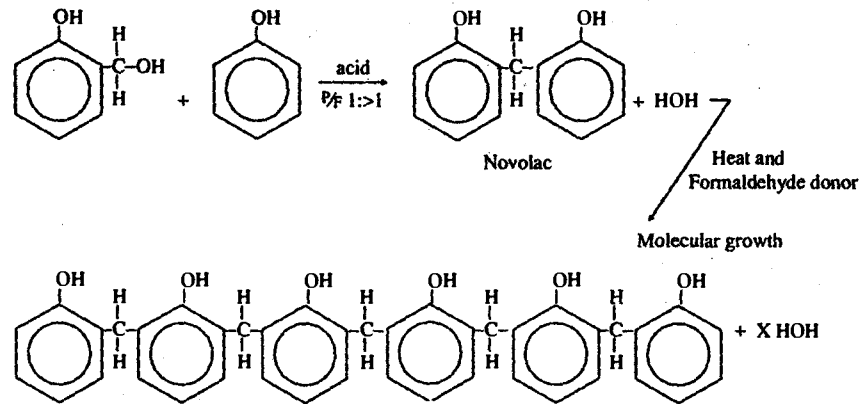


Figure 2.2 Addition, condensation, and linear growth of novolak molecule (from Marra, 1992).

formaldehyde as a hardener in addition to heat and is much more stable than the resols but must be kept dry (Maloney, 1977). Novolak PF adhesives are not generally recommended for use in wood-based composites because they use a strong acid catalyst which can damage the surface of wood particles and cause long term reliability problems. However, some waferboard plants use novolak resins in powder form and hexamethylene tetramine as a source of formaldehyde. Alkaline-catalyzed PF resins (resols) are generally used in exterior and structural wood-based composites such as OSB, plywood, LVL, MDF etc. A typical alkaline-catalyzed PF resin would be about 50% solids, pH about 10–12, contain phenol, formaldehyde and NaOH and have a molar ratio of about 1:2:0.75 (Skeist, 1990). Alkaline-catalyzed PF resin bonds have high strength and they are resistant to weathering (water and heat). Importantly, they have no problem with formaldehyde emission but are relatively expensive and have a dark color.

Resorcinol is a derivative of phenol, has an extra hydroxyl group on the benzene ring and this renders it extremely reactive with formaldehyde in forming the methylol compound, and then to the formation of methylene bridges to affect solidification. RF is cured without additional heat input and the curing speed

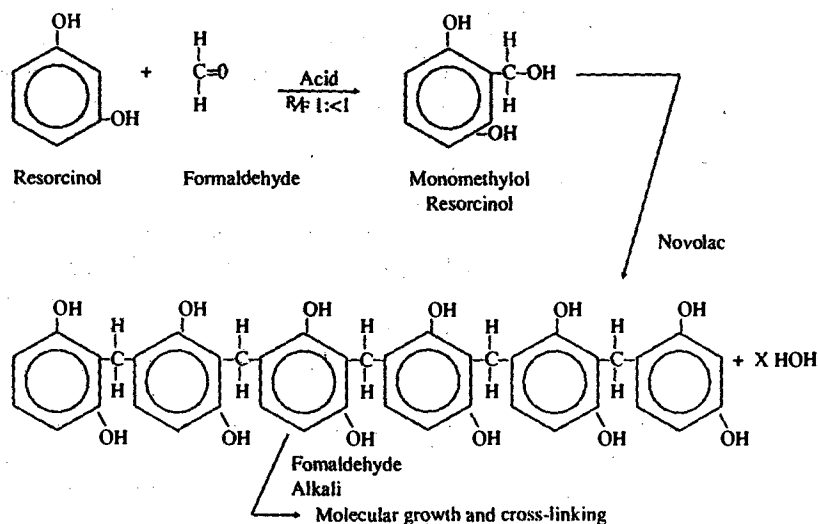


Figure 2.3. Addition and condensation reactions of resorcinol-formaldehyde (from Marra, 1992).

is very fast depending on the pH (Marra, 1992). pH ranges from 7-9, gives pot lives of 2-4 hours. Resorcinol is a comparatively expensive chemical and is rarely used in wood-based composites. The use of phenol-resorcinol-formaldehyde in wood-based composites is much more common than resorcinol-formaldehyde. Mixing of phenol and resorcinol accelerates curing of PRF resins and also enables the same bond strength that can be achieved with PF. PRF resins are generally used in lumber laminating and the I-beam industry where ambient-temperature curing is

required, although radio-frequency heating helps to accelerate the curing of PRF resins. PRF resin bonds are also waterproof and heat resistant.

### 2.2.2. Amino resins

Amino resins are the reaction products of aldehyde (mainly formaldehyde) with  $-NH_2$  or  $-NH$  groups containing compounds such as urea and melamine. The amino resins include urea-formaldehyde (UF), melamine-formaldehyde (MF) and melamine-urea-formaldehyde (MUF). UF resins are commonly used in the panel industry, and are generally in the form of an aqueous solution of acid-catalyzed urea-formaldehyde polymers. Urea has two amino groups with four reactive hydrogen sites which allow the formation of methylol groups (but only three sites may be methylolated due to steric hindrance with formaldehyde). The methylol groups are responsible for all further cross-linking to produce insoluble resin after full curing. The reaction also proceeds in two discrete steps: addition (methylolation) and condensation. The reaction between urea and formaldehyde is endothermic and takes place in an acid environment. After the condensation reaction, the resin can be stabilized for storage by increasing the pH of the liquid resin and cooling (Marra, 1992). The final curing stage of the resin is accomplished by decreasing its pH. The required acid is supplied by salts of strong acids and weak bases (e.g. ammonium chloride that dissolves and provides the corresponding acid).

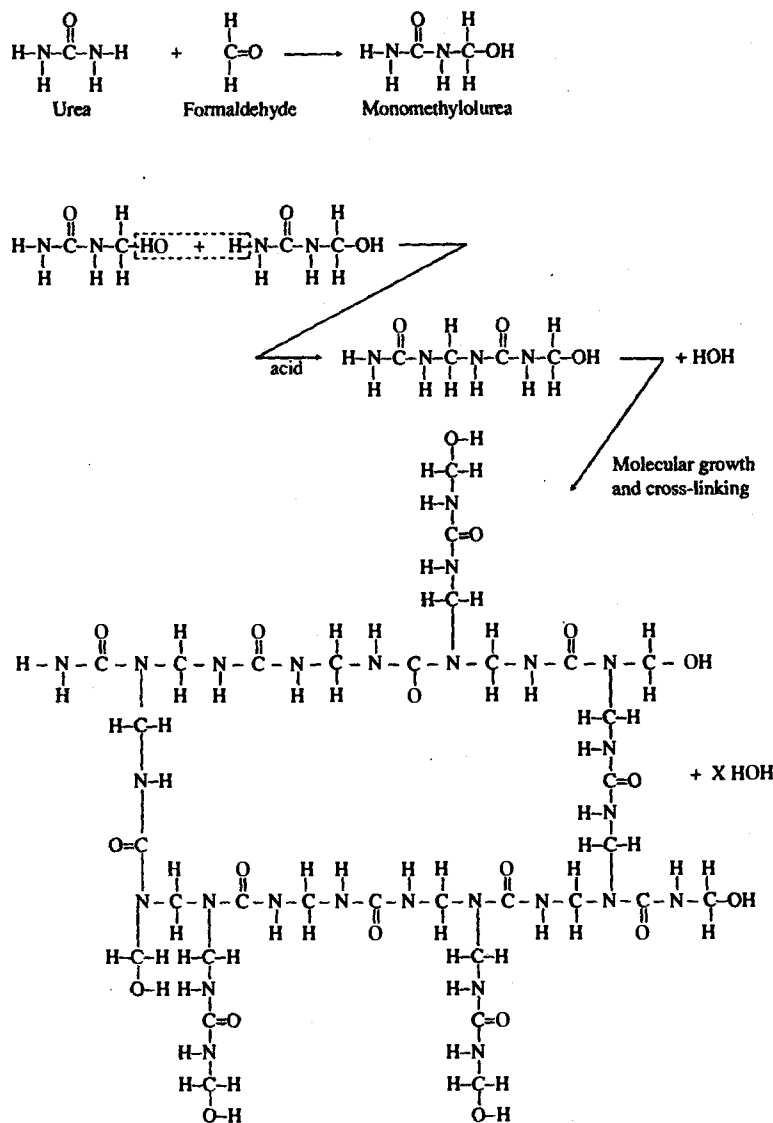


Figure 2.4 Addition, condensation, and cross-linking reactions of urea-formaldehyde (from Marra, 1992).

Urea based resins are very versatile. They can be made to cure at temperatures as low as 10<sup>0</sup>C (Davis, 1997) or at elevated temperatures. The molar ratio of formaldehyde and urea (F/U) generally varies from 1.2:1 to 2.0:1. Lower F/U ratios have lower free formaldehyde content and longer pot life, but they have

lower water resistance, lower strength and stiffness, and a slower curing speed (Steiner, 1973; Roffael, 1976; and Dinwoodie, 1977). The most common practice is to use molar ratios of 1.4:1 to 1.6:1.

Emissions of formaldehyde during hot pressing and of finished products have been a great problem of UF resins (Meyer, 1979; Marutzky, 1989). However, the main advantage of UF resins over PF resins is its curing speed. UF resins are also colorless and relatively cheap but are not currently resistant to weathering and are therefore not suitable for exterior use. The weathering resistance of UF resin may be improved by adding 15-20% melamine formaldehyde (Pizzi, 1983). It is also possible to increase the moisture resistance of UF resin by replacing some of the urea groups with melamine groups; this is known as melamine-urea-formaldehyde (MUF). The relative proportion of melamine to urea is about 40:60. MF is much more expensive than UF and also somewhat more expensive than PF.

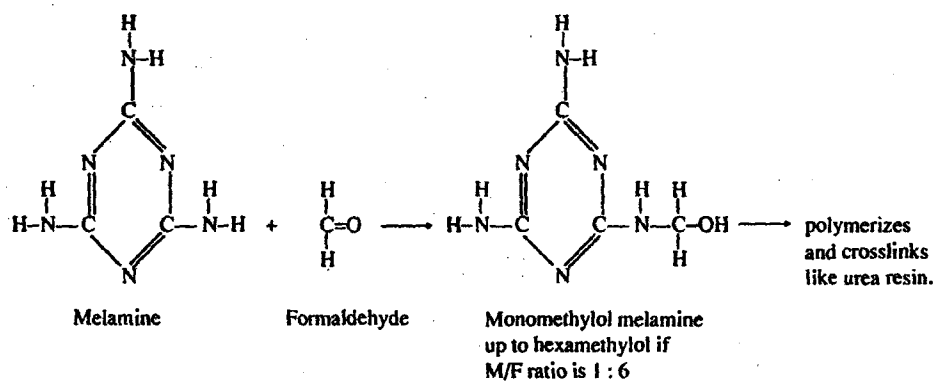


Figure 2.5 Reaction of melamine and formaldehyde (from Marra, 1992).

### 2.2.3. Isocyanate adhesives

Isocyanates are not yet widely used in wood-based composites although their importance is likely to increase in the near future. They are generally used in products where outdoor exposure and colorlessness are very important. A typical isocyanate resin is polymeric methylene-diphenyl-diisocyanate (PMDI), which is highly reactive. Isocyanate (IC) resins are very expensive but their bonds are highly durable and weather resistant and have no problem with free formaldehyde emission. These resins have strong polarity and very reactive radicals  $-N=C=O$ . Other than adhesion, IC resins have potential to form covalent bonds to any substrates that have reactive hydrogen. The resins can bond “anything to anything”. Indeed, their effectiveness can lead to unwanted sticking to press platens or cauls in panel pressing. Application of releasing agents is therefore required. However, in comparison to all other resins, less resin is needed to produce formaldehyde-free board with high moisture resistance and high dimensional stability. In addition, board density does not need to be as high as for those bonding with PF resins; this is due to better bonding behavior of isocyanate resins.

### **2.3. Overview of the internal behavior of fiber mats during hot pressing**

Many processes that occur in the conventional pressing of wood-based panels will also occur in sealed pressing systems and that is the reason that they will be reviewed here.



Many physical processes occur within conventional wood-based composites during hot pressing and these interact with each other as pressing proceeds. Heat and moisture move throughout the hygroscopic and porous mat. Heat is transferred from the press platens to the center of the mat and it approaches the temperature of the platens. Heat may be transferred by means of conduction, convection and diffusion of water vapor and air. Some vapor associated heat escapes from the edge of the mat to the atmosphere and this results in horizontal (in-plane) gradients as well as cross-sectional ones. Therefore, there is three-dimensional unsteady-state heat and moisture transfer (Bolton *et al.* 1989a). As time increases during the hot pressing process, the vertical position temperature distribution continuously varies until it approaches platen temperature, and moisture is re-distributed.

Evidently, in the hot pressing of most wood composites, phase change and subsequent convection of water vapor play a key role in the rapid transfer of heat into the center of the mat and therefore considerable movement of water within the mat in the vertical plane occurs. This phase-change of adsorbed water into vapor and subsequent diffusion and re-adsorption leads to the redistribution of adsorbed water within the system and to the development of three-dimensional gradients of moisture content (Bolton *et al.* 1989b). Recent work by Thoemen and Humphrey (1999) also suggest that air pressure gradients are also established, particularly in continuous presses.

So, during the consolidation of conventional wood-based composites, unsteady-state heat and moisture transfer and phase change result in ever changing

spatial distributions of temperature, adsorbed moisture and within-void partial pressure of water vapor within the composite. These affect spatial variations in densification in the consolidation direction since the viscoelastic properties of wood cell-wall material are dependent on temperature and moisture content. Such cross-sectional density profiles critically effect the physical and mechanical properties of the product; not least of these are the flexural properties of the composites. Furthermore, inter-fiber bonding characteristics and residual stress also differ throughout the composites as consolidation progresses. Indeed, the rate at which thermosetting adhesive bonds between fibers develop their strength is also affected by temperature variation during pressing (Ren and Humphrey, 1989). Manufacturers of conventional wood-based composites (mainly panels) have little control over the way all these mechanisms progress and interact.

#### **2.4. Chemistry, reactivity and accessibility of wood cell wall components**

In readiness for our attempts to identify a useful sequence of treatment chemicals in the present research, it is necessary to appreciate the chemical nature of the wood fibers with which the reactants must interact. A brief review of wood chemistry is therefore provided below before moving on to chemical treatments.

Wood consists of two major chemical components, known as lignin (18-25% in hardwoods and 25-35% in softwoods) and carbohydrate (65-75%). The carbohydrate portion of wood consists of cellulose (40-50%) and hemicellulose

(15-35% in hardwoods and 20-32% in softwoods). The relevant characteristics of each of these constituents will be summarized in turn.

#### 2.4.1. Wood cellulose

Cellulose is an unbranched, rigid, linear chain polymer composed of anhydro-D-glucopyranose units which are linked together by  $\beta$ -1-4-glycosidic bonds. The degree of polymerization (DP) of wood cellulose is typically about 9000-10,000 (Goring and Timell, 1962). Polymers containing cellulose have high tensile strength because of the covalent bonding within the anhydro-D-glucopyranose ring unit and between the pyranose ring units. Cellulose molecules have a strong tendency to form intra- and inter-molecular hydrogen bonds; these bonds impart rigidity to assemblages of such molecules and make them tough. Bundles of cellulose molecules are thus aggregated together in the form of microfibrils in which highly ordered crystalline regions alternate with less ordered amorphous regions.

Hydroxyl is the only functional site available in cellulose for non-destructive reaction to impart enhanced properties. Each monomer unit in the cellulose chain has three reactive hydroxyl groups: one primary (HO-6) and two secondary (HO-2 and HO-3). For bulky substitution, HO-6 groups possess the highest reactivity; this is because they are the least sterically hindered (Sjostrom, 1981).

In contrast to crystalline cellulose, the hydroxyl groups associated with non-crystalline amorphous regions are easily accessible and available for reaction. The hydroxyl groups present in the crystalline regions are not, or much less, accessible because of a high degree of inter-chain hydrogen bonding and close packing. Swelling by any agent increases the reactivity (West, 1988).

#### 2.4.2. Wood hemicelluloses

Hemicelluloses are the non-cellulosic cell wall polysaccharides. They are also polymeric materials and consist of various elementary sugar units, primarily the hexoses (six- carbon sugars, D-glucose, D-galactose, and D-mannose,) and the pentoses (five- carbon sugars, L-arabinose and D-xylose). In softwoods, the sugar units are mostly mannose and some xylose, but in hardwoods the sugar units are mostly xylose and little mannose. In hemicelluloses the linear polymeric chains are shorter (DP = 150-200), frequently branched, and their linkages are not always through the 1-4 positions. Galactose residues are often connected at the 6 position of a main chain. Due to the structural heterogeneity, branching and substitution (uronic acid groups and acetyl groups), it is difficult for hemicellulose chains to pack together closely. The poor packing also means that they are more accessible to chemical reagents. Most hemicelluloses are found in the amorphous regions of the cellulose chains and in close association with the lignin. They seem to act as a coupling agent between cellulose and lignin.

Due to the occurrence of chain branching and the lower degree of supramolecular order, hemicelluloses are likely to be amorphous (Timell, 1964; Timell, 1965) and are more accessible and more available for chemical reaction than highly ordered cellulose. In hemicellulose polymers, hydroxyl groups are abundant reactive sites. Also, hemicellulose polymers contain significant amounts of carboxylic acid groups (uronic acids) (Banks, 1990).

For esterification, Philipp *et al.* (1989) reported little difference between the HO-2 and HO-3 groups in reactivity. In the case of esterification, Croon and Timell (1960) observed that the OH-2 group was more reactive than the OH-3 group.

#### 2.4.3. Wood lignins

Lignin is a high molecular weight and complex three dimensional phenolic polymer consisting of an irregular array of variously bonded hydroxy- and methoxy- substituted phenylpropane units. Softwood lignin is composed of guaiacyl propane (or 3-methoxy-4-hydroxy-phenylpropane) monomers. In hardwood lignin, approximately half of the monomer units possess an extra methoxyl group giving syringyl propane (or 3, 5-dimethoxy-4-hydroxy-phenylpropane). Lignin acts as a cementing material on and around the carbohydrate fraction and is the most hydrophobic (water-repelling) component of the wood cell wall. Furthermore, lignin is thermoplastic in nature, having glass transitions at about 130-150<sup>0</sup>C (Biermann, 1993).

Experimentally, it has been found that lignin is a noncrystalline, amorphous material (Goring, 1971). As with polysaccharide, the most abundant functional group is hydroxyl. It is estimated that there is only one or sometimes two hydroxyl groups per monomer unit, or per 10 carbon atoms (Fengel, 1971). It was observed that the hydroxyl groups in lignin may react more readily initially in esterification and etherification reactions than do those of the cell wall polysaccharides (Rowell, 1980). Phenolic hydroxyl, benzylic hydroxyl, noncyclic benzyl ether and carbonyl groups are the reactive sites in lignin (Alder, 1977). The aryl ring may also be reacted with available electrophiles (Gierer, 1982a; Gierer, 1982b).

## **2.5. Brief review of chemical modification options for wood**

It is clear from the preceding discussion that chemically, wood is a three-dimensional complex polymeric material, consisting of cellulose, hemicelluloses and lignin and which contains large numbers of hydroxyl groups. Wood is one of the most versatile raw materials for a variety of reasons. Wood is reproducible, strong, easily processed and may be aesthetically pleasing. Despite the many advantages, it conversely is biodegradable, flammable, changes dimension with varying moisture contents, and is degradable by ultraviolet light, acids and bases. Wood's hygroscopic nature and potential for biological degradation has been attributed to the presence of a large number of free hydroxyl groups (Rowell, 1975). These hydroxyl groups play active roles in absorption of moisture through hydrogen bonding. Most of the wood-destroying organisms have specific enzyme

systems which attach themselves to these hydroxyl groups before hydrolyzing the wood substrate to easily digestible units.

Chemical modification of wood has been found to improve its dimensional stability and bio-resistance (Rowell, 1983). Chemical reaction between any functional site and any chemical reagent, with or without catalyst, to form a covalent or non-polar bond between the two is defined here as chemical modification. The specific configuration of the chemical components of the wood changed in chemical modification is usually achieved by substituting a portion of the hydroxyl groups. Such modifications can reduce bio-deterioration by preventing highly specific enzymatic reactions (Rowell, 1983). Blocking of such groups also changes the hydrophilic nature of the wood. Replacing hydroxyl groups with larger ones puts the wood in a permanently swollen state and makes it hydrophobic, thereby increasing its dimensional stability. Here however, we are not limited to the above mentioned definition of chemical modification. Included are some chemical treatments such as with ammonia, which affects some physical and chemical changes in the chemical components of the wood.

Chemical modification of wood for property improvement has been thoroughly reviewed by Rowell (1983) and by Banks (1990). The major types of covalent bonds formed by chemical modification of wood are esters, ethers, and acetals. The essential features of each of these will be considered here in turn. One of the specific objectives of this research is to find some chemical modification options which can be easily used in a sealed pressing system during pressing to

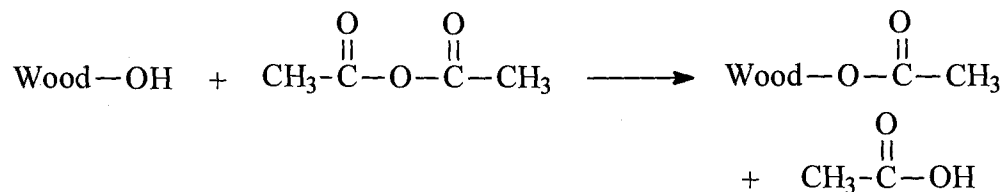
enhance the some desire properties of the furnish material as well as of the product object. Those desirable properties are plasticization, adhesion and, if possible, dimensional stabilization within the fiber networks. That is the reason behind the review of chemical modification options for wood. During review, we were concerned about other two criteria (i) vapor phase treatment, and (ii) compatibility of chemicals with each other for sequential treatment.

### 2.5.1. Esterification

Reactions of wood with acid anhydrides, carboxylic acids, acid chlorides, and isocyanates produce esters. Ester bonds are weaker than ether bonds. Various types of reaction will be considered below.

#### 2.5.1.1. Acetylation

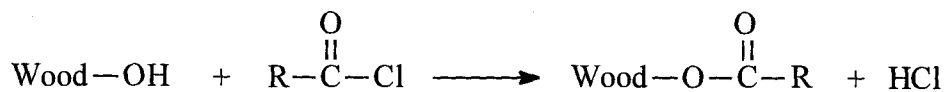
Acetylation has been the most studied of all the chemical modification methods for wood and is widely acknowledged as being potentially important



(Rowell *et al.* 1986a; Sheen 1992). Acetic anhydride was found to be the most suitable chemical for acetylation, which reacts with wood hydroxyls with or without a catalyst to form wood ester; acetic acid is released as a by-product.



Acid chlorides are also good chemical reagents for acetylation but have the disadvantage of releasing hydrochloric acid as a by-product (Singh *et al.* 1981).



Thioacetic acid has also been evaluated as acetylating agent (Singh *et al.* 1979) and was found to be highly reactive but did not yield Weight Percent Gain (WPG) values above 8 (Kumar and Agarwal 1982).



Ketene gas dissolved in acetone or toluene has also been used for acetylation.

Stamm and Tarkow (1947) carried out the first work on acetylation of whole wood with acetic anhydride. Goldstein *et al.* (1961) reported that the best acetylation condition is the vapor phase treatment with uncatalysed acetic anhydride in xylene at 100 to 130°C. More recently, Rowell *et al.* (1986a) reported a procedure that greatly shortens reaction time and simplifies the recovery of chemical by-products. According to this procedure, oven dry flakes, particles or fibers in a stainless steel mesh container were immersed in acetic anhydride without catalysts or co-solvents for 1 minute at room temperature and then treated with preheated (120°C) acetic anhydride in a stainless steel reactor for the desired level of time. After treatment, a vacuum was applied to the reactor and excess acetic anhydride and by-product acetic acid was collected from the bottom. The acetylated wood elements were then oven-dried.

Solid wood acetylated to weight gains of around 17% was found resistant to fungal and termite attack (Goldstein *et al.* 1961). Furthermore, anti-shrink efficiency (ASE) of about 70% have been achieved with weight gains of 20-25% (Tarkow *et al.* 1950). In acetylation with acetic anhydride, there is about 50% loss of reagent due to the formation of acetic acid. This acetic acid is corrosive to some metals and may reduce the strength of wood if not removed properly. Furthermore, acetylated wood exhibits no resistance against mold and stain fungi (Wakeling *et al.* 1992). However, the mechanical strength of wood was improved by acetylation (Tarkow *et al.* 1950; Goldstein *et al.* 1961; Agarwal *et al.* 1985) and Norimoto *et al.* (1987) reported that creep decreased with acetylation.

Acetylation improves the dynamic mechanical properties of wood by lowering the hygroscopicity and consequent equilibrium moisture content (EMC) of the cell wall in a given atmosphere (Akitsu *et al.* 1991). Yano *et al.* (1988) observed that resonant frequency of wood can be stabilized by acetylation. At weight gains of about 25%, Zhao *et al.* (1989) found that the dielectric constant and the EMC of the acetylated wood were decreased but the degree of crystallinity did not change. Plackett *et al.* (1992) observed a temporary reduction in the rate of surface degradation of acetylated wood due to UV radiation.

A lot of acetylation work has already been conducted on wood-based composite materials. Rowell *et al.* (1986b) reported a reduction in the swelling rate of flakeboards immersed in liquid water. They also observed that such flakeboards were much more stable than control boards in cyclic wetting and drying tests.

At constant relative humidity, as the level of acetylation increases, the equilibrium moisture content of the flakeboard made from acetylated flakes decreases. For low density particleboard made from acetylated or unmodified particles of *Albizzia falcata* (a fast-growing tropical timber species), Imamura *et al.* (1989) also found that the rate of thickness swelling in acetylated board samples was significantly less than in untreated controls and was independent of adhesive types; phenol-formaldehyde and isocyanate adhesives were used. Acetic anhydride treated boards produced slightly less swelling than similar thioacetic acid treated boards (Kumar and Morrell 1993). Rowell and Keany (1991) found that the EMC of acetylated bagasse fibers and fiberboard made from acetylated bagasse fibers were about one-third that of controls, at WPG 17.6%, at each relative humidity.

Particleboard made from acetylated particles showed better decay resistance than boards made from unmodified particles (Kumar and Morrell 1993). Acetylated flakeboard showed better resistance to dry wood termite attack, which was indicated by increasing termite mortality (Hadi, 1992). Acetylated flakeboard also showed better resistance to subterranean termite attack. At about 18% weight gain, the acetylated flakeboards are very resistant to brown-, white-, and soft-rot fungi and tunneling bacteria (Rowell *et al.* 1987; Imamura *et al.* 1986).

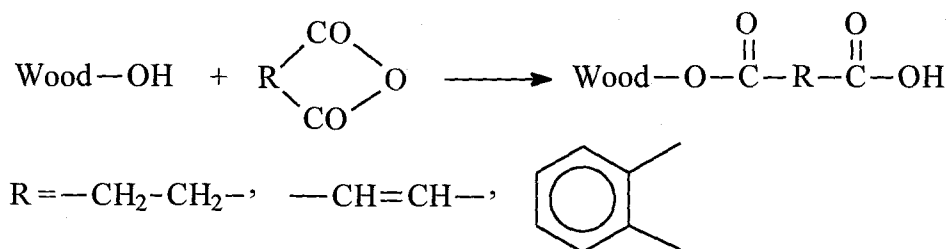
Youngquist *et al.* (1986) reported that due to the lack of wettability and penetration of adhesive, internal bond strength and bending strength of board made from acetylated flakes (with acetic anhydride) were lower than board made from unmodified particles. They also suggested that boards made from acetylated flakes

had more voids. Kumar and Morrell (1993) have found that modulus of rupture (MOR) in bending and internal bond strength of board made from thioacetic acid treated flakes were about 39% and 59% higher, respectively, than the control board. The mechanical properties of boards made from acetic anhydride treated flakes were higher than the control boards except that bending strength was much lower than the control boards.

Chowdhury and Humphrey (1999) investigated the effect of acetylation on the shear strength development kinetics of phenolic resin-to-wood bonds and reported that acetylation has relatively small effects on the curing rates of phenolic adhesives at the early and intermediate stages. However, they also have found that acetylation does have some effects on the final strength bonds.

#### 2.5.1.2. Reaction with dicarboxylic acid anhydrides

Reaction of dicarboxylic acid anhydrides with wood generates carboxyl groups bearing esterified wood. In this reaction, the product is left with an active functional group attached to the cell wall polymer surface, which can be used for further reaction.



Dicarboxylic acid anhydride treatment of wood has the advantage that no by-product is generated. Phthalic anhydride was the first dicarboxylic acid anhydride used for chemical modification (Risi and Arseneau, 1958). The hygroscopicity of phthalylated wood is higher than untreated wood because phthalyl groups are more reactive with water than hydroxyl groups of the wood (Popper and Bariska, 1972, 1973).

Recently Matsuda *et al.* (1984a, 1984b) prepared esterified wood bearing carboxyl groups by the addition reaction (esterification) of the wood (meal) with dicarboxylic acid anhydrides such as maleic anhydride (MA), succinic anhydride (SA), and phthalic anhydride (PA). These reactions were conducted in the presence or absence of N, N-dimethyl formamide (DMF) or dimethyl sulfoxide (DMSO) which acts as swelling agent. The dicarboxylic acid anhydrides reacted with the wood even at room temperature in the presence of DMF or DMSO. Even in the absence of solvent, the reaction proceeds at temperatures between 60 to 200<sup>0</sup>C. For maleic anhydride and phthalic anhydride esterified woods, they observed that the anhydride was added to the wood in the form of monoester. In the case of succinic anhydride esterified woods, the ester content increases with increase of the reaction temperature. They also observed formation of diester above about 100<sup>0</sup>C in the case of succinic anhydride esterified woods. Matsuda and Ueda (1985a) observed that hygroscopicity and initial weight loss temperature decreases with increase in the ester content. The decrease of hydrophobicity seems to decrease in the following order: phthalic anhydride (PA) residue > succinic anhydride (SA) residue > maleic

anhydride (MA) residue. Temperatures at which weight losses occur seem to decrease in the following order: Wood•MA > Wood•PA > Wood•SA.

Matsuda and Ueda (1985b) explored the thermoplasticity of esterified woods. They esterified wood meal with succinic anhydride, maleic anhydride and phthalic anhydride in the presence of a solvent [N, N-dimethyl formamide (DMF) or dimethyl sulfoxide (DMSO)] by simply heating for three hours at temperatures greater than 60°C. Following such treatment, the esterified wood meal could be molded into yellowish or reddish brown, semi-transparent sheets by hot pressing. It was observed that thermoplasticity increases with an increase in the monoester content of the esterified woods and the thermoplasticity decreases with an increase in the diester content of the esterified woods. These effects are probably due to a decrease in the thermal fluidity by crosslinking. The thermoplasticity of the esterified woods decreases in the order of SA > MA > PA.

Codd *et al.* (1992) observed that hepta-decenylsuccinic anhydride in the presence of the swelling agent dimethyl formamide linked to the wood hydroxyl oxygen, by opening its cyclic structure.

Clemons *et al.* (1992) esterified aspen fibres with MA and SA in hot xylene. Fibreboards made from esterified fibres had reduced moisture sorption and rate of swelling in liquid water. It was also observed that esterification of fibers with maleic and succinic anhydrides imparted thermoplasticity. Succinic anhydride esterified fibers had higher thermoplasticity than maleic anhydride esterified fibers.

It was also reported that esterification of fibers with dicarboxylic acid anhydrides increases compressive strength of fiberboard.

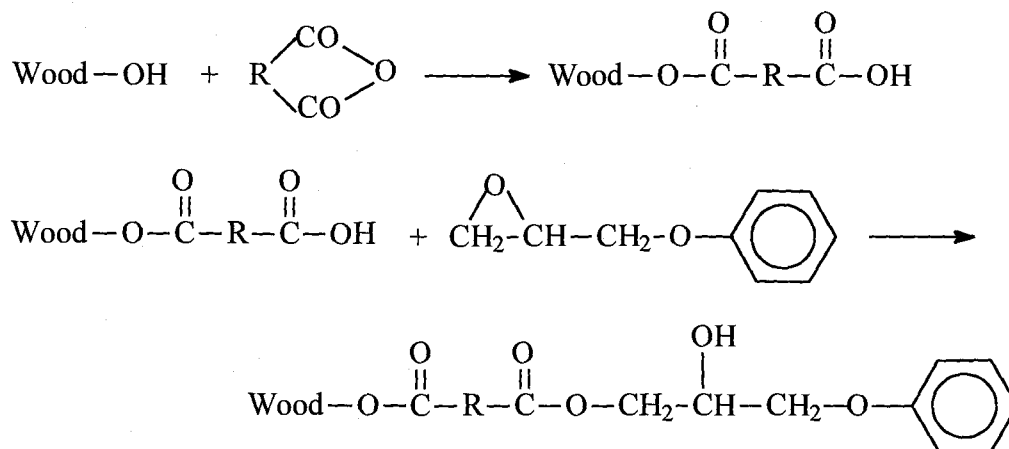
### 2.5.1.3. Oligoesterification

Addition reaction (esterification) of dicarboxylic acid anhydrides with wood (even in the absence of a solvent) results in active functional groups (carboxyl groups) bearing esterified wood (Matsuda *et al.* 1984a, 1984b). This material may undergo further addition reaction with epoxides such as phenyl glycidyl ether (PGE) (Matsuda, Ueda 1985c), epichlorohydrin (EpCl) (Murakami, Matsuda, 1990a), allyl glycidyl ether (AGE) and glycidyl methacrylate (GMA) (Matsuda, Ueda 1985d). When the epoxide-adducted esterified woods were subjected to stepwise addition reaction (alternately) with the anhydride and the epoxide, oligoesterified wood was produced (Matsuda, Ueda, 1985d).

Similarly, when the epoxide-adducted esterified woods were subjected to one-step chemical treatment with a mixture of the dicarboxylic acid anhydride and the epoxide, alternately addition reactions occurred, to obtain oligoesterified woods (Matsuda, Ueda 1985c).

From the above studies, Matsuda and Ueda observed that hygroscopicity of the oligoesterified wood decreases with an increase in the oligoester chain length and/ or terminating the oligoester chain with epoxide. They also examined the thermoplasticity of the epoxide-adducted esterified wood and the oligoesterified woods by hot pressing. This formed reddish brown, yellowish brown, yellow or

semi-transparent sheets (Matsuda, Ueda 1985e). In the case of epoxide-adduct esterified woods, the thermoplasticity decreased in the following epoxide order: PGE > AGE > GMA. In the case of oligoesterified woods, the thermoplasticity



decreased with the increase of the oligoester chain length and/ or terminating the chain with PGE.

At high temperature and pressure, oligoesterified wood such as wood-PA-GMA series (Matsuda *et al.* 1988a) gave plastic-like cross-linked wood boards without using any radical initiator; whereas the wood-MA-AGE series (Matsuda *et al.* 1988b) required a catalytic amount of dicumyl peroxide during hot pressing to give cross-linked plastic-link boards. Oligoesterified woods such as Wood-PA-EpCl series (Murakami, Matsuda 1990a) exhibit excellent decay resistance.

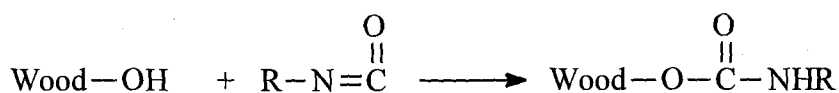
Wood-MA/ PA-EpCl oligoesterified woods yield highly dimensionally stable products with durable bonds (Matsuda *et al.* 1988c, 1988d). Murakami *et al.* (1989) reported that tensile and impact strengths decrease whereas bending and compressive strengths increase in the oligoesterified woods. Further, vibrational



properties of wood improve due to oligoesterification (Murakami and Matsuda 1990b), which has a direct relationship to acoustical properties.

#### 2.5.1.4. Reaction with isocyanates

Reaction between wood hydroxyls and isocyanates yield stable urethane bonds and produces nitrogen-containing ester.



This reaction is generally very fast and no by-product is produced with dry wood in this reaction. Isocyanates react with wood with or without catalyst. Dry wood is a prerequisite for isocyanate's reaction because they are very sensitive to moisture. Clermont and Bender (1957) exposed pre-swollen (in dimethyl formamide(DMF)) wood veneers to vapors of phenylisocyanate at 100-125<sup>0</sup>C for 1-2 hours and found up to 77% ASE. All treated veneers showed higher mechanical strength than controls and no color change was observed in this experiment. Baird (1969) treated DMF pre-soaked wood with ethyl, allyl, butyl, t-butyl, and phenyl isocyanate; butylisocyanate vapor in DMF gave best results and at 31 WPG, ASE of about 67% was reported. Baird also reported that at this weight gain toughness and abrasion resistance reduced by 25 percent.

Methyl isocyanate reacts very quickly with wood, even in the absence of catalyst. Rowell and Ellis (1979) reported about 40 WPG within 20 minutes, and at

16 to 28 WPG, ASE of 60 to 70% was observed. Splitting of the cell wall occurred at WPG above 26 and above this WPG, ASE decreases with increases of WPG.

Treatment with methyl isocyanate imparts resistance to brown rot. Ellis and Rowell (1984) reacted wood with ethyl, n-propyl, and n-butyl isocyanates in the absence of any catalyst and have found different degrees of dimensional stability. In the presence of 5% or less catalyst, phenyl isocyanates, 1,6-diisocyanatohexane, and tolylene-2, 4-diisocyanate produced non-bonded polymers in the wood voids and did not improve dimensional stability or decay resistance. The catalyzed n-butyl isocyanate gave the best results; 70% or more dimensional stability and higher resistance to decay were observed at 30 WPG.

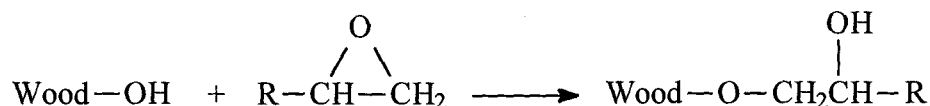
West and Banks (1986) reported that isocyanates react with lignin 10 times faster than they do the holocellulose. Martins and Banks (1991) observed the presence of a sorption-desorption hysteresis in isocyanate-modified wood.

### 2.5.2. Etherification

Ethers are formed by the reaction of wood with alkylhalides, allylhalides, epoxides, acrylonitrile,  $\beta$ -propiolactone (acid conditions) etc. Ether bonds are very stable. Each of these will be considered in turn.

### 2.5.2.1. Epoxidation

When epoxides are reacted with the hydroxyl groups of wood, etherification takes place as shown in the following reaction.



This is a base or acid-catalyzed reaction but is usually catalyzed with bases.

Advantages of this reaction are that stable ether bonds are formed, it generates no by-products, and the product is left with a new hydroxyl from which a polymer may begin to form. The early work was done with ethylene oxide (EO) in the vapor phase, catalyzed with tri-methylamine (McMillin, 1963). In this study, an ASE of 60% was obtained at weight gains of 20%, and the strength of the treated wood remained unchanged. Barnes *et al.* (1969) observed about 42% ASE at 12% weight gains.

Rowell and Gutzmer (1975) carried out detailed studies of the reaction of epoxides such as propylene oxide (PO) butylene oxide (BO) and epichlorohydrin (EPCL) with wood, catalyzed with triethylamine. They carried out the reaction at 120°C at 150 psi (1.0339 MPa) nitrogen pressure. The reactivity of epichlorohydrin and propylene oxide is much higher than that of butylene oxide. ASE of 50-70% was attained at a weight gain of between 20-30%. Good resistance to biological attack was observed in the modified wood.

Rowell *et al.* (1976) observed decreases in dimensional stability due to the breakdown of the cell wall structure above about 30% weight gain. Further, Rowell

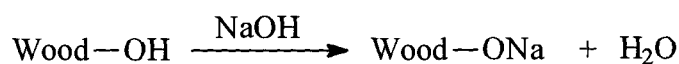
*et al.* (1982) reported 14% decreases of modulus of elasticity, 17% decreases of modulus of rupture and 10% decreases of crushing strength in the propylene oxide-modified wood.

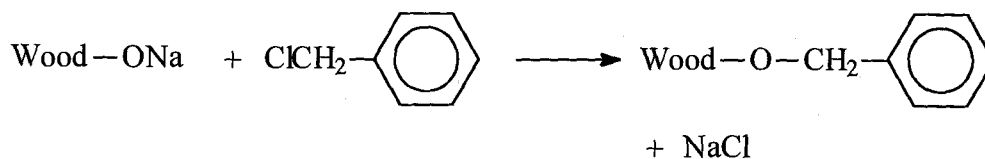
Guevara and Moslemi (1984) have studied the effect of alkylene oxides on wood dimensional stability. Results from their study showed that propylene oxide and butylene oxide plus the cross-linking agent trimethylol propane trimethacrylate, were the most efficient chemical treatments in controlling hygroscopic dimensional changes.

Rowell *et al.* (1986b) treated wood flakes with butylene oxide (catalyzed with triethylamine) before board formation. Flakeboard made from 20% WG's flakes, showed 25% less absorption of water and 50% reduction in thickness swelling than that of untreated flakeboard.

#### 2.5.2.2. Benzylation

Hon and Ou (1989) made the first attempt to impart appropriate plastic properties to the thermally non-flowable lignocellulosics materials by benzylation; benzyl chloride was used as the benzylation reagent. In this system, wood was first pretreated with sodium hydroxide as a swelling agent and water as a solvating agent to make the wood hydroxyl groups accessible. The reaction proceeds as follows:





Hon and Ou (1989) observed that the rate of reaction increased with increasing NaOH concentration and they used up to 40% aqueous NaOH solution. At low concentration, hydrolysis of wood components occurred. Hon and Ou also observed a significant effect of temperature on the benzylation reaction. The rate of reaction increased with increasing reaction temperature; benzylation could not be carried out at temperature below 60-70<sup>0</sup>C.

Density of the benzylated wood decreases with increases of WPG, due to the introduction of the large substituents into the cell walls. Wood materials may also be damaged during benzylation due to NaOH pretreatment. Glass transition temperature and activation energy decreased with increased WPG. Hon and Ou (1989) report that thermoplasticized woods were easily molded or extruded (by simply heating and pressing), which exhibited good mechanical strength for possible structural engineering applications. The researchers also reported that lignin inhibits benzylation. Products of the benzylation reaction were required to be washed with water and organic solvent such as methanol in order to remove by-product and residues of benzyl chloride respectively.

Kiguchi (1990a,b) prepared hot-melted wood surfaces by liquid phase benzylation and then by hot-pressing at 160<sup>0</sup>C. The hot-melted surfaces had high

levels of glossiness and showed good resistance to water, but the UV resistance was very poor.

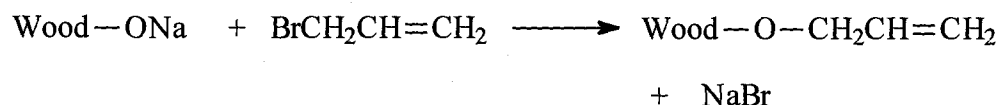
Kiguchi (1990b) prepared self-bonded particleboard from benzylated wood chips by hot pressing, without using any binder and reported good bending strength, as compared with commercial higher density particleboard. Water resistance and dimensional stability were also improved. Kiguchi and Yamamoto (1992) found that flexural strength of the self-bonded particleboard made from benzylated wood chips increased with increasing thermoplasticity of the wood but was a little less than the particleboards made from untreated wood chips and phenol-formaldehyde. Self-bonded particleboards made from benzylated wood chips with WPG more than 38, showed higher dimensional stability and decay resistance than PF bonded controls. The internal bonding strengths (IB) increased with increasing WPG and at about 51 WPG the IB of the benzylated particleboard was about two times that of the conventional one.

Benzylation of wood particles by the vapor phase method was examined by Kiguchi (1993) who observed that greatly thermoplasticized particles were produced in the vapor-phase benzylation below the boiling of benzyl chloride ( $140^{\circ}\text{C}$ ) after 2-4 hours.

### 2.5.2.3. Allylation

In allylation, before reaction, wood materials are pretreated with NaOH.

Allylation occurs when wood materials are treated with allyl chloride or allyl bromide as follows:



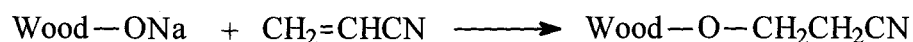
Kenaga and Sproull (1951) carried out the first work on allylation with allyl chloride in pyridine. They observed high initial ASE which was, however, lost after wet and dry cycling. Risi and Arseneau (1957) reported that the high ASE affected with allyl chloride in pyridine is not due to the formulation of allyl ether bonds with wood chemical components, but rather by the bulking with water soluble polymer allyl pyridinium. This would explain the poor water resistance of the product. Recently, Kiguchi (1990b) and Ohkoshi (1990) allylated wood blocks and wood chips with allyl bromide at 50-70<sup>0</sup>C after pretreatment with 10-50% NaOH. They reported that it was possible to bond allylated surfaces by hot pressing without using any adhesives. Kiguchi (1990b) also reported a lack of ultraviolet-ray resistance of the allylated surfaces.

Ohkoshi (1990) reported that the observed thermoplasticity is not due to the allylation but due to the high temperature and pressure during pressing. The thermoplasticity also varies the concentration of NaOH, pretreatment temperature and time and the pressing temperature. Ohkoshi also observed that the maximum

shear strength of the hot pressed bonded specimens was approximately equal to the shear strength of solid wood.

#### 2.5.2.4. Cyanoethylation

Reaction between wood and acrylonitrile results in cyanoethylated material. This reaction is catalyzed by alkalines such as sodium hydroxide. NaOH (aqueous solution) pretreatment gives good results.



Goldstein *et al.* (1959) reported that at a weight gain of 25%, cyanoethylated wood is highly dimensionally stable and decay resistant but had lower impact strength. Baechler (1959) treated wood with acrylonitrile in the presence of ammonium hydroxide catalyst. At WPG of 26, the ASE reported is 80 percent. After hot water extraction of the cyanoethylated wood, leached cyanoethylated wood blocks lost their dimensional stability and decay resistance. This may be caused by the reaction between ammonia and acrylonitrile to produce water soluble polymers.

Morita and Sakata (1986) pretreated wood with NaOH solution in the presence of the swelling agents NaI or NaSCN and then treated the pretreated wood with acrylonitrile. It was reported that cyanoethylation imparts thermoplasticity to wood and it was observed that the "flow temperature" is about 250°C. Morita and Sakata also observed lowering of flow temperature by chlorine solution post-



treatment of the cyanoethylated wood due to the plasticizing effect of chlorine solution on lignin.

Hon and San Luis (1989) reported that the softening temperature of cyanoethylated wood decreases with increase of N content. Kiguchi (1990b) found that the surfaces of hot-pressed (at 160<sup>0</sup>C) cyanoethylated wood blocks had very poor water resistance. This may be caused by the formation of amides in the hot press. More recently, Yamawaki *et al.* (1991) found auto adhesion of thermally melted cyanoethylated fibers by hot pressing at 240<sup>0</sup>C. They also found that chlorination of the cyanoethylated fibers enables pressing temperature to be reduced to about 130<sup>0</sup>C. Kiguchi (1990a) reported cyanoethylation of wood blocks imparts thermoplasticity to their surfaces and good resistance to ultraviolet light.

#### 2.5.2.5. Modification with maleic acid-glycerol mixture

Fujimoto *et al.* (1989) developed a new technology in the area of dimensional stabilization of particleboard. The chemical used in this treatment is called MG, which means a mixture of maleic acid and glycerol. The researchers treated wood flakes by spraying MG aqueous solution of different concentration to obtain 10% WG (as chemical) based on the oven-dry weight of the wood. The flakeboards made from flakes treated with MG were pressed at 210<sup>0</sup>C for 15 minutes with 6% PF. The thickness swelling of MG treated particleboard was found to be about 1/4 to 1/5 that of untreated particleboard. The mechanical properties, especially IB and MOE, of MG-treated particleboard were superior to

the control. Fujimoto *et al.* (1989) also suggested that MG-treatment fix the deformation of the wood, which is the main cause for the dimensional stability. The other causes are binder effect and water repellent effect of MG.

Fujimoto *et al.* (1991) reported that it is possible to improve the dimensional stability of the MG treated particleboard further by increasing the hot-press temperature, which indicates the cost for chemicals can be reduced by increasing the hot-press temperatures. Fujimoto (1992) also applied MG treatment to wood blocks. He treated them with 10-30% aqueous/ methanolic MG solution followed by heating at 160<sup>0</sup>C for 5 hours. In wet-dry cycle tests, MG treated blocks showed excellent ASE. In an outdoor exposure test, MG treated blocks retained their surface smoothness, which means that MG treated wood blocks are photo-stable.

#### 2.5.2.6. Methylation

The simplest ether, methyl ether is produced by the reaction of wood with dimethyl sulphate in the presence of NaOH or with methyl iodide in the presence of silver oxide (Rudkin 1950, Narayanamurthi and Handa, 1953). Methylation increases photostability but decreases mechanical properties (due to severe reaction condition) and no further studies have done with methylation.

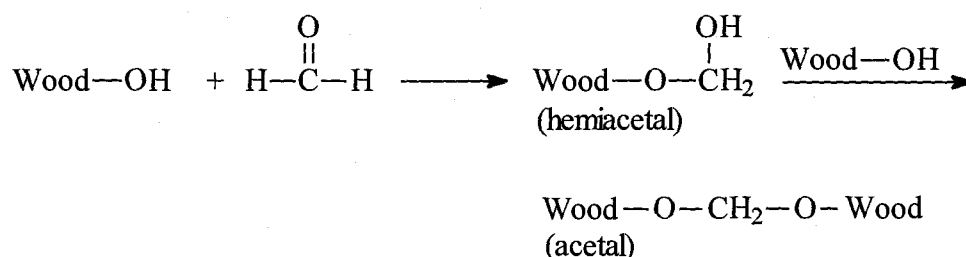
### 2.5.3. Acetyls formation

Acetyls are formed by reactions of aldehydes with wood hydroxyl groups.

Cross-linking may occur between hydroxyl groups on the same or different cellulose, hemicellulose, and lignin polymers.

#### 2.5.3.1. Formalization

Formalization occurs when wood cell wall hydroxyls react with formaldehyde (FA), as follows:



The reaction is also referred to as a cross-linking one and catalyzed by strong acids, such as HCl, HNO<sub>3</sub> (Tarkow and Stamm, 1953), zinc chloride (Stamm, 1959).

Tarkow and Stamm (1953) carried out the first work on formalization of wood with formaldehyde vapor in the presence of an acid catalyst. In this mechanism, small amounts of chemical addition impart large reductions in swelling. Tarkow and Stamm (1953) observed a 60% ASE at 5.5 WPG, while a weight gain of 7% showed a 90% ASE of wood (Tarkow and Stamm, 1953; Stamm, 1959). Stamm and Baechler (1960) reported that a WPG of 2 is enough to resist fungal attack.

Tarkow and Stamm (1953), and Stamm (1959) observed that reduction of the mechanical properties in formaldehyde treated wood may be due to the hydrolysis of cellulose. The wood becomes brittle after the treatment, which may be due to the short, inflexible cross-linking of the -O-C-O- linkage. Minato and Yano (1990) reported that the reduction in mechanical strength can be minimized by carrying out the formalization with formaldehyde vapor in the presence of SO<sub>2</sub> as catalyst.

Akitsu *et al.* (1991) found that vibrational properties of wood can be improved by formaldehyde treatment. Akitsu *et al.* (1993) reported that this improvement is due to the dimensional stabilization of the wood and reduction in internal friction. Improvement of dimensional stability of medium-density fibreboard has been found with vaporous FA treatment (Minato *et al.* 1992). SO<sub>2</sub> catalyzed tetraoxame gave the highest ASE (> 60%).

#### 2.5.3.2. Non-formaldehyde cross-linking

The other aldehydes used for cross-linking are non-formaldehyde reagents such as glyoxal, glutaraldehyde, and dimethyloldihydroxyethyleneurea (DMDHEU). Nicholas and Williams (1987) treated wood with a 10-20% aqueous solution of dimethylolethyleneurea in the presence of an aluminum chloride and a tartaric acid catalyst and observed only up to 60% ASE without any impaired to mechanical properties. Militz (1993) also reported about 50% ASE for dimethylolethyleneurea treatment but he did not notice any significant decay

resistance. Minato and Yasuda (1992) observed that treatment with DMDHEU did not result in sufficiently high ASE but treatment with glyoxal and glutaraldehyde showed up to 70% ASE.

#### 2.5.4. Treatment of wood with ammonia

##### 2.5.4.1. Introduction

On the basis of the solvent properties of liquid ammonia, Schuerch (1952) suggested that liquid ammonia should be able to penetrate the lignin fraction of plant cell walls. Stamm (1955), using thin sections of softwoods and fiberboards, was the first researcher who recognized that ammonia can cause plasticization in wood and also reported that liquid ammonia swelled wood to a much greater extent than does water. Schuerch (1963) conducted a more comprehensive study of plasticizing wood with liquid ammonia and was able to show that, indeed, wood can be effectively plasticized and quite easily formed into a variety of shapes. Schuerch also observed that the formation of new shapes were much easier and permanent when plasticizing with ammonia than plasticizing with steam. Davidson (1968) reported that plasticization of wood was possible by treating the wood with gaseous anhydrous ammonia at room temperature under an ammonia vapor pressure of 0.99 MPa (145 psi). Davidson also mentioned that the presence of moisture (about 10-12%) in the wood enhanced the rate of sorption of ammonia from the gas phase.

In many ways, the action of ammonia on natural fibers is similar to that of water or steam except that it appears to be a more effective plasticizer. The work of Bariska *et al.* (1969) demonstrated some similarities between the sorption of ammonia vapor by wood and the sorption of water vapor by wood. Weight percent gain with ammonia is generally higher than with water. We know the molecular weights of ammonia (17) and water (18) are almost the same. The higher weight gain with ammonia than with water is a clear indication that more wood substance is taking part in the sorption process.

Bariska *et al.* (1969) and Davidson and Baumgardt (1970) also reported that plasticization of wood was possible by treating the wood with gaseous ammonia, when the relative vapor pressure of the gaseous ammonia was close to saturation. Schuerch (1964) reported that cell wall collapse and deterioration of the molded product may occur at high levels of plasticization.

#### 2.5.4.2. Effect of ammonia on wood

##### 2.5.4.2.1. *Chemical changes*

Schuerch (1963, 1964) suggested that the chemical effect of anhydrous liquid ammonia on wood during the plasticizing process is generally mild although Kalninsh *et al.* (1967) reported that some chemical changes may occur.

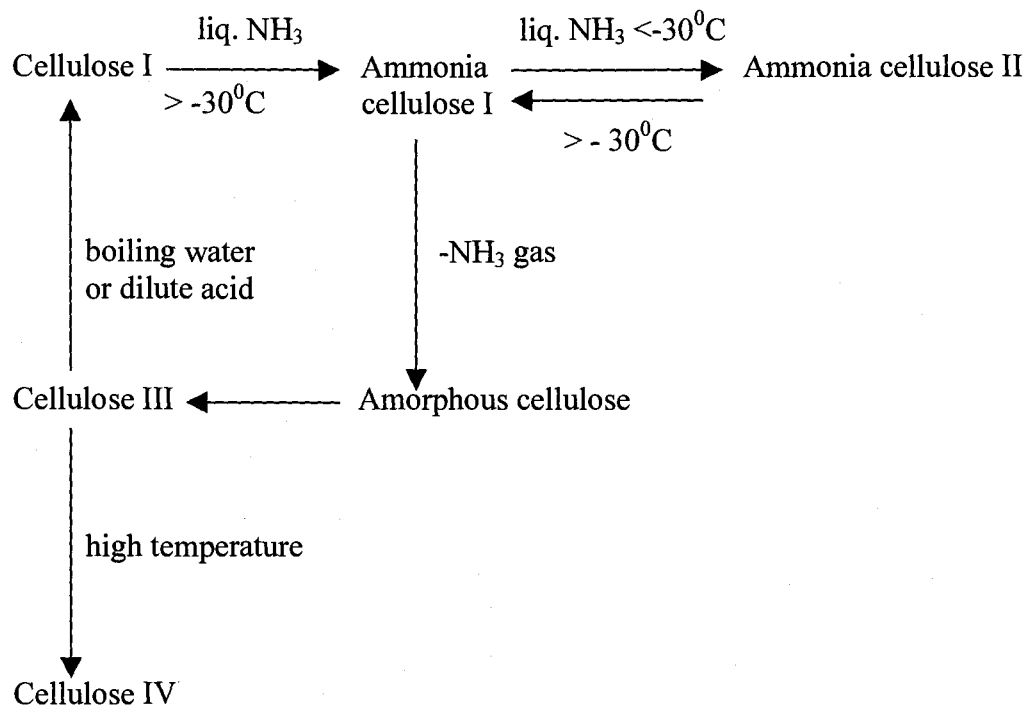
The general mechanism of the plasticizing process is that ammonia breaks the hydrogen bonds within both amorphous and crystalline regions of the

carbohydrate portion of the cell wall and within the lignin fraction of the cell wall. This allows polymers to flow over one another. After removal of ammonia by evaporation, new hydrogen bonds form at new locations. In this way, a new cross-linking structure occurs, which result a substantial level of permanent set.

Barry *et al.* (1936) reported that liquid ammonia not only swelled the amorphous regions but also penetrated into the crystalline regions of the cellulose and thereby forms an ammonia cellulose crystal structure. The distinguishing feature of the liquid ammonia treatment is the penetration and relaxation of the cellulosic crystal lattice. Liquid ammonia reacts strongly by an acid-base reaction with cellulose hydroxyl groups, but it is too small in size to dissolve the cellulose, although through its penetration into crystallites the distances between the chain increases.

Schuerch (1964) presents the following diagram for the crystal lattice changes that occur in the cellulose-ammonia systems. This is based on the work of Howsmon and Sisson (1954).

It appears from this diagram that a plasticized state is obtained upon treating the cellulose with liquid ammonia at a temperature above  $-30^{\circ}\text{C}$  and subsequent removal of the ammonia. Depending on how the ammonia is exchanged, three different crystal lattices are obtained. These are cellulose I, III, and IV. According to Schuerch (1964), a treatment of 15 minutes in liquid ammonia is needed for cotton in order to reorganize 70% of the macromolecular structure of cotton while 4 hours are needed for a complete rearrangement. This rate may be an indication of



chemical reactivity rather than the limited diffusion in wood. It appears that both of the treatment conditions such as temperature and duration, as well how the fibers are subsequently treated, critically affect the structure of the crystal cellulose lattice that is derived.

Based on the work of Yan and Purves (1956), Schuerch (1964) has written that when hemicelluloses are treated with liquid ammonia for about five hours at 25°C, then they undergo deacetylation and acetamide formation. Ammonium salts or amides may be formed by conversion of uronic acid groups. The effect of these changes to the macromolecular structure of wood is relatively small and can be minimized by lowering the temperature. Reorientation of hemicelluloses in the cell wall may occur due to their solubility, but the loss is very small because it is



difficult to diffuse out of large pieces. In the case of fibers, their rate of diffusion out may be higher and the loss may increase with increasing temperature.

Kalnins et al. (1967) reported that when wood is treated with 25% ammonia solution, then a portion of the carbohydrate-to-lignin bonds are broken and free active groups of lignin become available. Subsequently, the lignin recondenses. Chemical changes clearly influence physical properties; lignin becomes plastic by swelling with ammonia.

Schuerch (1964) suggested that there are significant amounts of tackiness of the lignin-liquid ammonia system at temperatures below room temperature. Generally, lignin does not show tackiness or softness below about 130°C (Biermann 1993).

Schuerch and Davidson (1971) have also observed color changes in wood when treated with anhydrous ammonia. These may be due to a number of chemical reactions. According to Schuerch and Davidson (1971), oxidation of hydroquinones or phenols may result in the formation of quinoidal structures. Further, moisture content of wood has a great influence on the color change by ammonia treatment; greater extent of color changes observed with higher moisture content.

#### *2.5.4.2.2. Morphological changes*

According to Erinsh and Odintsov (1967), when wood is treated with aqueous solutions of ammonia, the internal surface area and void volume increases. This suggests that significant changes occur in the submicroscopic structure and

capillaries in the cell walls. Treatment with aqueous solutions of ammonia at concentrations above 20% can cause breaking up of the microfibrils into finer elementary fibrils; these are able to move relative to one another when subjected to external stresses. Associated changes in properties will be considered below.

#### *2.5.4.2.3. Physical and mechanical property changes*

Bariska (1975) observed collapse of wood after ammonia treatment and drying, due to the reduction of the volume of the cell lumina and the partial reduction of the pore volume of the cell walls.

Tangential and radial swelling and density of wood are increased by liquid ammonia treatment. At the same time, the hygroscopicity decreases (Mahdalik *et al.* 1971). Bending strength and tensile strength increase only slightly, where as toughness decreases with liquid ammonia treatment. Such increases in strength may be due to enlargement and associated increases in bulk properties of samples (rather than increases in material properties). This inference is supported by the work of Mahdalik *et al.* (1971). Ozo-insh and Yukna (1967) observed about 15 to 20% reduction in the ultimate strength of unpressed birch wood during static bending and compression along fibers after treatment with ammonia solution in room temperature (at 20<sup>0</sup>C). According to Bariska and Schuerch (1977), when wood is saturated with ammonia, it shows a large time-dependent plastic deformation and creep with stress but the amount of elastic deformation is comparatively little

compared to normal wood. Best results can be obtained by deforming the ammonia-saturated wood slowly and/ or intermittently.

#### 2.5.4.3. Application of ammonia in wood-based composites manufacture

Shaines (1970) bonded a decorative paper overlay to a wood substrate by impregnating the paper sheet with liquid ammonia and applying pressure up to about 20.5 MPa and temperatures up to 148<sup>0</sup>C. Graf *et al.* (1971 and 1972) reported the production of boards and moldings from ammonia treated wood particles, sawdust or pulp without using any adhesives. Boards so produced by compressing and heating to high temperatures have mechanical properties that resemble those of conventional resin bonded boards. However, the specific gravity of the boards made from ammonia-treated materials is about twice that of the conventionally resin bonded boards (Graf *et al.*, 1971 and 1972).

#### 2.5.5. Selection of candidate chemical treatment methods for the sealed pressing system

It has already been pointed out in Section 1.3 that one of the aims of this research is to select viable chemical reactants which will stimulate desirable transformations of fibers within a network during pressing in the sealed pressing system, and to demonstrate that the sealed pressing system might be used simultaneously for chemical treatment and pressing. The desirable transformations

within the fiber networks are plasticization, adhesion and, if possible, dimensional stabilization.

Some chemical treatments result in auto-adhesion of fibers within the network under the influence of heat and pressure but other chemical treatments do require application of adhesive as a binder. Interaction of some adhesives with some treating chemicals is a problem in one-step treatment and pressing processes. For that reason, epoxide treatment or treatment with non-formaldehyde cross-linking agents is not achievable before PF (resole) adhesive cure. However, epoxide treatment is possible with novolak type PF adhesive.

Another requirement of the chemical treatment sequence to be used is that a single temperature must be applicable at all of the stages of treatment and pressing sequence. It is not yet feasible to affect rapid temperature changes in the sealed pressing system. Such provisions may, however, be feasible in future enhancements.

It was pointed out in Section 2.5.2.2 that benzylation of NaOH pretreated wood with benzyl chloride effectively imparts thermoplasticity to lignocellulosic materials, and thereby auto-adhesion at high temperature (about 200<sup>0</sup>C) and pressure pressing. However, products of benzylation must be washed with water and an organic solvent (such as methanol) to remove byproduct NaCl and residues of benzyl chloride respectively. Such washing would be difficult in the sealed pressing system since it is designed to operate with gases and not liquids. As for benzylation, allylation of NaOH pretreated wood with allyl chloride or allyl

bromide also produces the same byproducts. Acetylation with acetic anhydride is another very good chemical modification method for imparting dimensional stability and bio-resistance to lignocellulosic materials (discussed in Section 2.5.1.1); it does, however, release acetic acid as a byproduct. Due to the non-removability of the byproducts, treatments like benzylation, allylation, and acetylation are not, therefore, appropriate for the sealed pressing system.

From the above discussion, it seems that treatment with diisocyanate, acrylonitrile, formaldehyde and ammonia in the sealed pressing system might be possible. However formaldehyde, acrylonitrile, and monomers of isocyanates are toxic chemicals. Extra precautions are required from the starting point of the in-let to the end point of the out-let in the sealed pressing system. In future developments of the concept, however, these chemicals may be viable since the system is sealed. It should be noted that isocyanates (urethanes), though toxic, have considerable potential for future use.

Treatment with gaseous ammonia (for plasticization of the wood cell wall materials) appears, from the above literature review, to be is one of the easiest and simplest treatment methods to adopt. It may also be appropriate to demonstrate that the sealed pressing system may be used simultaneously to affect chemical treatment and pressing of mats. Ammonia treatment has been found, in the present research, to be particularly interesting because of its new found effects on PF adhesives. The interaction of ammonia with PF adhesives is, therefore, discussed below.

## 2.6. Curing behavior of alkaline catalyzed phenol-formaldehyde (PF) adhesives

In the absence of a convenient means of transporting an adhesive system into the fiber mat during pressing, and considering that  $\text{NH}_3$  may be used as a softening agent, adhesive must be added before mat formation. The following discussion explores the use of alkaline catalyzed PF adhesives.

PF resins of very high alkalinity (pH's between 10 and 13) are generally used in wood-based composites to avoid acid hydrolysis of the lignocellulosic materials.

It is also well established and accepted that the curing rate of PF (resole) resins accelerates at very high pH i.e. (Pizzi, 1983; Skeist, 1977). This is due to an increase in the functionality of phenolic nuclei as nucleophiles, which is a consequence of the ionization of the phenol to the phenate ions as shown in Figure 2.6. The effect of pH on the curing rate of PF resins is well established as shown in Figure 2.7. The solid line in the figure up to pH 9 is experimentally verified data. The dashed line for pH values above 9 indicates extrapolated or assumed behavior of PF (resole) adhesives. However, until recently there was no experimental verification of this trend in the literature regarding the reactivity of PF (resole) resins over a pH of 9. Pizzi and Stephanou (1994a) measured the reactivity of PF (resole) resins beyond pH 9 and their important findings are considered below in Section 2.6.1. This information is important because we are considering that gaseous  $\text{NH}_3$  may be used to soften the mats of fiber-PF (resole) mixtures.

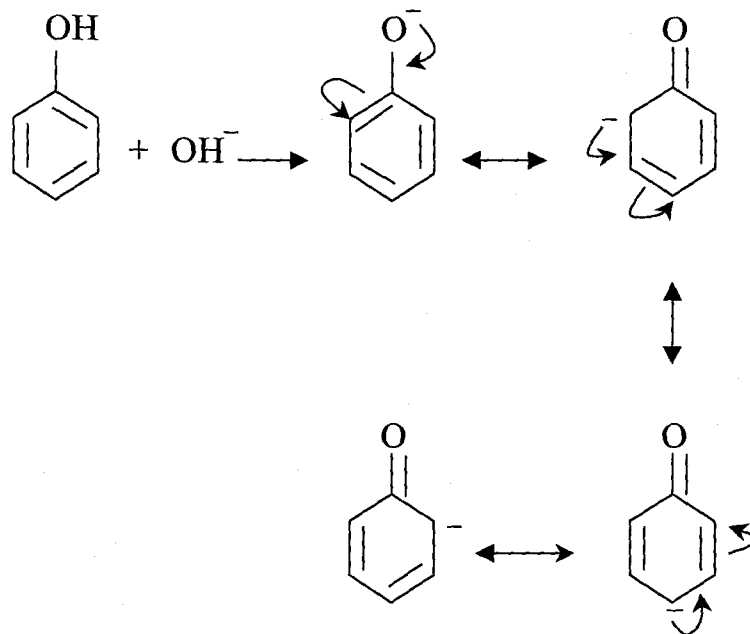


Figure 2.6 Ionization of the phenol to form phenate ions.

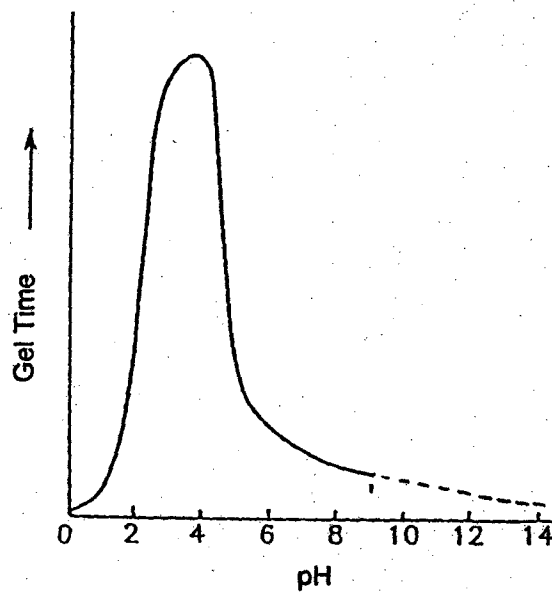


Figure 2.7 Gel time versus pH curve of PF resin. The dashed line indicates extrapolated assumed behavior (from Pizzi and Stephanou, 1994a).

### 2.6.1. Curing behavior of PF resin under very alkaline conditions

Pizzi and Stephanou (1994a) found that under very high pH conditions, the reaction and curing behavior of PF resin is unexpectedly very different from that previously assumed. They reported that the curing rate of PF resin slows down markedly beyond a pH of 9, instead of accelerating as previously assumed. This effect is demonstrated in a reproduction of Pizzi and Stephanou's graph (Figure 2.8).

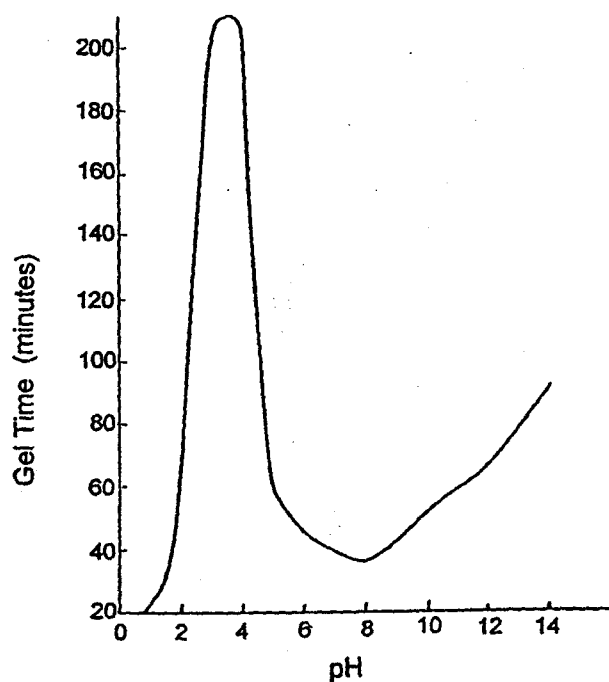


Figure 2.8 Experimentally derived gel time versus pH curve of a PF resin over a very wide pH range (from Pizzi and Stephanou, 1994a).



### 2.6.2. Acceleration of the curing of alkaline catalyzed PF (resole) adhesive

In the foundry industries, very alkaline PF resins are used to bind sand. Esters such as propylene carbonate, methyl formate and glycerol triacetate, are added in the liquid (called  $\alpha$ -set) or vapor phases (called  $\beta$ -set) to accelerate the rate of curing of the resin at room temperature (Lemon, 1990).

Pizzi and Stephanou (1994b) applied this concept to alkaline resol PF resins used in wood-based composites. Gel times of the resins were measured at 94<sup>0</sup>C after addition of 2.5%, 5%, 7.5% and 10% by mass (based on solid content of the resin) of methyl formate, propylene carbonate, glycerol triacetate and phenyl acetate at pH 11.26. It was found that with increasing addition of an ester, curing speed increased correspondingly as shown in Figure 2.9.

Propylene carbonate (boiling point 87<sup>0</sup>C) stimulates very fast curing at relatively low concentrations, but at higher concentrations the effect decreases. Another ester, methyl formate (MeF) also shows very good curing acceleration and has a lower boiling point (33<sup>0</sup>C). A degree of volatility is necessary for use in the sealed pressing system. Methyl formate is therefore a strong candidate.

According to Pizzi and Stephanou (1994b), acceleration of the curing of PF resin by esters is due to an increase in the number of cross-linking sites in the PF resin. Fragments from the dissociation of ester provide different, and additional, cross-linking than that of methylene linkages in unaltered PF-resins. Pizzi and Stephanou suggested a number of possible reasons for acceleration of the curing of PF resin by esters. Those are listed in turn below.

- I. The presence of the equivalent of another tri-functional reagent (compared to di-functionality of formaldehyde instance);
- II. A phenolic nucleus on which a methylol group is already present may change from a tri-functional to at least a tetra-functional reagent (or even more functional if more than one propylene carbonate reacts);
- III. Higher concentrations of reagents (the ester being a proper reagent as shown in Figure 2.10 and not a catalyst).

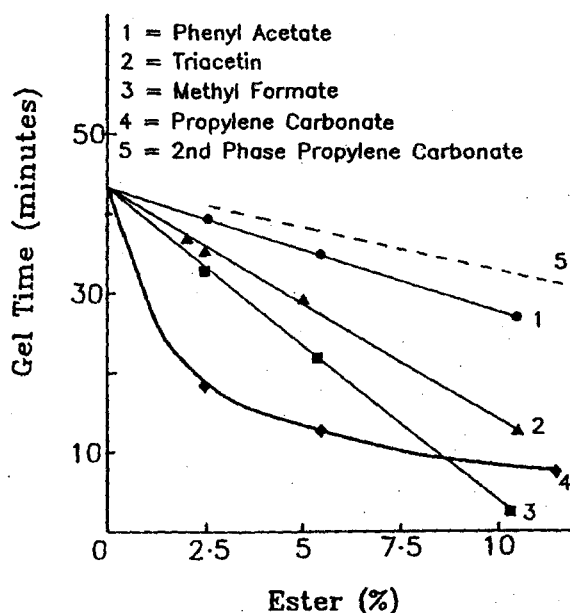


Figure 2.9 Dependence of gel time of a PF resin at pH 11.26 on percentage and type of ester added (from Pizzi and Stephanou, 1994b).

Other esters may also follow the above mechanism but, due to their lower functionality, their reactions will be slower than that of propylene carbonate.

Pizzi and Stephanou (1994b) made particleboard by using triacetin-accelerated PF-resins and found excellent internal bond strength even when hot pressed at press times as low as 2.5 minutes.

From the above discussion, it is clear that resole PF resins are very stable at high pH. It may, therefore be possible to treat fiber-PF (resole) mix with gaseous ammonia for softening the fiber mats without stimulation of resin cure. Ammonia is a weak base. It is assumed that it would not bring any big change in the pH of the

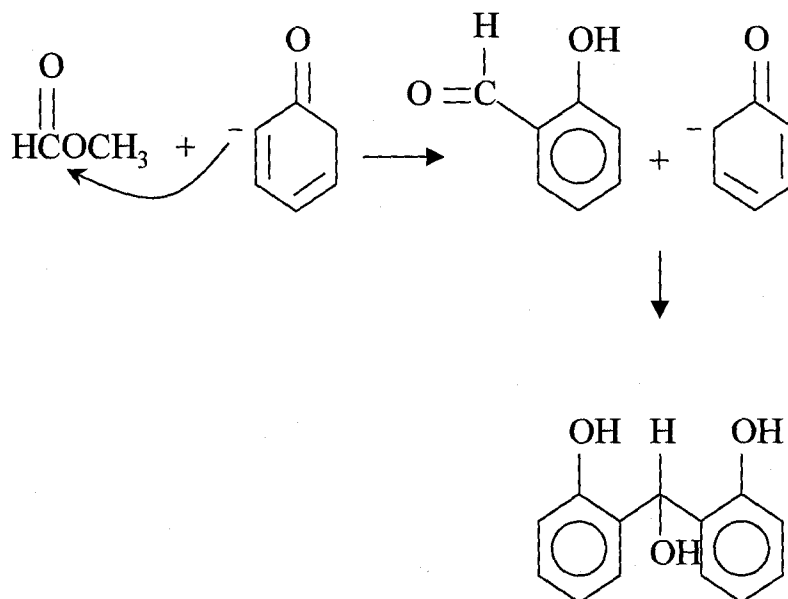


Figure 2.10 Reaction between ester and phenolic nucleus shows ester acts as a reagent.

resin in the mat. After ammonia treatment, it may therefore, be possible to accelerate the curing of PF resin in the mat by injecting MeF vapor.

## 2.7. Sealed pressing systems

The concept of sealed pressing was first introduced in the literature by Shen (1973 and 1975) when used for the injection of high pressure steam into PF bonded particleboard. Shen designed a pressing system with specially designed press platens and a sealing frame, by which he was able to inject and remove steam from both upper and lower platens. Each platen, of size 610 x 610 x 127 mm, had a closed steam heating system within them and a steam injection system (manifolds) near the surface as shown in Figure 2.11. Manifolds were 76.2 mm apart and 12.7 mm below the platen surface. A number of perforations 2.38 mm in diameter and

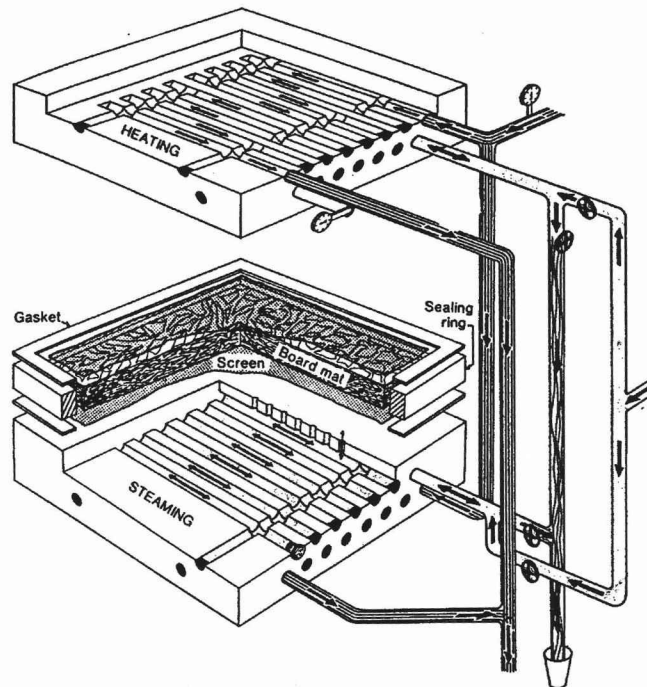


Figure 2.11 Sealed steam press (from Shen, 1973).

12.7 mm apart were in rows on the platen surfaces. A frame made from steel plate was used for peripheral sealing; this also served as a stop between the press platens and determined the final thickness of the board. Asbestos gaskets were used between the sealing frame and the press platens to make the system enclosed during final pressing. Shen also reported that injection of steam through both platens affected an improvement in heating uniformity

Similar to Shen's sealed steam injection pressing system, Thoman and Pearson (1976) designed and developed another sealed steam injection press. The platens were 508 x 457 mm in size and consisted of 5 steam injection and heating channels. The channels were 12.7 mm in diameter and 76.2 mm apart from each other and consisted of 30 perforations of 2.38 mm diameter and 12.7 mm apart. Thoman and Pearson examined the effect of steam injection on selected strength and physical properties of particleboard made in their designed pressing system.

Ren and Humphrey (1999) designed and developed a special cylinder and piston type sealed pressing system to quantitatively study the thermo-hygro rheological characteristics of furnish materials used in the manufacture of wood-based composites. A sealing 'o'-ring was used at the periphery of the upper part of the piston to provide an enclosed system with the cylinder portion of the press. At the circumference of the cylinder portion, there were holes to supply vapor of specified temperature and humidity through the edge of the sample and also to measure the internal vapor pressure and temperature.

### CHAPTER 3. EXPERIMENTAL OBJECTIVES OF THIS RESEARCH

The main approach of this research is to consolidate pre-formed fiber networks in a specially developed sealed pressing system under highly controlled (dynamic) chemical, thermal and mechanical (stress) conditions. Reactants will be transfluxed through the porous matrix of fibers in the vapor phase. This will be done in such a way as to trigger a desirable range of reactions to stimulate localized softening followed by adhesion and, finally, dimensional stabilization.

Before identifying the specific experimental objectives, the essential consequences of the earlier analysis of chemical modification issues will be briefly stated below.

The limited number and types of sealed pressing systems developed to date were reviewed in Chapter 2. It is clear from that review that it is impossible to adapt any existing equipment to conduct chemical vapor treatment and pressing of the pre-form fiber network *in situ* with highly controlled chemical and thermodynamic conditions. A pressing system will therefore be developed.

A wide range of chemical treatment methods for property enhancement of wood were analyzed in Chapter 2. This was with the aim of developing viable chemical treatment methods which will stimulate desirable transformations of fibers within a network during pressing in the sealed system. From the analysis, it seems that treatment with isocyanate, epoxide, acrylonitrile, formaldehyde and ammonia might be conducted in the sealed pressing system. Treatment with

gaseous ammonia was found to be one of the easiest and simplest treatment methods to demonstrate that the sealed pressing system may be used to simultaneously affect chemical treatment and pressing of mats.

Adhesives used to bond wood-based composites were briefly discussed in Chapter 2. Two widely used adhesives in wood-based composites are amino (urea formaldehyde) and phenolic (phenol formaldehyde) resins. Use of urea formaldehyde (UF) resin is somewhat limited in wood-based composites due to the lack of water resistance and emission of carcinogenic formaldehyde. However, the significant and increasing use of MUF (melamine urea formaldehyde) and urethane adhesives (particularly in Europe) must not be overlooked. Phenolic adhesives have, however, been selected for the present work.

Alkaline catalyzed PF resins (resoles), generally at pHs of 10 to 13, are used in the US wood-based composites to avoid acid hydrolysis of the lignocellulosic substrate (Pizzi and Stephanou, 1993). It has been well established that the rate of curing of resole PF resins accelerates with increases in pH. Pizzi (1983) explained that the nucleophilic functionality of phenols is increased by the ionization of the phenol to form phenate ions, without changing the activity of the aldehyde. Literature (Pizzi, 1983; Barth, 1977) has information regarding the gel times (suggesting reactivity) as a function of pH up to a pH of 9. Pizzi and Stephanou (1994a) carried out experiments to determine the gel time of resole PF adhesive as a function of pH at 94<sup>0</sup>C over the entire pH range at a constant solids content of

50%. They reported that the rate of curing of the NaOH-catalyzed PF resin (resole) slows down markedly and unexpectedly above a pH of approximately 9.

Lemon (1990) reported that alkaline phenolic resin at pH of about 12 (called  $\beta$ -set and originally formulated for the foundry industry) cured extremely fast with the injection of methyl formate (MeF) gas. Pizzi and Stephanou (1994b) found that the rate of curing of the PF (resole) resin increasingly accelerates with the addition of esters such as propylene carbonate, methyl formate, and triacetin (glycerol triacetate). They clarified the mechanism of ester acceleration of PF (resole) curing and quantified the effects of different esters. It was also shown that esters do not act strictly as a catalyst but become part of the bond.

Considering all the above facts, the experimental objectives of this thesis were:

- I. Design and construct a miniature laboratory sealed pressing system to demonstrate that it can be used for chemical vapor treatment and pressing of pre-formed fiber networks.
- II. Conduct a qualitative examination of the action (mainly softening) of gaseous ammonia on pre-formed fiber networks in the above sealed pressing system.
- III. In a complementary investigation, to evaluate the effect of  $\text{NH}_3$  and MeF on wood-PF-resin bond strength development rates of small, standardized test bonds formed at room temperature by using an Automatic Bond Evaluation System (ABES). In this way, to observe the likely interaction of  $\text{NH}_3$ , MeF



and PF adhesive in the bond formation process. This study was carried out with a view to qualitatively anticipating the likely response of bonds between fibers in the sealed pressing system.

- IV. Formation trials of composite samples by pressing PF resinated fiber mats with ammonia for expected softening of the fiber cell wall in the above stated sealed pressing system, followed by MeF vapor to accelerate the curing of resin.
- V. Evaluate a limited range of physical and mechanical properties of fiber disk trial samples formed in the sealed pressing system and to consider future potential of the approaches.

## CHAPTER 4. MATERIALS AND METHODS

### 4.1. Introduction

The main concern of this thesis was to consolidate pre-formed fiber networks in a sealed pressing system under highly controlled thermodynamic and chemical conditions inside them. The earlier review of literature shows that no such equipment exists to perform such types of work. An important aspect of this thesis was, therefore, to design and construct a miniature sealed pressing system with provision for sequential chemical gas injection and removal together with control of thermal and mechanical (stress) conditions.

Another objective of this research was to evaluate the interaction of  $\text{NH}_3$ , MeF and PF adhesive in the bond formation processes by using an Automated Bonding Evaluation System (ABES). Here our assumption was that this would provide us with qualitative prediction of the likely response of the bonds between fibers in the sealed pressing system to the sequence of chemicals. For injection of chemicals in the liquid and vapor phases into test bonds, the ABES system was specially modified.

### 4.2. Materials

In this research, wood fibers were selected as the material to be used because they have high specific (density adjusted) stiffness and strength, are

permeable to fluids and are amenable to modification during consolidation. In addition, the cell walls are accessible to, and reactive with, some polar chemicals, and are hygro-thermo-viscoelastic.

#### 4.2.1. Mats from dried fibers

Wood fiber furnish was obtained from the Evanite Hardboard Mill (Corvallis, Oregon). Most of the raw material entering the Mill is plywood mill residues (30-40%), wood chips of virgin wood (30-40%) and urban wood waste (30-40%). The wood fibers consisted of about 60-70% Douglas fir (*Pseudotsuga menziesii*) and 30-40% Hemlock (*Tsuga heterophylla*). These raw materials are defiberated in the mill with a thermo-mechanical defiberator (TMP method). The production conditions within the defiberator are typically 125<sup>0</sup>C, 0.86 MPa vapor pressure, and 50-100 seconds residence time. The fibers for the present research were extracted from the process near to a port of the defiberator and therefore didn't contain any adhesive or wax. The reasons for using these fibers are: (i) they were consistent in supply, (ii) were manufactured in an industrially viable process, and (iii) they were readily available. Having been extracted from the plant at a moisture content (MC) of approximately 70-75%, the fibers were dried in a hot-dry room at 50<sup>0</sup>C and 10% relative humidity (RH) and then conditioned in a standard room at 19 ± 1<sup>0</sup>C and 60 ± 2% RH until constant weight was reached. The MC of the conditioned fibers was 10%.

#### 4.2.1.1. Mat formation for ammonia softening studies

Circular fiber mats of 97 mm diameter were manually formed by sprinkling previously dried fibers into a specially designed cylindrical disk former and then gently pressing manually with a piston. A metered quantity of conditioned fibers was used for each mat. This quantity was selected so that a target density (oven-dry weight basis) of  $525 \text{ Kg/m}^3$  could be achieved after compressing to a thickness of 5.00 mm in the sealed pressing system. In order to separate agglomerations of fibers before mat forming, they were tumbled inside a specially made cylindrical container with variable speed impeller. Mats for the preliminary ammonia softening studies did not include adhesive.

#### 4.2.1.2. Mat formation for sample formation trials

Previously conditioned fibers were used to form circular disks of 97 mm diameter. Quantities of fibers were metered to enable disks with target densities (oven-dry weight basis) of  $550 \text{ Kg/m}^3$  and  $750 \text{ Kg/m}^3$  to be created when compressed to a thickness of 5.00 mm. Liquid resole PF adhesive (see Section 4.2.4) was applied at a rate of 15% based on the oven-dry weight of fibers. Adhesive was sprayed by a single action air spray as the fibers were tumbled inside a container by the agitation action of an impeller to produce a uniform fibrous mix. Considerable effort was devoted to the design of the spraying system in order to maximize adhesive dispersion. This design is explained below. After spraying,

another short period (about 1 minute) of tumbling was continued in order to obtain an even dispersion of the adhesive and also to break up any clumps. The blended furnish was then transferred very carefully and hand formed by sprinkling into a circular disk former and manually pre-pressed with a specially made plunger.

Adhesive spraying system: A single action air spray gun built from parts of a commercial airbrush (type: Badger Mod. 250) was mounted in the lid of the spraying container (Figure 4.1). The container has some minute holes (0.5mm dia.) to allow air to be expelled. A specially designed impeller was also mounted in the lid of the container, the end of which was connected to a variable speed motor. During spraying, the impeller agitated the fibers vigorously for uniform distribution of the resin. The resin was kept in a slightly pressurized container. Air pressure at the spray gun and a slave valve in the feed line for the resin spray were both activated simultaneously by a solenoid pilot valve. Air pressures of 0.20 MPa at the spray gun were used. Variables influencing the spray mist (spray nozzle setting, air pressures etc.) were optimized experimentally to yield the finest spray mist possible and to avoid sputtering. Intermittent operation of the spray gun results in dry out of the liquid resin at the gun. After each batch of spraying, cleaning of the spray gun was therefore usually necessary.

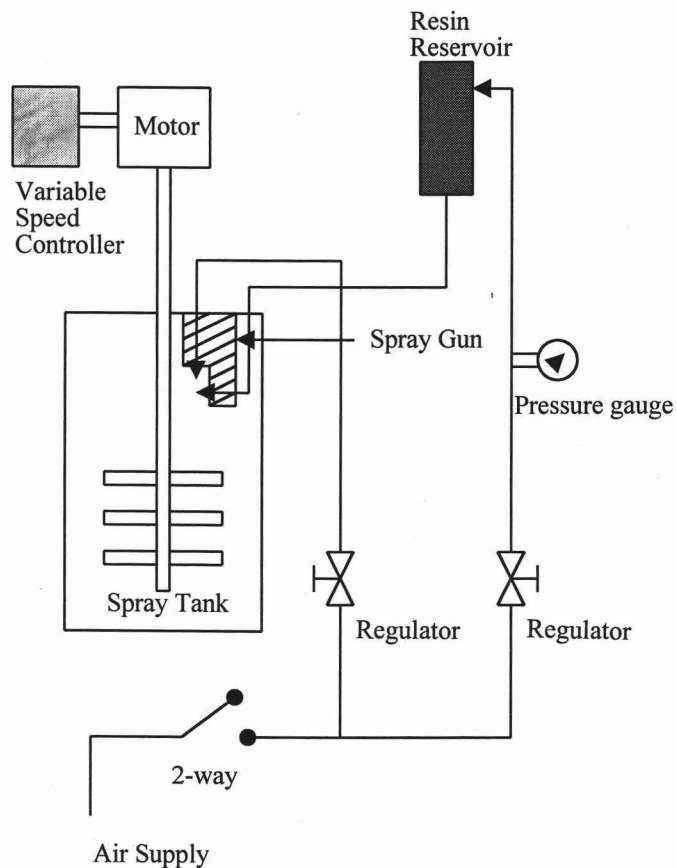


Figure 4.1 Adhesive spraying system.

#### 4.2.2. Fiber mat material for preliminary ammonia softening studies

In addition to fibers, some pre-formed wet fiber mats which are used to make hardboard were also collected the from Evanite Hardboard Mill. The mass of fibers (oven dry basis) per unit area was approximately  $2.8\text{-}2.9 \text{ Kg/m}^2$ . This was done in order to perform some preliminary studies of the softening action of gaseous ammonia (treatment time and treatment temperature) on fiber materials. It was much easier to cut disks from pre-formed mats than to hand form them from

separated fibers. Tests with these disks were preliminary; the viability of pressing techniques with ammonia was confirmed. The main studies were conducted with manually formed disks as above.

Following extraction from the plant the mats were dried in a kiln to a MC of 6% at  $100 \pm 5^{\circ}\text{C}$  and conditioned in the standard room at  $19 \pm 1^{\circ}\text{C}$  and  $60 \pm 2\%$  RH until constant weight has been reached. The final MC of the mats was about 10%. Since these were extracted from the plant immediately before pressing, they did contain additives (1% PF resin and less than 1% cationic wax). Care was taken to kiln dry the mats quickly after extraction from the plant in order to avoid onset of fungal attack. The mats were then cut into circular disks of 95-97 mm diameter with a laboratory band saw and plastic template.

#### 4.2.3. Wood strips for adhesion studies

Sliced maple (*Acer macrophyllum* Pursh) veneers (0.8 mm thick) were cut into strips 25.0 X 120.0 mm and used to evaluate the individual and combined effects of  $\text{NH}_3$ , and MeF on shear strength development rates of phenol-formaldehyde (PF) resin-to-wood bonds. During selection of wood strips, we were very careful about the uniformity among them. These pieces were conditioned at 40% RH and  $21^{\circ}\text{C}$  to a moisture content of 7.6%. No attempt was made to control growth ring orientation on the surfaces of the pieces, although longitudinal cells ran lengthways (in the 120.0 mm direction).

#### 4.2.4. Adhesive

A commercially available alkaline catalyzed phenol-formaldehyde (PF) adhesive of the resole type (pH 12, solid content 50%) was kindly donated by Borden Chemical, Inc. The reasons for selecting this particular adhesive have already been discussed in Chapters 2 and 3.

### **4.3. Experimental methods**

#### 4.3.1. Evaluation of strength development of miniature test bonds

An Automated Bonding Evaluation System (ABES) developed by Humphrey and Zavala (1989) and subsequently improved by Humphrey (1993, 1999) was modified and used to evaluate the effect of  $\text{NH}_3$  and  $\text{MeF}_3$  on wood-PF resin bond strength development. This system is described below.

##### 4.3.1.1. The automated bonding evaluation system (ABES)

The principal functions of the Automated Bonding Evaluation System (ABES) are schematically represented in Figure 4.2. ABES enables the strength development characteristics of a variety of adhesive and adherend combinations to be explored in an accurate and time efficient manner. The system enables the effect of temperature on the strength development rate of thermoset adhesives to be



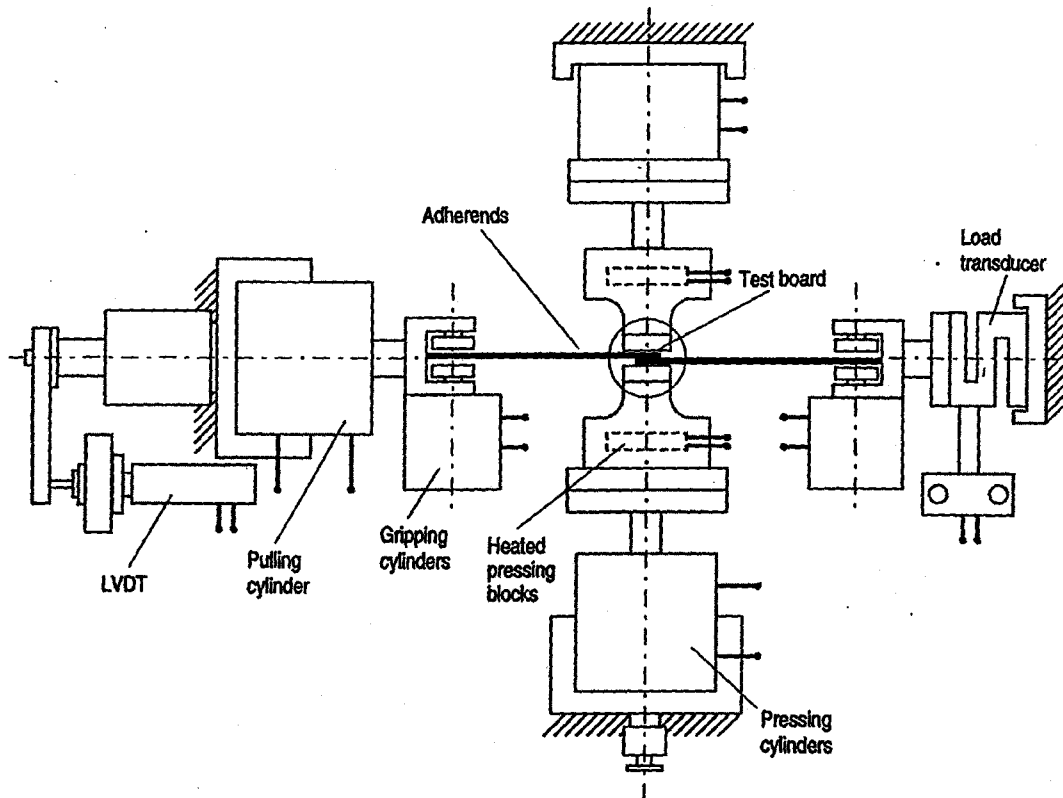


Figure 4.2 Schematic showing principal functions of ABES (from Chowdhury and Humphrey, 1999).

characterized at temperatures ranging from ambient to 200<sup>0</sup>C. ABES may be used to explore many types of bonding system such as thermosets, thermoplastics, isocyanates etc.; it may also be used as a miniature materials testing device to measure tensile modulus and strength of materials. An overview of the main bond forming and testing module of the system is shown in Figure 4.3.

In this system, small adhesive bonds are formed under highly controlled conditions of temperature, pressing load, and time. Almost immediately after each bond is cured to the required level, it is tested to destruction in shear mode. Tensile

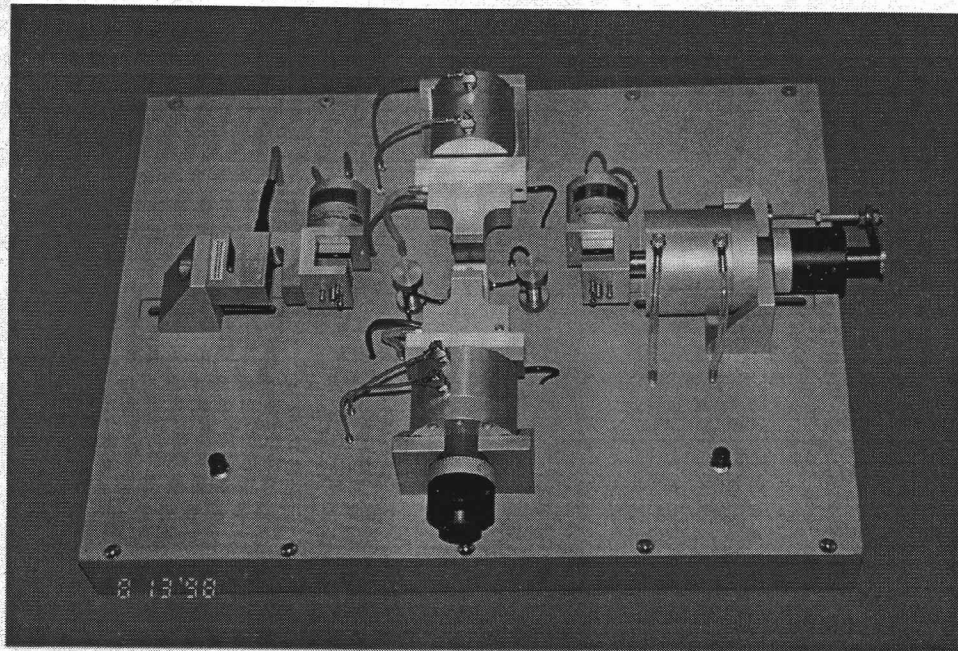


Figure 4.3 An overview of the main bond forming and testing module of ABES.

load and gripping head movement (sample elongation) are monitored digitally during bond pulling, and shear-stress-to-failure (area-corrected peak load) is calculated (Humphrey, 1999).

By using relatively thin adherend strips (typically 0.8 mm for wood bonding studies), a broad range of near-isothermal conditions may be achieved shortly after the beginning of bond forming periods (where the heated blocks close on the overlap). In this way, near-isothermal bond strength development may be achieved shortly after the beginning of bond forming periods (necessary for adhesion kinetics studies).

Repetition of the bond forming and testing procedure for a range of pressing times (while holding temperature constant) enables isothermal bond strength accumulation with time to be plotted. Each point on such a plot therefore corresponds to a similar glue bond that has been cured under controlled conditions of temperature, time and pressure and immediately thereafter automatically pulled to measure its accumulated shear strength. Repeating this procedure for a number of different pressing temperatures enables a family of such isothermal bond strength accumulation plots to be constructed. This data, in turn, enables the reactivity of bonding systems (effect of temperature on rates of isothermal bond strength development) to be explored.

Humphrey (1996) has modified the ABES and made provision for computer controlled cooling of bonds immediately prior to their being pulled. This is achieved with a pneumatically driven and spring-loaded PTFE cooling head (Figure 4.4). This function enables ABES to be used to explore the thermoplastic characteristics of adhesive systems, including those that are predominantly thermosetting. For the present investigation, the PTFE heads have been pressed onto the bond area, and by modifying the PTFE heads, they have been used as a means of injecting chemicals into bonds. Figure 4.5 represents the basic principle of such bond formation with chemical injection as developed in the present research.

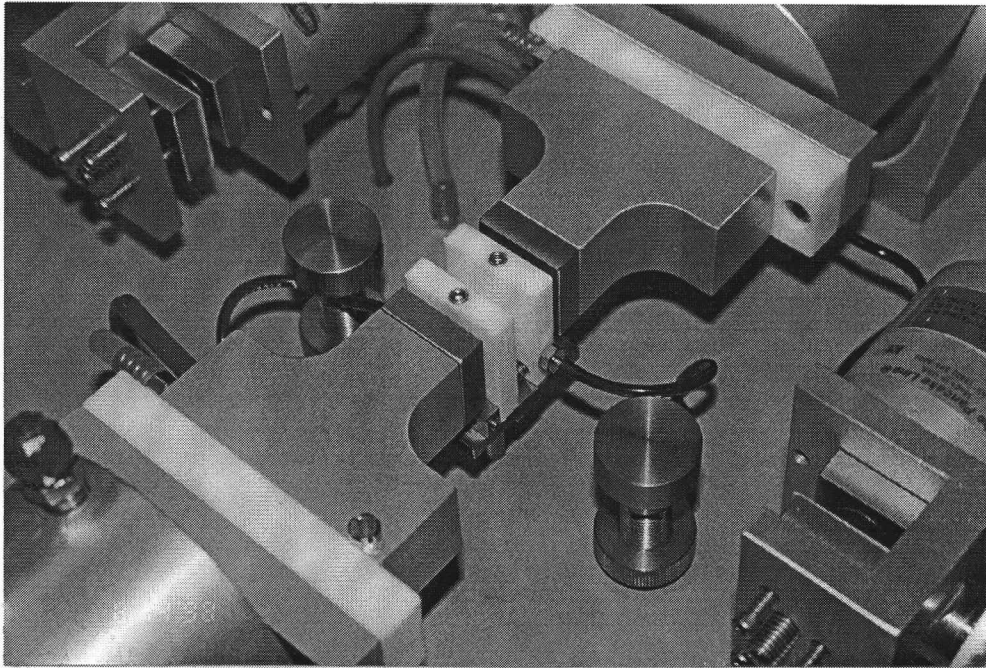


Figure 4.4 A close-up of the bond-pressing zone with bond cooling-head in the elevated position.

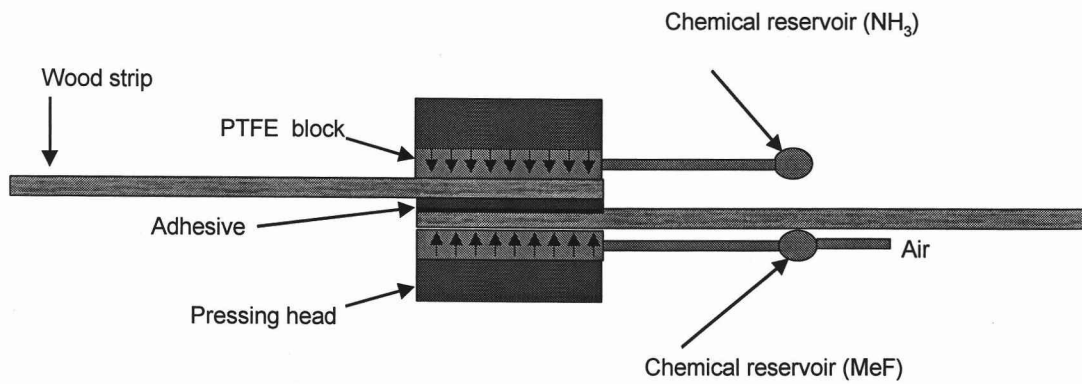


Figure 4.5 Basic principle of bond formation with chemical injection.

#### 4.3.1.2. Refinement of ABES

The ABES was modified in this research as shown schematically in Figures 4.5 and 4.6, in order to inject liquid and/ or vapor in the press during the bond formation processes. For this purpose, the cooling air supply connections to the PTFE blocks were disconnected. One of the PTFE blocks was connected with a miniature chemical (MeF liquid) container and the other PTFE block was connected to a small  $\text{NH}_3$  gas container (volume about  $62.0 \text{ cm}^3$ ) as shown in Figure 4.7. The supply of  $\text{NH}_3$  to the bond was controlled manually by a 2-way valve. Supply of MeF to the bond was automatically computer controlled by air

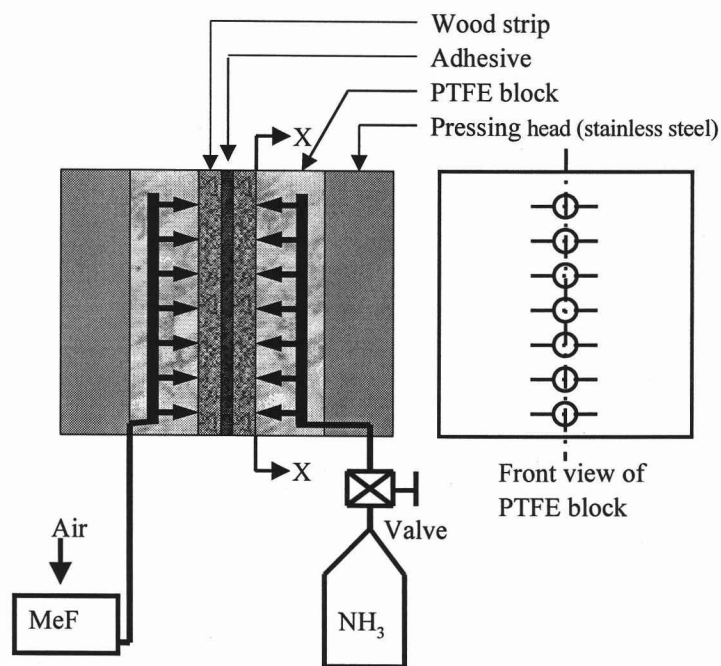


Figure 4.6 Vertical cross-section of the modified pressing heads of ABES.

pressurization of the liquid chemical container. About 62 cm<sup>3</sup> of NH<sub>3</sub> at 0.41 MPa (pressure inside the container) was applied to each of the selected bonds at a 0.14 MPa pressure.

The penetration of NH<sub>3</sub> through the wood to the bondline was sensed in some preliminary trials by putting red litmus paper in between them. Control of

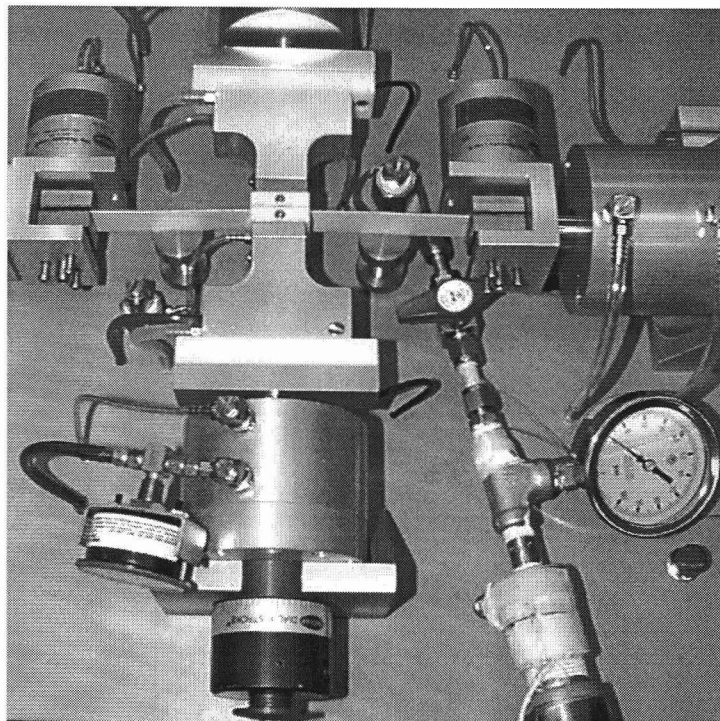


Figure 4.7 A close-up of the bond-pressing zone with sample being injected with chemicals.

the amount of liquid MeF supplied to each of the selected bonds was not sophisticated. Attempts were, however, made to maintain approximately equal quantities of chemical to each of the selected bonds. Approximately 0.25 cc of MeF

was supplied to each of the selected bonds out of which some of MeF was spread outside of the bond area. There was also a chance that the distribution of MeF through out the bond area might not be uniform. The penetration of MeF through the wood strip was tested by putting a drop of MeF on one surface of the wood and observing that penetration on the other surface of the wood strip was very rapid. Clearly, the chemical is highly polar and also of low viscosity.

#### 4.3.1.3. Bond pressing and testing sequence

The alkaline-catalyzed and filled PF adhesive of the resole type which was used for fiber mat formation (kindly donated by Borden Chemical, Inc.), was also used in the bond strength development tests.

To form each bond, one surface of one end of one wood strip was coated with adhesive over a 25 X 8 mm area. A pair of strips (one without adhesive coating) were lapped together and placed in the testing device with an 8 mm overlap. A bonding pressure of 1.1 MPa was used for all tests. The use of a very slight excess of adhesive and a constant pressure during bond pressing meant that a small amount of "squeeze-out" occurred, and the remaining adhesive was almost constant among bonds (approximately  $0.08 \text{ Kg/m}^2$ ). All tests were done at room temperature.

After a pre-selected curing time, bond forming pressure was reduced, the free ends of the specimens were gripped pneumatically, and the bond was pulled to effect failure in shear mode. Forming time and shear strength (corrected for

bonding area) were automatically recorded for each bond. For each treatment type, at least 17 bonds were tested (except delay MeF treatment, in which 11 bonds were tested) over a range of pressing times (0 to 604 seconds). Figure 4.8 schematically shows the number of bonds formed and tested for each of the

Treatment	Range of pressing time (Sec.)	Number of bonds formed & tested
Control	0 - 604	20
NH <sub>3</sub>	0 - 604	19
MeF	0 - 604	20
NH <sub>3</sub> + MeF	0 - 604	17
MeF (delay)	0 - 604	11

Figure 4.8 Bonds formed and tested for different types of treatment.

different treatment types. From those recorded data, graphs of bond strength versus pressing time were drawn. Bonds were formed with five different types of treatment:

- I. control (without NH<sub>3</sub> or MeF),
- II. NH<sub>3</sub> gas was injected to the bond 4 seconds after press closure to explore the effect of NH<sub>3</sub> on bond strength development rate. The reason to pass NH<sub>3</sub> gas 4 seconds after press closure was to allow the press to apply desired maximum (1.1 MPa) pressure on the bond. Application of gas prior to the attainment of full press force would have led to gas escape at the PTFE-wood interface.



- III. MeF (liquid) was injected to the bond 8 seconds after press closure to explore the effect of MeF on bond strength development rate. The reason to pass MeF 8 seconds after press closure was to keep same time sequence as in sequential treatment (IV).
- IV.  $\text{NH}_3$  and MeF were injected sequentially into to the bond 4 seconds and 8 seconds after the press closure respectively to explore the combined effects of  $\text{NH}_3$  and MeF on bond strength development rate.
- V. MeF was injected to the bond 400 seconds after press closure to explore the action of methyl formate at the later part of pressing process.

To assess the effect of different chemical treatment on bond strength statistically, five bonds of each type (control, injection of  $\text{NH}_3$ , injection of MeF, and injection of both  $\text{NH}_3$  and MeF) were formed at 308 seconds of pressing time and then tested in shear mode. The results of these tests will be presented and discussed in Chapter 5.

#### 4.3.2. A sealed pressing device

A miniature sealed circular hot pressing system with provisions for chemical reactant (vapor phase) injection and removal as loads are applied dynamically was developed. Figure 4.9 represents the basic principle of the sealed press. This system can be used first as a chemical treatment vessel under controlled conditions of temperature, pressure, and chemical. In this way, it may be used to

explore the possibilities to create miniature composite products with uniform or non-uniform micro-structure, as we desire. It can also be used for materials (mat) characterization purposes; properties such as fluid permeability, thermal conductivity, and hygro-thermo-viscoelasticity may be explored. Development of such a trial miniature type sealed pressing system was one of the primary objectives of this research project.

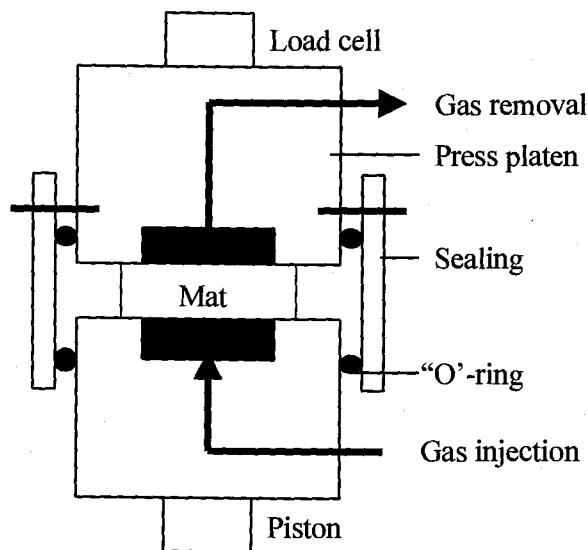


Figure 4.9 Basic principle of the sealed press.

#### 4.3.2.1. Performance needs and design strategy

In light of the above and prior discussion, it is evident that the sealed pressing system should perform the following basic functions:

- I. Controlled application of uniaxial compressive stress (with options for dynamic stress or position control),
- II. Platen temperature control,
- III. Reactant injection and removal through pressing faces,
- IV. Peripheral sealing,
- V. Internal sensing of selected material conditions.
- VI. Capability of computer control and data acquisition.

Circular samples were used in the research because they do not contain square corners which may perturb uniform boundary conditions in the horizontal (X-Y) plane. Sample size was limited by the load capacity (44.59 KN) of the available servo-hydraulic material test machine (MTS) system. From the previous work of Haselein (1997) working with identical material, it was known that a load of approximately 6.2 MPa (900 psi) is required to compact dry fiber (TMP) mats at 20<sup>0</sup>C to a density of 850 to 900 Kg<sup>m</sup><sup>-3</sup>. A sample diameter of 96.00-97.00 mm was therefore possible.

Based on this sample diameter, the diameter of the circular pressing platen was selected to be 105.00 mm. This oversize was necessary because of design issues discussed below.

#### 4.3.2.2. Mechanical design

The pressing system consists of five main portions:

- I. The upper portion of the pressing system,

- II. The lower portion of the pressing system,
- III. Collar which provides peripheral sealing of the pressing system,
- IV. The external gas supply and removal system and
- V. The hydraulic control system.

The present discussion is limited to the pressing system itself and the gas supply/removal system. The upper and lower portions of the pressing system are identical. As shown in Figure 4.10 and 4.11, each portion (upper and lower) of the pressing system consists of six different parts: porous plate, back plate, gas supply block, heating block, thermal barrier, and connecting column. Since the design of each part was given very careful consideration, they will each be considered in turn here. Furthermore, since this system may be adopted by other worker in the field, engineering drawings of each part are provided in Appendix A.

The upper portion of the pressing system was connected to a load transducer, which was in turn attached to the top cross-beam of the servo-hydraulic test machine (MTS). The lower portion of the pressing system was connected to the hydraulic piston of the MTS machine. The piston can be driven up or down by hydraulic power from a power unit and control (Moog) valve. An internal LVDT of 150 mm range was applied to measure the position of the press.

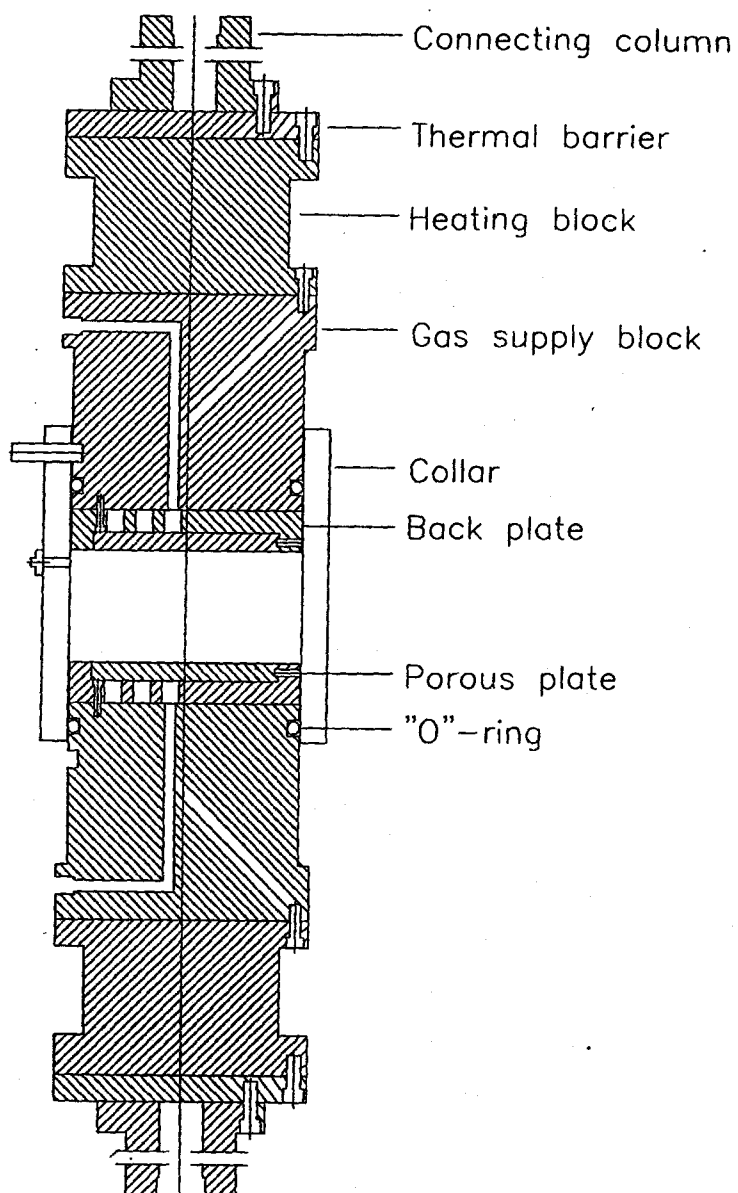


Figure 4.10 Schematic showing the upper and lower portions of the sealed pressing system.

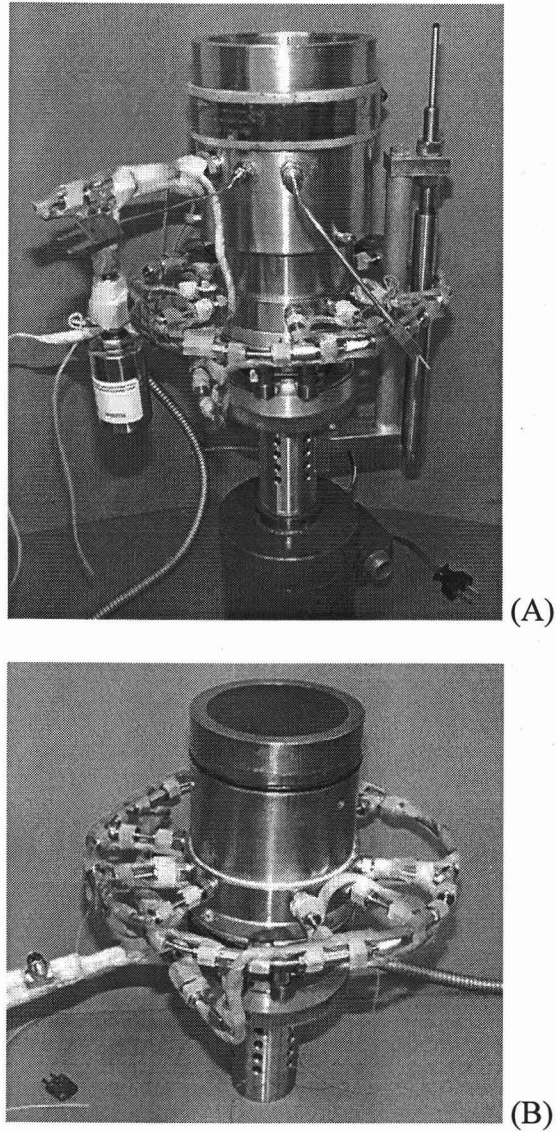


Figure 4.11 An overview of the upper portion (A) and the lower portion (B) of the pressing system.

#### 4.3.2.2.1. Porous plate

The size of the porous plate is 85.00 mm in diameter and 8.00 mm in thickness. It is attached to, and situated inside, the back plate i.e. the back plate

covers the outer surface and periphery of the porous plate, leaving the inner surface of the porous plate free. The porous plate is made up of porous graphite (25% porosity). Material properties including permeability, strength (especially compressive and bending strength), and heat stability were considered when selecting the material for the porous plate. In future development of the technique, porous ceramic platens may be appropriate. Shrinkage during firing of "green ceramic" does, however, present some difficulties. The main functions of the porous plate are:

- I. To distribute the chemical reactant across the sample uniformly but with future possibilities for zoned injection and removal (this may require use of porous plates with a micro-tubular structure to avoid lateral translation of gas),
- II. To transfer the heat energy from the back plate to the mat (mainly by gas transfer and some by conduction), and
- III. To act as a pressing platen with future possibilities for shaped surfaces.

#### *4.3.2.2.2. Back plate*

To avoid corrosion by chemicals, while achieving acceptable heat transfer, stainless steel was used for the back plate. The outer surface of the back plate is attached to the inner surface of the gas supply block. The inner surface of the back plate covers the outer surface and periphery of the porous plate. This plate contains nine systematically arranged hollow sections which meet nine axial holes from the

gas supply block. These hollow sections act as a reactant reservoir to insure continuous and uniform distribution of reactant to the mats through the porous plate. This may also provide future potential for zoned treatment.

#### *4.3.2.2.3. Gas supply block*

The gas supply block is also made of stainless steel to avoid corrosion and to insure acceptable heat transfer. The outer surface of the block is attached to the inner surface of the heating block. It has nine radially drilled holes which intersect with nine axially drilled holes (5 mm dia) lying on three pitch circles. The radial holes are also 5.00 mm in diameter; counterbored 7.80 mm threaded (Swagelok) by 10.00 mm deep, with mill necessary spots for "o"-rings. These nine radial holes are fitted to the external reactant supply and removal system. The function of these radial and axial holes is to supply and remove the reactant via the back plate. Another function of this block is to transfer the heat energy from heating block to the mats through the back plate and porous plate. An "o"-ring was fitted in a groove circumferentially around this block. This "o"-ring is responsible for sealing between the pressing platen and the collar. A high-temperature tolerant "o"-ring material was selected to also be resistant to ammonia and methyl formate. After considerable research an ethylene propylene polymer was found to provide the best combination of properties under the hostile environment generated.

The block has three radial holes at the circumference 120 degree apart, 8.00 mm diameter and 5.00 mm deep, which facilitated the locking of collar and block.



#### 4.3.2.2.4. Heating block

The heating block is made with high heat conductivity aluminum to insure rapid heat transfer and therefore aid in efficient temperature control. This block is 70.00 mm in vertical height and 115.00 mm in diameter. Electrical band-heaters (650 W and 120 V, 88.90 mm (3.5") internal diameter and 38.10 mm (1.5") width, maximum operating temperature 320<sup>0</sup>C) were mounted in grooves circumferentially around the heating blocks. Subminiature thermocouple probes (3.175 mm dia, copper-Constantine with 304 SS sheath) were fitted inside the block through a radial hole to measure the temperature of this block. Temperature controllers (self-tuning with proportional, integral and derivative functions) were used to control the temperatures of the two heads. The ends of these blocks are attached to thermal barriers. To insure good heat transfer and to avoid large temperature variations in the heat transfer from the pressing platens to the mats, the thermal mass was large.

#### 4.3.2.2.5. Thermal barrier

The heating block is attached to a thermal barrier to prevent heat loss, to protect the load cell and the piston from the influences of temperature, and to avoid the effects of thermally-induced distortion of the MTS frame. The thermal barrier is made up of low thermal conductivity glass-epoxy composite (trade name G-11) supplied by AFC, Illinois. The thermal conductivity of this material is about 0.29

$W^0K^{-1}m^{-1}$  and the tensile strength is about 255.04 MPa (37,000 psi). This barrier is 115.00 mm in diameter and 13.00 mm in thickness. The other surface of this thermal barrier is joined to the connecting column.

#### 4.3.2.2.6. *Connecting column*

The connecting column is hollow and cylindrical in shape with one internally threaded open end through which the sealed pressing system connects with the load transducer and piston of the MTS machine. The column is also made of stainless steel and is 100.00 mm in length. It has provisions to supply cool air inside the hollow cylinder and to remove hot air from inside the hollow cylinder caused by the small amount of heat which is transferred through the thermal barriers to the connecting column.

#### 4.3.2.2.7. *Collar*

The collar which provides peripheral sealing of the pressing system, is made of stainless steel. Peripheral sealing of the platens enables one to control the thermodynamic and chemical environments inside the pressing chamber. It has three radial holes at its upper side 120 degrees apart, 8.00 mm diameter, which facilitate locking of the collar to the upper press platen. The collar also has another three holes at the middle, which facilitate the fitting of pressure transducers and sub-miniature thermocouple probes. An Electrical band-heater was also mounted

circumferentially around the collar and PID temperature controller was used to control its temperature.

#### 4.3.2.2.8. *Safety stop*

From previous experience, it was known that sometimes the piston of the MTS machine goes beyond the control range and moves up or down unpredictably, which is dangerous for maintaining sealed conditions in the pressing system when harmful chemicals may be inside. For that reason, an easily removable safety stop was designed. This could be placed in between the connecting column of the lower portion of the pressing system and the lower frame of the MTS machine to prevent unwanted downward movement of the piston. The safety stop is in two parts which, when installed, are held together by a steel ring. The stop is capable of withstanding the full force of the MTS machine.

#### 4.3.2.3. External gas supply and removal system

The nine radially drilled holes of the gas supply block were fitted with a peripheral stainless steel tubing system. In order to avoid localized condensation of treatment chemicals (principally MeF), it was necessary to heat all external supply lines. Rope heaters (OMEGALUX, 400 W, and 120 V) were therefore wrapped around the circular stainless steel tubing system and several hand-made miniature thermocouples probes were installed at a range of positions on the tubing.

The chemical gas was supplied to the pressing system through the lower portion of the pressing system and removed from the pressing system after desired period of time through the upper portion of the pressing system. Figure 4.12 schematically represents the external gas supply and removal system.

The controlled gas injection system consisted of the following main components:

- A proportionally opening electronic servo-valve which supplied desired amounts of gas into the pressing chamber for chemical treatment of the pre-formed fiber mats;
- A manifold which supplied required chemical gas from the source to the proportionally opening electronic servo-valve;
- Chemical gas container tanks with their own regulators;
- Manual 2-way control valves to activate selected gas supplies.

A gas bomb of volume  $62.0 \text{ cm}^3$  was connected at the very end of the gas injection system to facilitate the direct injection of any desired gas (in present research MeF) to the system. An electrical band-heater was mounted around the gas bomb and a temperature controller was used to control its temperature. Heating tape was also warpped around the fittings of the gas bomb and two hand-made thermocouples were installed around the bomb to measure and control its temperature.

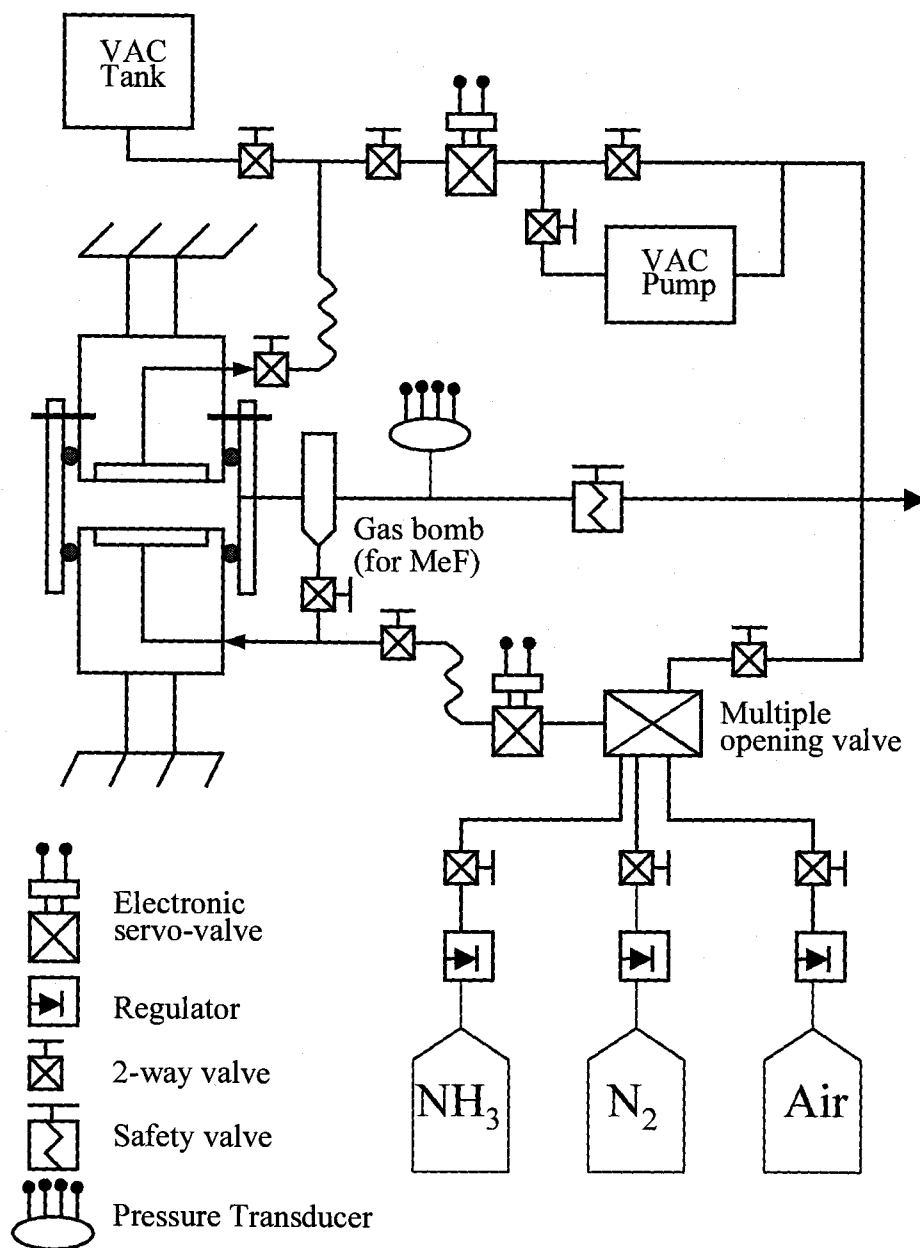


Figure 4.12 Schematic representation of the external gas supply and removal system.

The controlled gas removal system consisted of the following main components:

- A proportionally opening electronic servo-valve which removed desired amounts of chemical gas from the pressing chamber;
- A manually controllable 2-way valve through which the gas removed from the pressing chamber (via the proportionally opening electric servo-valve) passed into the fan-assisted vent;
- A vacuum pump which removed most of the air from the pressing chamber prior to test if necessary; and
- A vacuum tank, which sucked and removed the desired chemical from the pressing chamber at desired times.

The chemical gas safety control system consisted of the following main components:

- A manually adjustable safety valve employed with the pressing chamber to avoid possible pressure overshooting damage or explosion of the pressing system.

#### 4.3.2.4. Platen position control and load measurement

The original function generator of the MTS machine was replaced by a stand-alone computer control system to improve the performance of the machine and experimental system. Figure 4.13 shows the complete test system.

Almost all of the experiments and pressing operations were carried out in the position (mat thickness) control mode. A small number of experiments were also conducted under load control; this was to examine the softening action of  $\text{NH}_3$ .

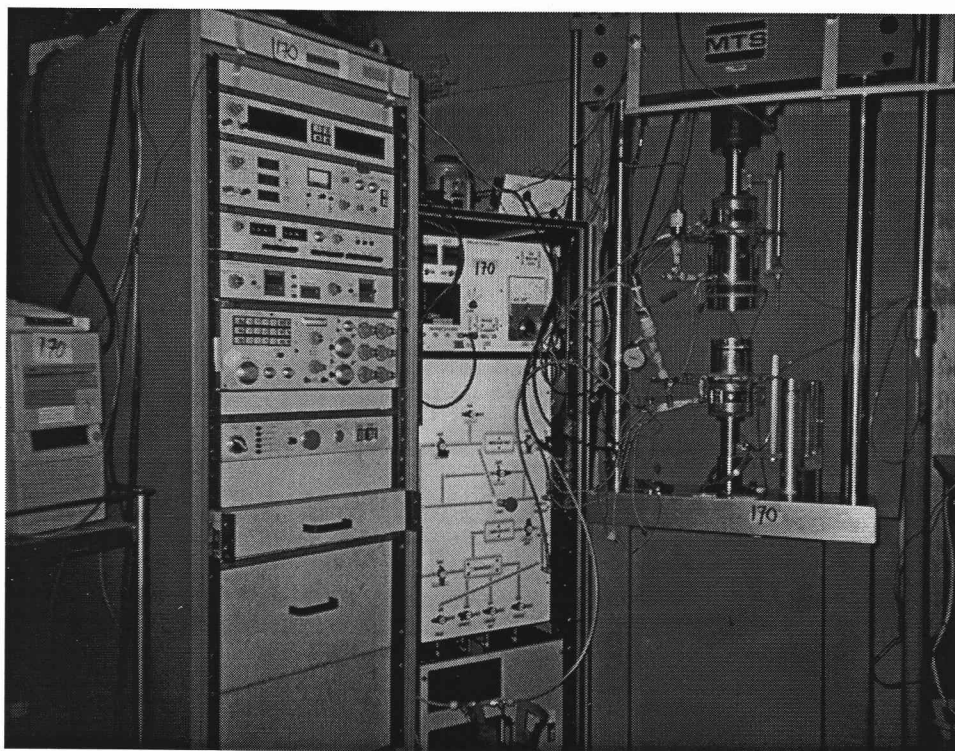


Figure 4.13 An overview of the complete test system.

A Strawberry Tree Program<sup>®</sup> (see Appendix B) was used to sequentially control head position. Desired closing and pressing cycles for each experiment were programmed into the software. The operating worksheet then converted the digital data to analog form by means of a converter; this signal was transmitted to the MTS microprocessor. The signal analysis and control cycle were repeated every

0.2 seconds. An external LVDT of 50 mm range was directly assembled beside the sealed press for precise measurement. This was connected beyond the thermal barriers of the sealed pressing system to minimize the influences of temperature. Installation of the LVDT directly on the pressing heads improved the precision of measurements by omitting vibration and the effects of thermally induced distortion of the MTS frame. During consolidation and treatment, the movement of the piston was measured by both of the LVDTs (external and internal).

The resultant stresses (in the form of load) in the pressing system were sensed by the load cell and recorded with the data acquisition system. Throughout the experiments, position and load were measured by the LVDT and load cell, and recorded to the computer with the data acquisition system.

#### 4.3.2.5. Temperature control and measurement

Most of the experiments for the present study were carried out at relatively low temperatures, but the system has the capability to be run at temperatures ranging between ambient and about 200<sup>0</sup>C. Components were designed with high heat conductivity to maximize the internal rate of heat transfer. Further, to minimize temperature variations when cold materials were inserted, certain portions were of high thermal mass. Four electrical band-heaters were used to provide heat for both platens, the collar, and gas bomb. Individually controlled rope heaters were used around the surrounding tubing system for heating. Subminiature thermocouple probes were used to monitor the temperature of the heated platens,



collar, and internal environment of the pressing chamber. Three self-tuning controllers with proportional, integral and derivative functions (PID) were used to control the temperature of both platens and the collar. Solid state AC voltage controllers were used to control the temperature of the surrounding tubing systems and a variac was used to control the temperature of the gas bomb.

#### 4.3.2.6. Gas pressure measurement

A pressure transducer (Omega: Model PX931-1KSV) was used to monitor gas pressures inside the sealed pressing system. The signal was directed to the computer through the analog-to-digital data acquisition system. Figure 4.14 shows the gas pressure measurement arrangement. In addition to measurement of gas

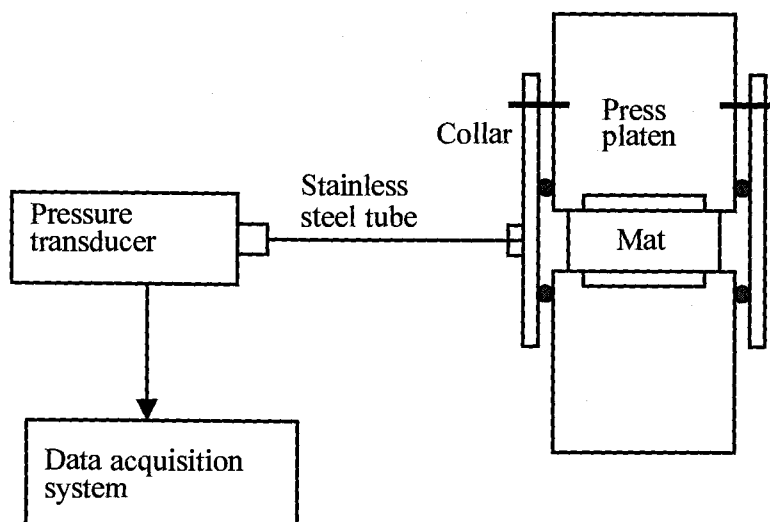


Figure 4.14 Gas pressure measurement arrangement.

pressure inside the sealed pressing system, gas pressures at the center of the mat were also measured in some selected experiments. This was done by carefully placing one end of a small diameter stainless steel tube at the geometric center of the mat, the other end of which was connected to a pressure transducer which was recorded digitally. This probe was used to explore the magnitude of fluid pressure gradient within sample when external conditions were altered. A sample of such a test is shown as Appendix C.

#### 4.3.2.7. Computer control and data acquisition system

By using a Dynares analog Strawberry Tree<sup>®</sup> card, a computer control and PC-based data acquisition system has been developed (Figure 4.15). Terminal Panels T71 and T31 were used in the data acquisition system. The Strawberry Tree<sup>®</sup> data acquisition system was programmed using icon-based software (PC-Workbench). A worksheet to control pressing system and collect the necessary data included the following functions:

- I. Controlling the movement of the hydraulic piston i.e. position or mat thickness;
- II. Measuring the position and load by LVDT and load cell respectively;
- III. Collecting and recording temperature and gas pressure data.

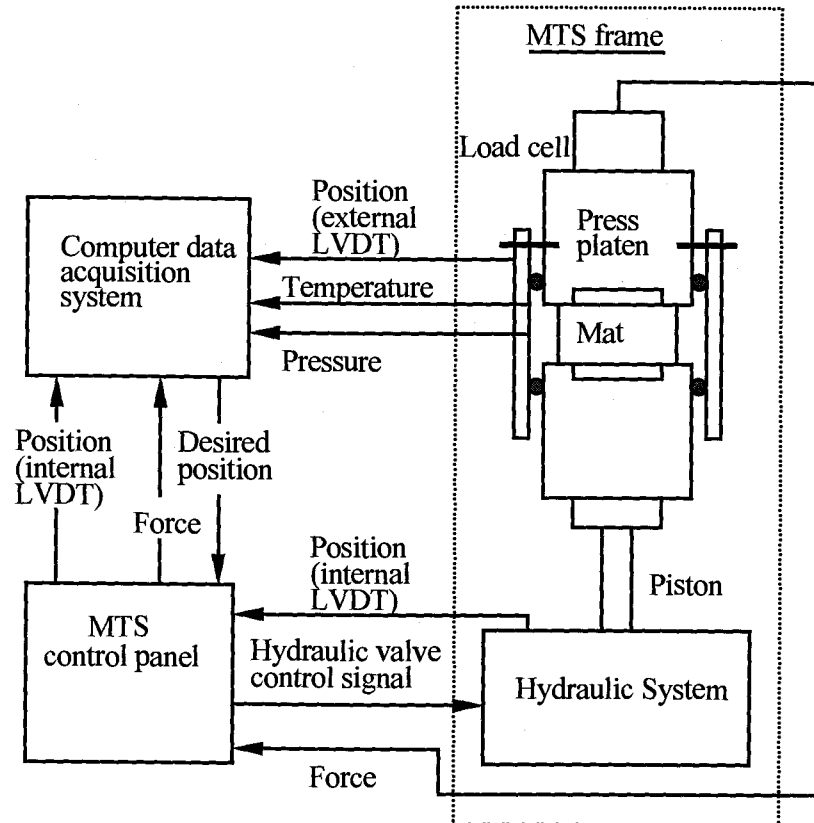


Figure 4.15 A schematic of the computer control and data acquisition system.

#### 4.3.3. Chemical treatment and pressing sequence

Two different types of experiment were conducted as follows:

- I. Examination of the softening action of gaseous ammonia on pre-formed TMP fiber mats under a range of environmental conditions, and
- II. Formation trial of composite samples by exposing resinated TMP fiber mats to gaseous ammonia followed by MeF vapor. Resole PF resin was used; this

was catalyzed by the methyl formate after the mat had been softened with the ammonia.

#### 4.3.3.1. Softening action of gaseous ammonia

As mentioned in the literature review, Davidson (1968) reported that plasticization of wood was possible by treating it with gaseous anhydrous ammonia at room temperature under an ammonia vapor pressure of 0.99 MPa (145 psi). No results could be found of research work done on the softening action of gaseous ammonia on fiber mat. Consequently no prior information was available about times, vapor pressures or temperatures necessary for softening of fiber mats.

In wood-based composite panel manufacture, consolidation of mats in the thickness direction during pressing induces internal stresses both within and between the particles. Consequently high pressures are necessary to compact mats to the desired thickness during pressing. In conventional pressing operations, heat and water are used to affect necessary softening. Treatment with gaseous ammonia to soften the wood cell wall material may provide an alternative means of affecting such softening without heat. Such softening may reduce the build-up of internal stresses in panels during pressing. This may in turn also reduce the springback of the densified panel after press opening. Irreversible swelling of the panels may thus be reduced and less bonding will be required to produce composites of a given strength.

In light of the above discussion, this preliminary part of the study was carried out to evaluate the effect of gaseous ammonia treatment time, treatment temperature, and vapor pressure on the softening of fiber mats. In treatment time and temperature studies, the softening action of  $\text{NH}_3$  was compared in terms of density development with pressing time under controlled pressure. In studies in which ammonia vapor pressure was the independent variable, the softening action was compared in terms of percentage of the reduction of the press-induced internal residual stress at constant platen position. Each aspect of the study will be considered in turn.

#### *4.3.3.1.1. Treatment time effects*

Evanite Hardboard mill's pre-formed fiber mats were used in this experiment. Circular specimen mats of 95-97 mm diameter and 19 to 21 mm thick were conditioned to 10% MC prior to being consolidated in the sealed pressing system operating in load control mode. The weight of mats were recorded. In each test, the specimen with mesh wire screen was placed on the lower platen of the sealed pressing system and gently pre-pressed to 16 mm. The stainless steel mesh wire (diameter 97 mm, thickness 0.125 mm, pore diameter about 0.08-0.09 mm) was included to prevent penetration and possible blocking of the graphite pores.

After pre-pressing by manually controlling all the necessary valves in the gas in-let and out-let system the sample was treated with ammonia gas at 0.62 MPa partial pressure and  $19^{\circ}\text{C}$ . Mats were exposed to the gas for a range of times after

which the gas was vented. In this part of the study, treatment time was the only variable. The treatment times were 0 (control), 10, 30, 60, 100, 200, 300, 450, 600, 750 and 900 seconds. Following treatment, the samples were pressed at 8.4 MPa pressure for 120 seconds. The closing and opening rate of the press was 1 mm/sec. Figure 4.16 schematically shows the treatment cycle of  $\text{NH}_3$  for the experiments. In this figure, stages A and B represent  $\text{NH}_3$  treatment and pressing periods

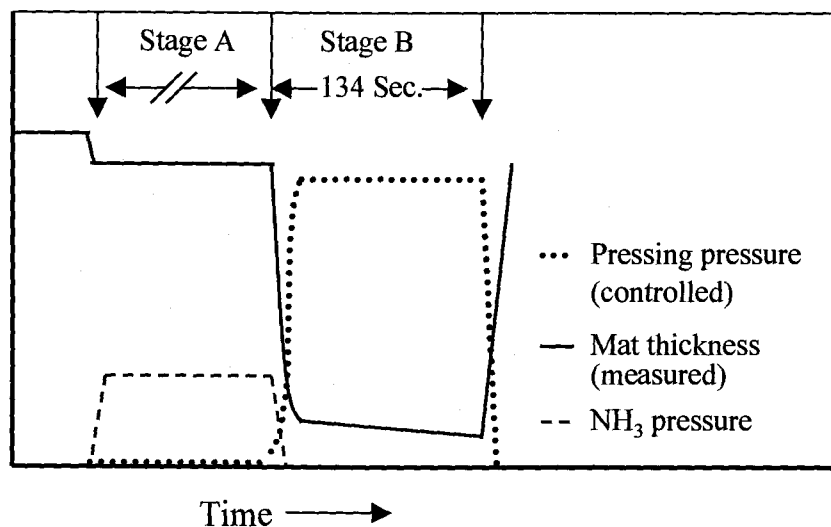


Figure 4.16 Sequence for the  $\text{NH}_3$  treatment time experiments.

respectively. During these pressing periods, time (s), load (N), mat thickness (mm), partial pressure of ammonia (MPa), and temperature ( $^{\circ}\text{C}$ ) of the environment inside the sealed pressing chamber were recorded digitally. After press opening, the thickness and diameter of the sample was measured with digital calipers. Fiber mats retained some ammonia after press opening.

From each experimental data file, the data was processed to observe how the density of the mat developed with pressing time. The diameter of the mat after pressing was used in the density calculation. In other words, no attempt was made to collect for small changes in diameter that occurred at intermediate stages of the cycle. The density was calculated by using the following equation (5.1) as below:

$$\text{Density}_{\text{time}} = \frac{\text{Weight of fiber mat}}{\text{Thickness}_{\text{time}} * \Pi * (\text{Radius of mat})^2} \quad (5.1)$$

Where:

Density<sub>time</sub> = density at a particular pressing time,

Thickness<sub>time</sub> = thickness at the above particular pressing time.

To compare between the different treatments, density values at one time point of pressing (after 30 seconds) were extracted. Graphs of treatment time vs. density (after 30 seconds of compaction with constant pressure) were then plotted to display the effect of treatment time on the softening action of NH<sub>3</sub>. Results (density versus treatment time) for these experiments will be presented and discussed in Chapter 5.

#### 4.3.3.1.2. Treatment temperature effects

Treatment temperatures of 20, 30, 40, 50, 70, 90 and 100<sup>0</sup>C were used to observe the effect of temperature on the softening action of gaseous ammonia. This was done in order to ascertain whether heating would be necessary in the sealed

pressing system to affect necessary softening. A constant relative vapor pressure (RVP) of  $\text{NH}_3$  was used to keep the amount of  $\text{NH}_3$  constant. The maximum RVP of  $\text{NH}_3$  was limited by the saturated vapor pressure of  $\text{NH}_3$  at room temperature. This value was 0.74 MPa (108 psi). This pressure corresponds to 11% relative vapor pressure of  $\text{NH}_3$  at  $105^\circ\text{C}$ . In the literature, the saturated vapor pressures of ammonia were available up to  $105^\circ\text{C}$ . Furthermore, safety issues became greater when dealing with toxic gases and higher pressures and temperature. Therefore, it was decided to use 11% RVP of  $\text{NH}_3$  when investigating temperature effects. From Braker and Mossman (1971), the partial pressure of ammonia at 11% saturation was calculated, these data are shown in Figure 4.17.

Though RVP's of  $\text{NH}_3$  were constant, the density of the  $\text{NH}_3$  decreased with increase of temperature among the experiments. In retrospect, it may have been more informative to maintain gas density constant among all treatments rather than RVP.

Prior to each test, time was allowed for the pressing system to reach the desired temperature, and the sample was then pre-pressed to 16 mm in the sealed pressing system. After pre-pressing by manually controlling the necessary valves including electronic servo-valves in the gas in-let and out-let system, the sample was treated with ammonia gas (11% relative vapor pressure) for 300 seconds. Treatment temperatures were 20, 30, 40, 50, 70, 90, and  $100^\circ\text{C}$ . Following the pre-treatment, each sample was pressed at a constant pressure of 8.4 MPa for 120 seconds. The closing and opening rates of the press were 1 mm/sec. Figure 4.18



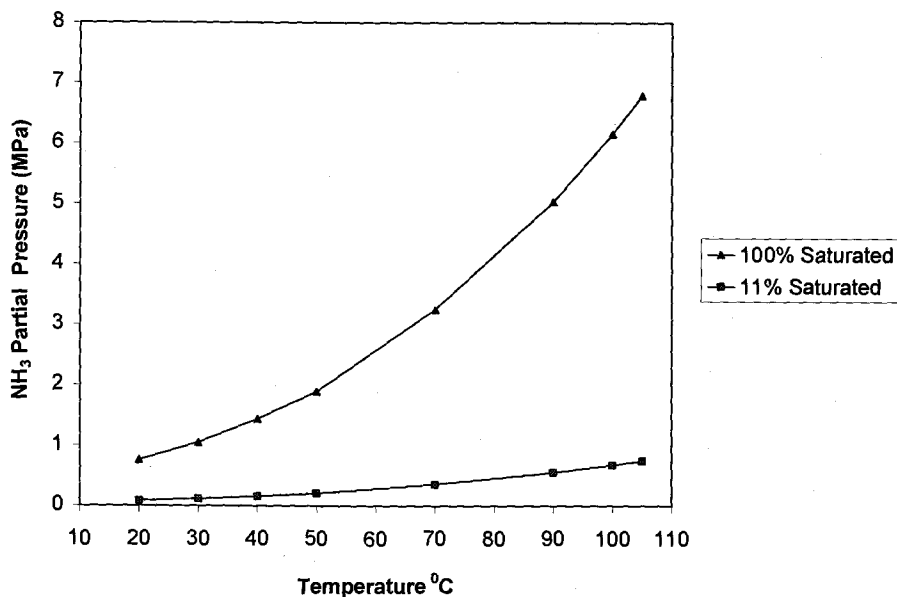


Figure 4.17 100% saturated and 11% saturated vapor pressure of ammonia with temperature (derived from Braker and Mossman, 1971).

schematically shows the treatment cycle of NH<sub>3</sub> employed. In this figure, stages A and B represent NH<sub>3</sub> treatment period and pressing period respectively. During the treatment and pressing period, time (s), force (N), mat thickness (mm), partial pressure of treating gas (MPa), and temperature (°C) were recorded digitally. After press opening, the thickness and diameter of the sample were measured. Similar to treatment time experiments, density development during pressing was calculated by using equation 5.1. Results (density versus treatment temperature) for these experiments will be presented and discussed in Chapter 5.

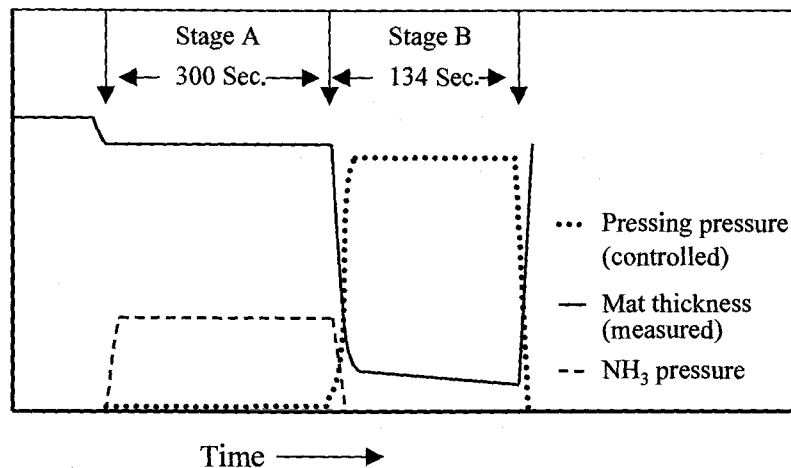


Figure 4.18 Sequence for the NH<sub>3</sub> treatment temperature experiments.

#### 4.3.3.1.3. Ammonia vapor pressure effects

The aim of this experiment was to examine the reduction of induced internal residual stresses in the compressed fiber mat (due to NH<sub>3</sub> softening) with different vapor pressure (partial pressure) of ammonia gas. This was again conducted in order to assess the conditions required in the sealed pressing system to achieve useful softening levels at any acceptable rate. Reduction of induced internal stresses in the compressed fiber mat due to ammonia treatment was inferred by monitoring the reduction of force necessary to hold the mat at a constant density (often termed counterpressure).

Manually formed circular mats (97 mm diameter), as described in the specimens preparation section were used in this experiment. For each test, a very carefully pre-formed mat was transferred to the sealed pressing system. The sample

was pre-pressed to 18 mm thickness and then the pressing and treatment chamber was evacuated. The mat was then compressed to a thickness of 5.00 mm (corresponding to a target density of  $525 \text{ Kg/m}^3$  on an oven-dry weight basis) at a closing rate of 1 mm/sec.

After 60 seconds of press closure,  $\text{NH}_3$  gas of the required vapor pressure was passed into the compressed mat for 60 seconds and treated; the vessel remained charged with ammonia for a further 240 seconds. The total pressing time was therefore 300 seconds. Figure 4.19 schematically shows the treatment cycle where stages A and B represent pressing period (only) and  $\text{NH}_3$  treatment during pressing respectively. The partial pressures of ammonia employed were 0.0345, 0.0621, 0.1034, 0.1103, 0.1379, 0.1585, 0.1723, 0.2068, 0.2757, 0.3102, 0.4274, 0.5652 and 0.7444 MPa. This wide range of pressures were used in order to find out some optimum value for fiber softening. All experiments were carried out at room temperature ( $19^\circ\text{C}$ ). During the pressing cycle, time (s), load (N), mat thickness (mm), partial pressure of  $\text{NH}_3$  gas (MPa), and temperature ( $^\circ\text{C}$ ) were recorded digitally.

Load was converted to pressure acting on the mat (hereafter referred to as counterpressure) by subtracting the partial pressure of  $\text{NH}_3$ . These manipulations were performed in the spreadsheet. Graphs of corrected mat pressure versus pressing time were drawn for each of the treatment vapor pressure values employed.

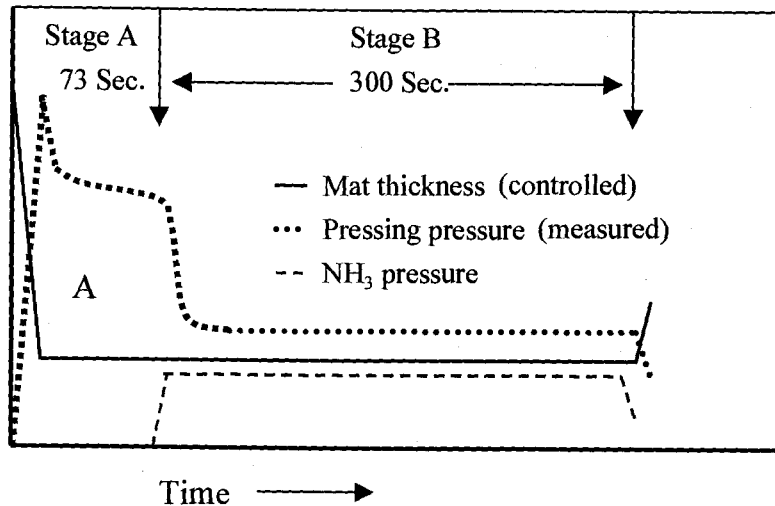


Figure 4.19 Sequence for the NH<sub>3</sub> treatment vapor pressure experiments.

From each of the treatment vapor pressure graphs, the reduction in counter-pressure due to NH<sub>3</sub> injection was collected and converted to a percentage of the reduction of pressure (press induced) based on the press-induced internal residual pressure just before ammonia treatment.

Limitations of the servo-hydraulic testing machine led to mat thickness variations of  $\pm 0.75$  mm among tests. Due to this variation, the press-induced internal residual forces before ammonia treatment were not the same in all experiments in this part of the study. An attempt was therefore made to correct all data to a reference thickness of 5.00 mm. For this purpose, a correction curve was established. For this purpose, mat thickness and corrected mat pressure applying just before ammonia injection were regressed against each other. Forces were then

back corrected to their equivalent at 5.00 mm. Clearly an assumption of linear elasticity was made.

Following application of all necessary corrections and adjustments, graph of pressure reduction (%) versus treatment vapor pressure was drawn to compare the softening action of ammonia at different partial pressure values. These results will be presented and discussed in Chapter 5.

#### 4.3.3.2. Composite sample formation trials

Some composite samples were formed by pressing resinated TMP fiber mats with the sequential injection of  $\text{NH}_3$  and MeF vapor.

Circular mats (as described in the specimen preparation section) of fiber-PF-resin mix with target compressed (to 5.00 mm) densities of  $525 \text{ Kg/m}^3$  (lower) and  $750 \text{ Kg/m}^3$  (higher) were manually formed. All sample formation experiments were carried out at a temperature of  $40\text{-}42^\circ\text{C}$  (above the boiling point of MeF). For the formation of both lower and higher density samples, samples were formed by treating the mats according to the following four sequences.

- (I)  $\text{NH}_3$  and MeF sequentially (GAM),
- (II)  $\text{NH}_3$  only (GA),
- (III) MeF only (GM), and
- (IV) Control (G).

Where: G represents resin, A represents  $\text{NH}_3$  and M represents MeF.

In these experiments, very carefully pre-formed mats were transferred into the sealed pressing system. In most of the experiments, the gas bomb at the very end of the gas injection system was pre-filled with 22-23 c.c. of liquid MeF and pre-heated to 80°C. This heating was necessary to ensure that condensation of MeF did not occur and there was a sufficient phase gradient to ensure that the MeF migrated into the specimen disk. The sample was pre-pressed to 18 mm thickness before the pressing and treatment chamber was evacuated. The press was then closed to affect a mat thickness of 5.00 mm at closing rate of 1 mm/sec. Due to some limitations of the MTS, some variation in position occurred. The total pressing time of the mat was 500 seconds.

In the NH<sub>3</sub> and MeF sequential treatment experiments, as shown in Figure 4.20, after 20 seconds of press closure, NH<sub>3</sub> gas (0.15 MPa) was passed into the pressing chamber for 22-25 seconds and was subsequently vented from the system. The mat was then washed cyclically with N<sub>2</sub> gas at about 0.34 MPa for 22-25 seconds. After venting the N<sub>2</sub> gas, the pressing system was re-evacuated and then MeF vapor was passed let in by opening the MeF vessel. MeF was held there for the remainder of the pressing period. At the end of the pressing cycle, the press was opened to 18 mm and the residual MeF was purged from the press and again flushed with N<sub>2</sub>. After removing the mats from press, their thickness and diameter were measured.

In the case of the NH<sub>3</sub> treatment, a similar procedure as described above was followed except that MeF was absent and no washing with N<sub>2</sub> was included

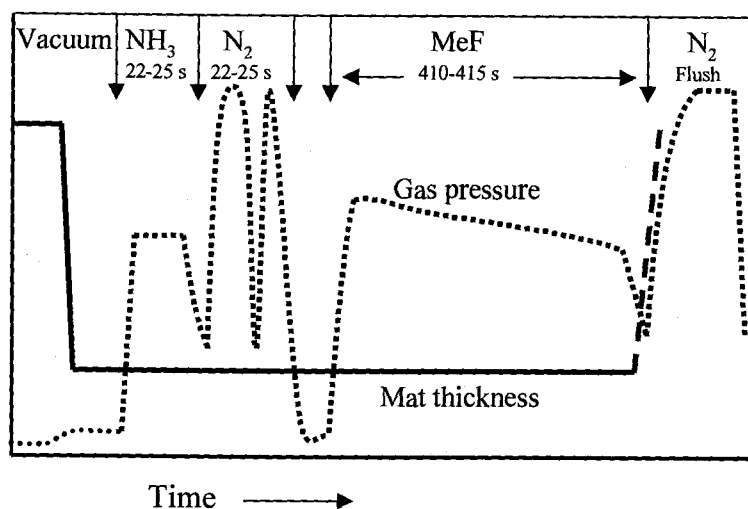


Figure 4.20 Sequence for the NH<sub>3</sub> and MeF treatment during sample formation trials.

(see Figure 4.21). In the case of experiments with MeF alone, instead of passing NH<sub>3</sub> after 20 seconds of press closure, MeF vapor was passed into the pressing chamber and it was there for the remaining period of the pressing cycle (see Figure 4.22).

Attempts were also made to form some control samples at 40-42<sup>0</sup>C without ammonia or methyl formate. These samples did not, however, hold together. In addition, some samples were also formed by using a conventional hot press (HP). Pressing conditions of HP samples were 160<sup>0</sup>C, 28 MPa (for high density samples) and 16 MPa (for low density samples), and a pressing time of 500 seconds. These were formed for comparative purposes.

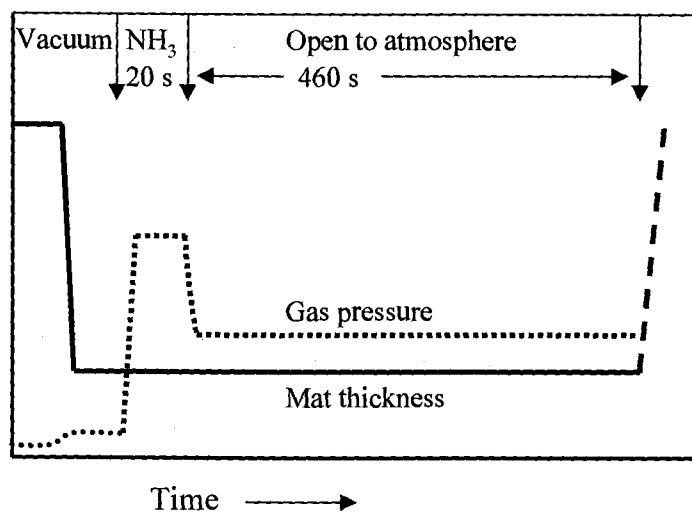


Figure 4.21 Sequence for the NH<sub>3</sub> treatment during sample formation trials.

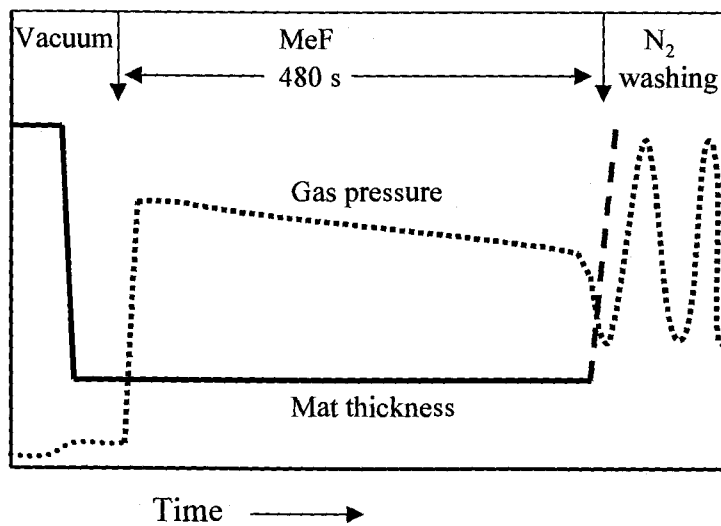


Figure 4.22 Sequence for the MeF treatment during sample formation trials.



#### 4.3.4. Characterization of trial fiber disks

Once formed, all samples were put into a standard room at 60% RH and 19°C for at least a week prior to being tested. Figure 4.23 schematically shows the tests performed on each set of samples.

Sample Type	Tensile strength		MOR		MOE		Thickness swelling (%)	
	HD	LD	HD	LD	HD	LD	HD	LD
G	3	3	3	3	3	3	3	3
GA	3	3	3	3	3	3	3	3
GM	3	3	3	3	3	3	3	3
GAM	3	3	3	3	3	3	3	3
HP	3	3	3	3	3	3	3	3

Where: G = resin, GA = resin and NH<sub>3</sub>, GM = resin and MeF, GAM = resin, NH<sub>3</sub> and MeF, HP = hot pressed, HD = high density, HL = low density.

Figure 4. 23 Tests performed on each set of samples (numbers indicate replications).

##### 4.3.4.1. Static bending tests

Three-point static bending tests were performed on rectangular samples cut from circular sample disks (Figure 4.24) to measure for modulus of rupture (MOR) and modulus of elasticity (MOE). Tests were performed using a screw drive

Universal Testing Machine, on three specimens of each set. A miniature-supporting frame was specially made for the tests (Figure 4.25). The test differed from the ASTM D 1037 (1989) standard for our specimen sizes, which were 12 mm X 90 mm X 5 mm samples with 70 mm span. The loading (cross-head) speed was 10 mm/min.

Before each test, width and depth (thickness) of the each specimen were measured and recorded. During the test 5 data points were collected per second

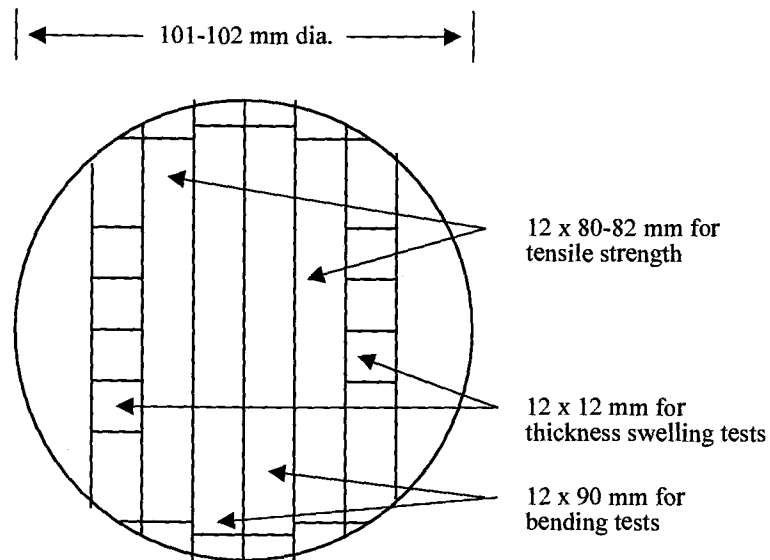


Figure 4.24 Cutting patterns for the specimens.

with an analog to digital data acquisition system. Data of load (N) were recorded in the computer. From loading speed, 10 mm/min., deflection per data points were calculated as follows (equation 5.2):

$$\text{Deflection per data point} = \frac{10 \text{ mm}}{60 \text{ Sec.} * 5} \quad (5.2)$$

The deflection at each point was calculated by multiplying the deflection per data point by the number of the respective data point. Then a load-deflection curve was drawn for each of the tests.

Modulus of rupture (MOR) and modulus of elasticity (MOE) for each test were calculated by using the following equations (5.3 and 5.4):

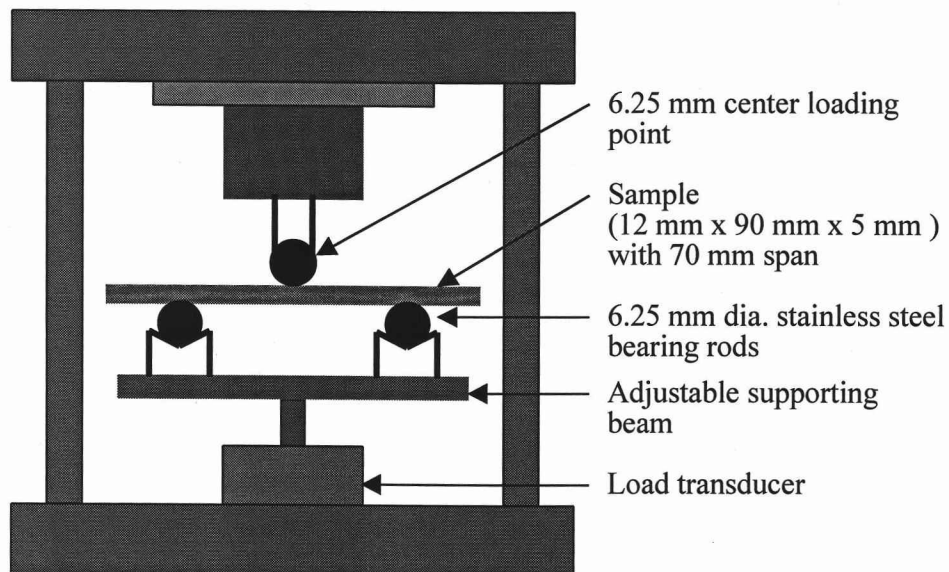


Figure 4.25 Bending tests arrangement.

$$MOR = \frac{3 PL}{2 b d^2} \quad (5.3)$$

and

$$MOE = \frac{L^3}{4bd^3} * \frac{\Delta p}{\Delta \delta} \quad (5.4)$$

Where:

P = maximum load, (N),

L = length of span, (mm),

b = width of specimen, (mm),

d = depth (thickness) of specimen, (mm)

$\Delta p/\Delta \delta$  = slope of the load-deflection curve within proportional limit.

#### 4.3.4.2. Tensile strength

Tensile strength tests (parallel to surface) were performed using the Universal Testing Machine (model TTBML of Instron), on three specimens of each set. Samples were tested and each specimen measured 12 mm X 80-82 mm X 5 mm and a 16 mm span was used. The loading speed was 1 mm/min.

Width and depth (thickness) of the each specimen were measured and recorded before each test. Maximum load in lb required for tensile failure of the each specimen was recorded. The tensile strength was calculated using the following equation (5.5):

$$\text{Tensile strength} = \frac{P}{b d} \quad (5.5)$$

Where:

P = maximum load, N,

b = width of specimen, mm, and

d = depth (thickness) of specimen, mm.

#### 4.3.4.3. Thickness swelling test

Samples were cut into 12 mm X 12 mm specimens and soaked in water at room temperature. Changes in thickness were measured at 0.083, 0.166, 0.25, 0.5, 1, 2, 4, 6, 8, and 24 hours to observe the rate of thickness swelling. The percentage increase in thickness was calculated based on the initial thickness by using equation (5.6). Four specimens of each set sample were tested for the thickness swelling test.

$$\text{Thickness swelling (\%)} = \frac{(t_a - t_i)}{t_i} * 100 \quad (5.6)$$

Where:

$t_i$  = initial thickness of specimen,

$t_a$  = thickness after water soaked (desired level of time).

## CHAPTER 5. RESULTS AND DISCUSSION

### 5.1. The sealed pressing system

In accordance with the objectives of this research, a new automated experimental technique has been developed for sealed pressing of pre-formed fiber networks. This may be used to evaluate the effects of specific conditions on the natural fiber networks. The system may also be used to make miniature products under highly controlled (dynamic) thermal, mechanical (stress) and chemical conditions. The system has provision for chemical (vapor phase) injection and removal and thence provides opportunities for chemical treatment or modification of the fibers during the pressing operation. Details of design and construction were discussed in Chapter 4. Following are some brief discussions of the calibration of some parameters of the sealed pressing system and evaluation of its performance.

#### 5.1.1. Pressure cross-check, and dead-volume and flow resistance measurements

Fluid pressure differentials between ambient atmosphere and within the press clearly lead to the creation of a reactive force on the ram. A cross-check was carried out to explore the correlation of these two parameters in order to evaluate the accuracy and consistency of the measurement and control systems. For this purpose, the press while empty (no mat) was closed to a specified opening (50 mm). Air was introduced at a range of known pressures and consequent ram forces

were recorded, which were then converted to absolute ram pressures. Figure 5.1 represents the comparison between measured pressures (based on load transducer

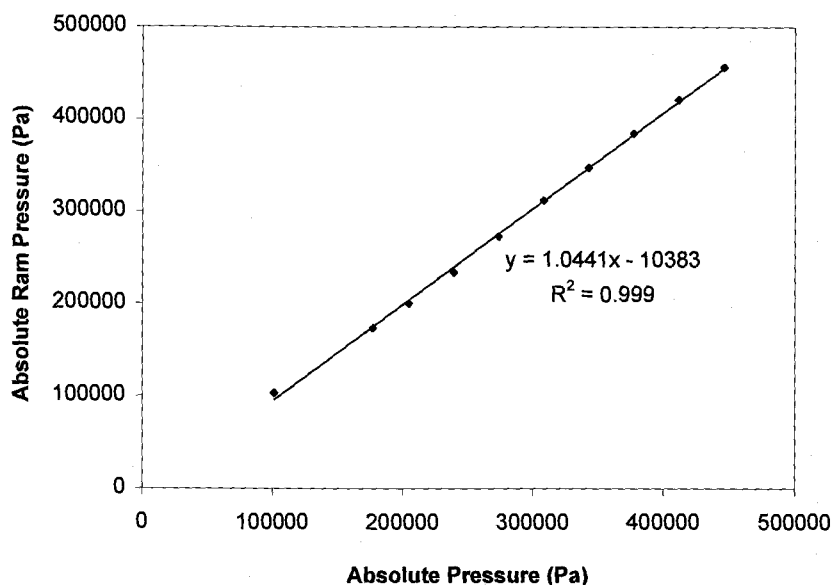


Figure 5.1 Pressure cross-check of the sealed pressing system.

signals) with supplied air pressures (absolute). The graph shows that there was a small deviation between the two in the range of  $\pm 2.42\%$ . This deviation is attributable to both the combined inaccuracies of the transducers involved and to frictional drag at the 'o'-ring seal. This drag was minimized by coating of the cylinder with PTFE and periodic subsequent smearing of the 'o'-ring with silicone grease.

In addition to the above cross-check of gas pressure versus pressing force, total dead volume of the pressing system and resistance to gas flow into the

pressing chamber were evaluated. For the former, changes in ram force (which were then converted to pressure) as a consequence of controlled head movements (from a 50 mm starting position) were made with the in-let and venting valves closed. From this data, total system volume was calculated (based on the assumption of isothermal ideal gas behavior). Care was taken in this procedure to allow time for adiabatic heat generation due to volume changes to be dissipated. System dead volume was needed in subsequent use of the apparatus in order to calculate mass of reactant necessary to affect a target concentration. The dead volume of our present system is  $0.000136 \text{ m}^3$ . This valve corresponds to the fully closed press condition.

Resistance to reactant flow from the supply system into the treatment chamber is an important issue. This is particularly so since the porous graphite platens could limit efficiency. In order to derive effective permeability of the device, a range of pressure differentials between inlet and outlet ports were applied and consequent mass flow (of air) was measured electronically. Thus from this measured volumetric flow rate, and related known pressures, flow resistance (R) of the pressing system was calculated by using the following equation based on Newtonian viscous flow.

$$R = \frac{(P_1^2 - P_2^2) * t}{2\eta P V_p}$$

Where:

$V_p/t$  = is volumetric flow rate at a particular pressure of P ( $\text{m}^3/\text{Sec}$ ),



$P_1$  = is the in-let pressure (Pa),

$P_2$  = is the pressure in the out-let (Pa),

$\eta$  = is viscosity of fluid (N.Sec.m<sup>-2</sup>),

$R$  = is resistance to flow (m<sup>-3</sup>).

The supplied fluid (air) pressure and consequent measured flow rate is given in the Table below.

The supplied air pressure and consequent flow rate of the sealed pressing system.

Air Pressure (Pa)	Flow rate (m <sup>3</sup> /Sec) (at pressure of 102325 Pa)
128896	0.0001097
142682	0.0001582
156467	0.0002037
170253	0.0002444
308110	0.0006844
377039	0.0008260
445968	0.0009676
514896	0.0011328
583825	0.0012980

Figure 5.2 shows flow resistance plotted against flow rate. This figure indicates, as expected, that with increase of flow rate, resistance to flow also increases. That means at higher pressure flow is limited in the system.

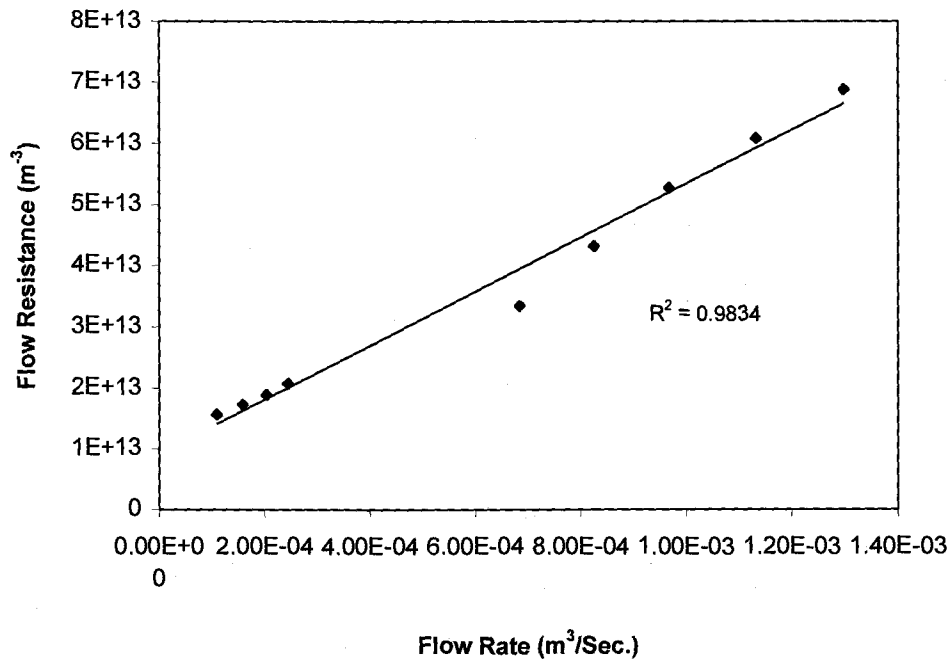


Figure 5.2 Flow resistance versus flow rate in the pressing system.

#### 5.1.2. Position cross-check

The pressing system may be operated in either position or load control modes. In either case, it is important to be able to accurately control separation of the pressing surfaces or measure deformation when applying compressive loads to samples. This was, however, a limitation of the MTS system available.

Performance could clearly be improved considerably by mounting the pressing system on a superior servo-hydraulic setup. An indication of the quality of control may be seen in Figure 5.3 which represents the linkage between requested (from control software) and measured positions of the lower platen with respect to the

upper platen one. The figure shows that the measured position varied within  $\pm 0.75$  mm from that requested.

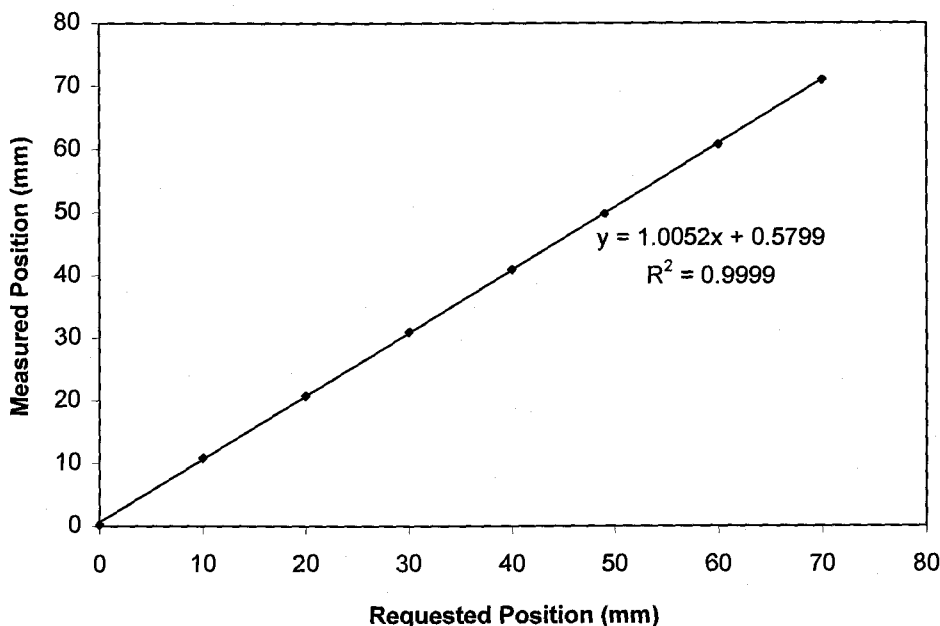


Figure 5.3 Position cross-check of the sealed pressing system.

### 5.1.3. Calibration of proportionally opening electronic servo-valve control system

Considerable effort was devoted to the design and construction of servo-control systems capable of maintaining a target (pre-set) gas pressure inside the press chamber under dynamically changing chamber conditions (including chamber volume, gas sorption into mats, and gas temperature changes). For this purpose an analog control device was developed. Signals from a pressure transducer connected to the chamber were electronically compared to target values provided by the

operator. Error signals were then amplified and used to activate a proportionally opening solenoid valve (MKS) to direct supply gas to the chamber (when a pressure deficit prevailed). When chamber pressures exceeded target values (principally during press closing when chamber volume decreased) a solenoid operated venting valve was activated. Both gas injection and venting sides of the control unit were proportional (valve opening proportional to error) which maximized control accuracy. Figure 5.4 represents the calibration of the

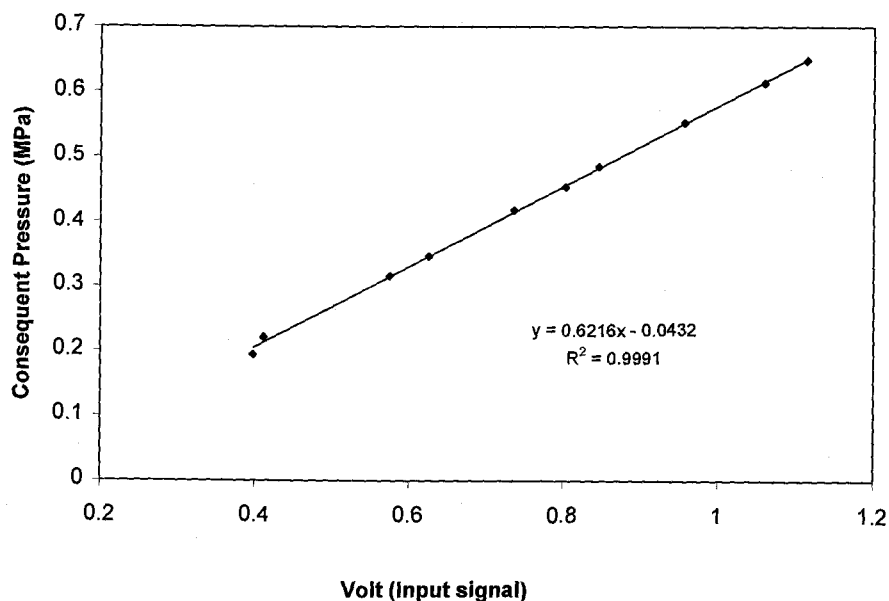


Figure 5.4 Calibration of the proportionally opening electronic servo-valve control system.

proportionally opening electronic servo-valve. The figure shows that 1 Volt input signal led to a gas pressure of 0.621 MPa.

## **5.2. Softening action of gaseous ammonia**

According to Davidson (1968), wood can be plasticized by treating it with gaseous anhydrous ammonia at room temperature under an ammonia vapor pressure of 0.99 MPa (145 psi). It has already been made clear that no report of the softening action of gaseous ammonia on fiber networks has been found in the literature. In this research, the effectiveness of gaseous ammonia as a softening agent on fiber networks in terms of treatment time, treatment temperature and treatment vapor pressure was examined by using the newly developed sealed pressing system. It has thereby been demonstrated that the pressing system can be used for chemical treatment of furnish materials.

### 5.2.1. Ammonia treatment time and temperature effects

As mentioned earlier, in the treatment time and temperature experiments, the effectiveness of gaseous ammonia as a softening agent for fiber networks was compared in terms of density development under controlled load with pressing time after ammonia treatment.

In this experiment, variously treated mats were therefore compressed under a constant pressure of 8.4 MPa and their consolidation was recorded with time. As would be expected, the mat behaved viscoelastically. One example plot of the variation of mat thickness with time is shown as Figure 5.5. The development of a viscoelastic model of the material under different ammonia treatment conditions is

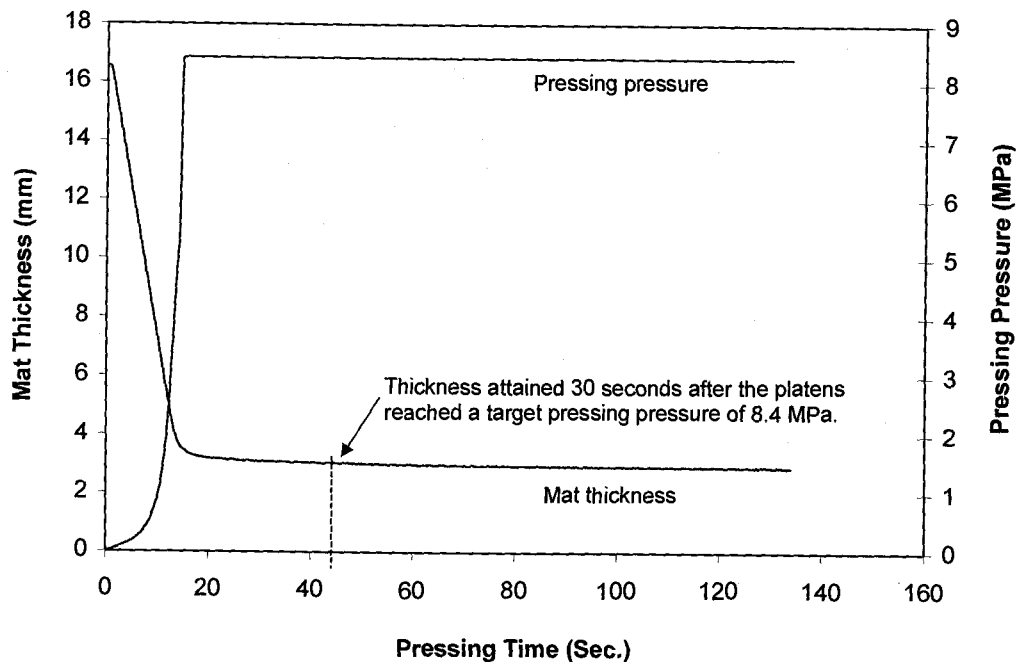


Figure 5.5 A typical plot of mat thickness variation with pressing time (in this case following 300 seconds of ammonia treatment).

beyond the scope of the present work since only proof of the viability of ammonia softening was necessary here. Such rheological analyses have, however, been conducted in earlier related projects at OSU (Ren, 1992 and Ren and Humphrey, 1999) and a 5-element modified Burger's model (with each element being non-linearly correlated with temperature, moisture content and mat density) has been developed. The sealed pressing system may be used in future studies to derive data to enable such material property models to be developed which account for chemical modification (such as ammonia softening).

For the purposes of the present study, curves of time versus mat thickness under force control have been used in a highly simplified fashion to infer the effects of ammonia on softening. Figure 5.6 shows the effect of ammonia treatment time on the density attained 30 seconds after the platens reached the target pressing pressure of 8.4 MPa. Here, density development reflects the softening action. There is some variability among the values of density developed with treatment time. Still, this figure indicates two important findings.

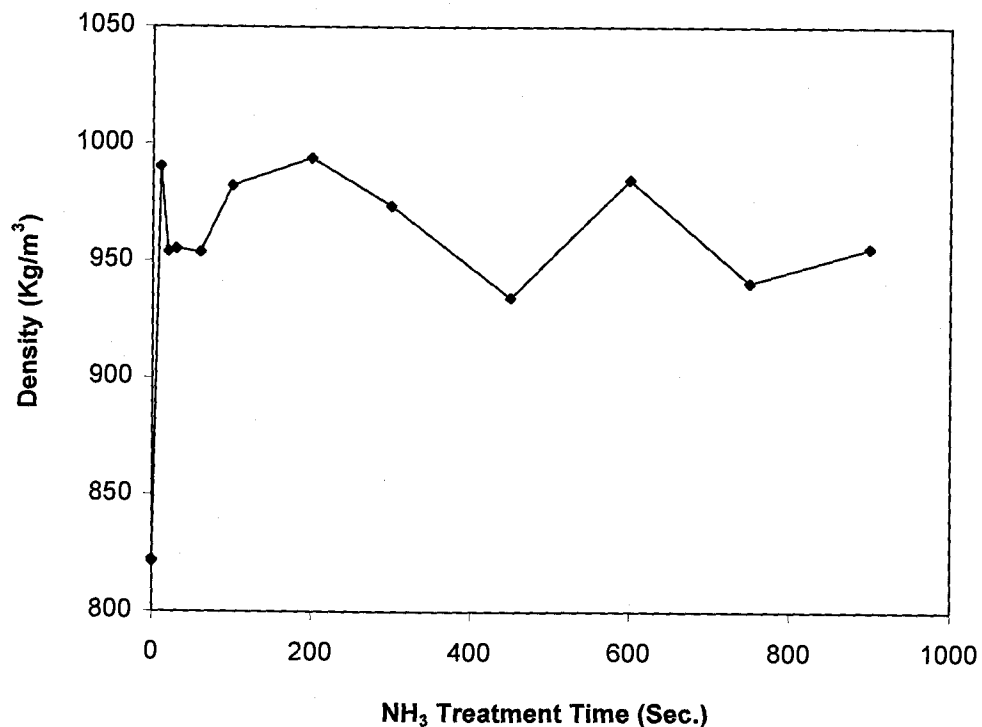


Figure 5.6 Effect of ammonia treatment time on density development (30 seconds after the platens reached a target pressing pressure of 8.4 MPa).

- I. There is a big difference in density values between the control (without ammonia pre-treatment) and all of the ammonia treated fiber networks; and
- II. The figures also show that treatment time is not an important factor in affecting ammonia softening of fibers. Small treatment times may be sufficient to produce significant and useful levels of softening in fiber networks -- at least under the concentration and temperature conditions used in this experiment.

Similar to Figure 5.6, Figure 5.7 represents the effect of ammonia treatment temperature on density attainment after 30 seconds of pressing at constant pressure. In ammonia treatment temperature experiments, the fiber networks were treated

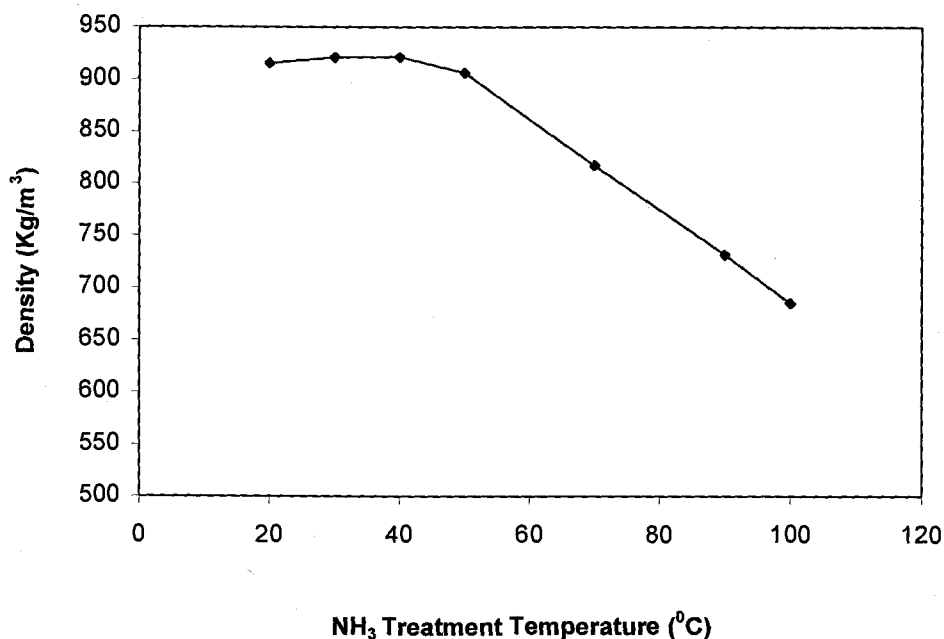


Figure 5.7 Effect of ammonia treatment temperature on density development (after 30 seconds of pressing with constant pressure of 8.4 MPa).



with ammonia of 11% relative vapor pressure. Figure 5.7 shows that at lower temperatures, such as between 20<sup>0</sup>C to 40<sup>0</sup>C, there is no remarkable change in the values of the density developed and implied softening. However, above 40<sup>0</sup>C the softening effect decreases. This result is surprising since one may expect that increasing temperature would increase the mobility and action of ammonia molecules in the walls of wood fibers. This result may be due to the decrease in ammonia density with the increase of temperature since constant relative vapor pressures were used during these experiments. Davidson and Baumgardt (1970) indicated that in the case of solid wood, softer and more easily formable material would result at higher temperature but all of those experiments were carried out at room temperature and below. In retrospect, an increase in softening action with temperature may have been detected here if the density of ammonia (and consequent number of available molecules) were kept constant rather than percentage of saturated pressure (where vapor density decreases with temperature). In light of this result, it was elected to conduct experiments with varying gas pressure (see Section 5.2.2 below) in order to clarify this and other issues.

#### 5.2.2. Ammonia treatment vapor pressure effects

This part of the experiment was done in a different way than the ammonia treatment time and temperature experiments. This experiment was carried out to explore the rate at which ammonia penetrates and subsequently softens mats after they have been compressed to a target density.

Softening would, it was anticipated, lead to a reduction in counterpressure (force needed to maintain a fixed platen position). Clearly, once closure of the press was complete, stress relaxation would occur due to the visco-elastic nature of the fiber networks even in the absence of ammonia. Figure 5.8 shows a typical response of counterpressure (corrected for variables identified in Section 4.3.3.1.3) with respect to treatment with ammonia vapor at a pressure of 0.42 MPa and 55% saturation. According to this figure, as press closing proceeds, the counterpressure increases to a peak at target mat thickness. The compressed fiber mat subsequently sustained stress relaxation which initially progressed at a rapid rate (approximately 1.6 MPa/sec) and then progressively slower rates. At a selected point after press

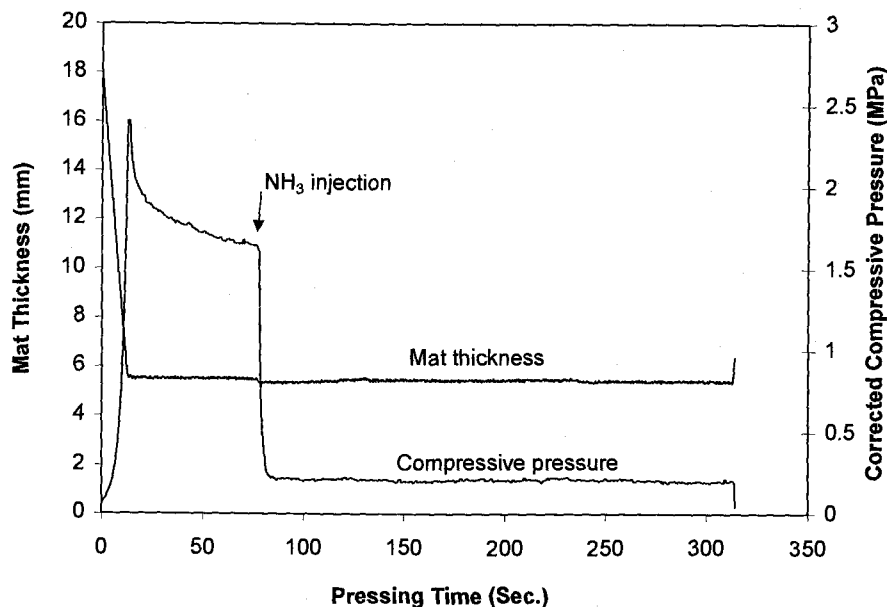


Figure 5.8 Stress relaxation with ammonia injection after press closure (with ammonia vapor pressure of 0.42 MPa).

closure and once the stress relaxation rate had decreased substantially (60 seconds after press closure the rate had levelled off to 15 KPa/Sec) ammonia gas was injected into the mat.

Importantly, a big drop of pressure was evident almost instantly upon ammonia injection (Figure 5.8), which represents the softening action of ammonia. Figure 5.9 shows that the rate of softening (rate of compressive pressure drop) of the fiber network by ammonia gas is very rapid. The results indicate that compressed natural fiber networks are very much accessible to  $\text{NH}_3$  gas. The rate of

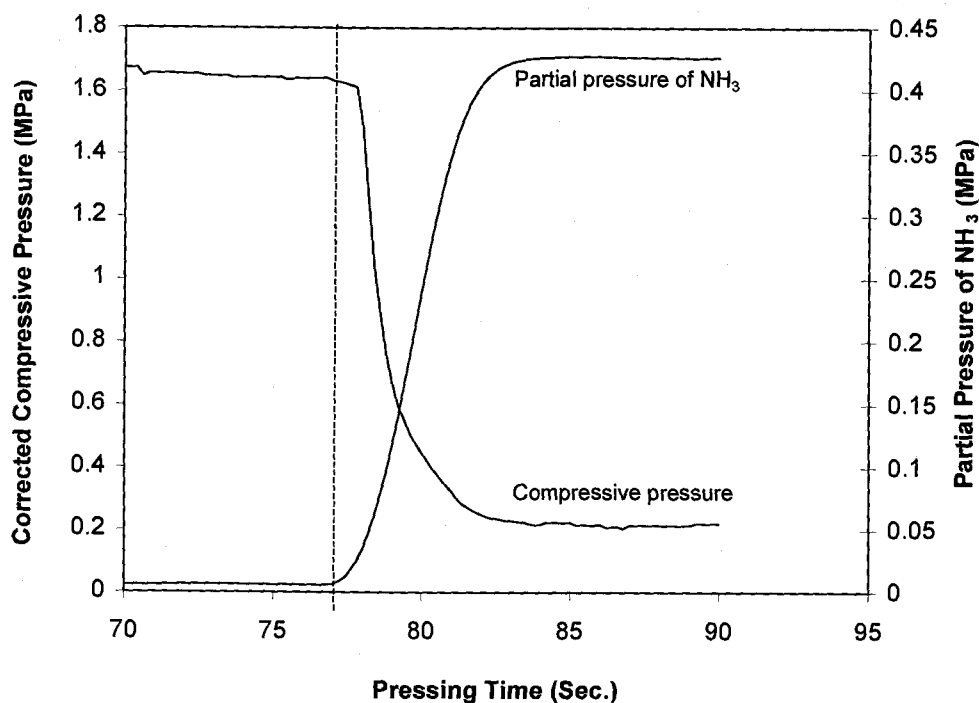


Figure 5.9 A typical close-up of the compressive pressure drop curve upon  $\text{NH}_3$  injection (with  $\text{NH}_3$  vapor pressure of 0.42 MPa).

penetration of  $\text{NH}_3$  gas into compressed fiber networks must be very fast – indeed, much faster than the limited diffusion in wood. The chemical reactivity (action) of  $\text{NH}_3$  gas on individual fibers in the network also appears to be very fast which results in significantly fast softening of the fiber network. The findings (fast softening rate) of this experiment might open a new era in the possibilities of processing (for softening) of fibers or fiber networks in an industrial process.

An attempt is here made to numerically relate the rate of ammonia pressure increase to associated decrease in counterpressure. For this purpose the quotient of counterpressure divided by ammonia pressure is plotted against time elapsed after ammonia introduction. The shape of Figure 5.10 supports the assertion that ammonia pressure and associated reduction in counterpressure closely track

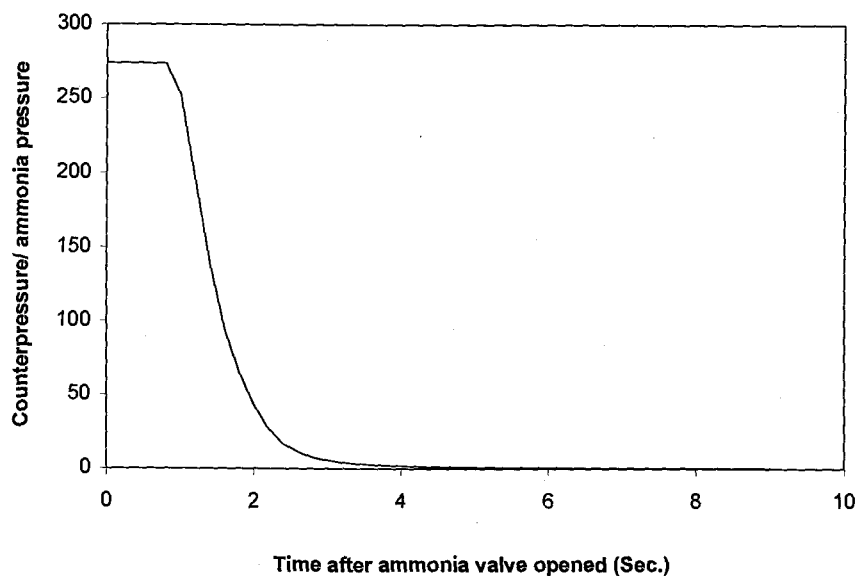


Figure 5.10 Quotient of counterpressure over ammonia pressure versus elapsed time.

each other and that there is little time delay in the material's response. This assertion is further supported by the fact that once ammonia pressure has stabilized, there is very little subsequent change in counterpressures. This suggests that penetration of ammonia to the core of the sample is very rapid and that there is little delay in the action of ammonia within the cell wall.

These findings appear to contradict the suggestion of Schuerch (1964) mentioned in Section 2.5.4.2.1 that there are time-dependent chemical transformations associated with  $\text{NH}_3$ -wood interaction. Alternatively, if slow reactions do occur, then they appear not to be associated with softening. The speed of the effect also suggests that the permeability of mats compressed to relatively high levels ( $525 \text{ Kg/m}^3$  in this case) is not limiting. Measurements of the permeability of similar mats in a related study (Haselein, 1998; Haselein and Humphrey, 1999) suggest that the mats had a permeability of  $10^{11} \text{ m}^2$  at a density of  $525 \text{ Kg/m}^3$ . This compares with values in the order of  $10^{16} \text{ m}^2$  for solid wood (Douglas fir heartwood) in the transverse direction.

Measurements were made of gas pressures at the core layer of sample mat during pressing (where ammonia treatment was followed by methyl formate injection). This was done by inserting a stainless steel tube into the mat prior to its consolidation and connecting this tube to a gas pressure transducer. In the resultant graphs (an example of which is presented as Appendix C), it is clear that rapid changes in external ammonia pressure were rapidly translated to the core.

One of the main reasons that initial experiments with ammonia were conducted on unconsolidated (loose) mats was that it was expected that penetration would then be unrestricted by resistance to flow (high permeability). Evidently, this appears not to be a limitation.

Figure 5.11 represents the effect of the level of the ammonia vapor pressure on its softening action on fiber networks. This effect has been expressed as the percentage reduction of counterpressure compared to that prevailing immediately before ammonia injection. The figure indicates that initially, at low vapor pressures of ammonia, with the increase of the level of ammonia vapor pressure the

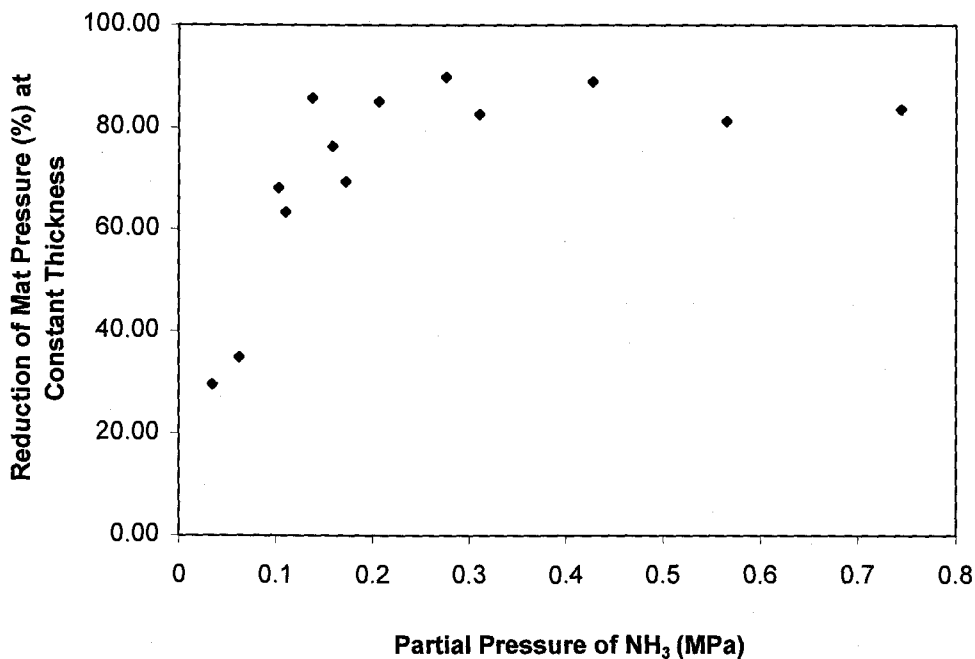


Figure 5.11 Effect of ammonia partial pressure on its softening action on fiber networks.

percentage reduction of pressure also increases and then the graph flattens at higher levels (above 0.16 - 0.20 MPa) of ammonia treatment vapor pressure. This trend suggests that low vapor pressures (say about 0.16 MPa) of ammonia might be sufficient to produce the desired level of softening in the fiber networks. This finding also has a significant impact on the possibilities of using  $\text{NH}_3$  gas as a softening agent for fibers or fiber networks in future industrial processes.

Overall, the findings of this part of the studies indicate that moderate vapor pressures of ammonia can rapidly and efficiently soften fiber networks at room temperature.

### **5.3. Bond strength development studies**

This part of the research was carried out to understand the likely interaction of ammonia, methyl formate (MeF) and phenol-formaldehyde (PF) adhesive in the bond formation processes operative in mat formation. An objective was to derive a qualitative understanding of the likely response of bonds between fibers in the sealed pressing system.

The set of bond strength development data at room temperature (for PF adhesive-to maple bonds) is shown in Figure 5.12. Each point in this figure represents the bond strength developed at that particular pressing time. This figure shows that at the early stages of bond formation (the first 200 seconds), bond strength development was almost linear with bond forming time. It is interesting to note that the PF developed about 1.5-1.6 MPa of bond strength at room

temperature, albeit at a very slow rate. Although this strength is only modest and the rate is low, it does show that the adhesive had some reactivity at room temperature. This set of data was used as a control to compare the effect of ammonia, methyl formate, and both on the strength development of PF adhesive-to-maple bonds.

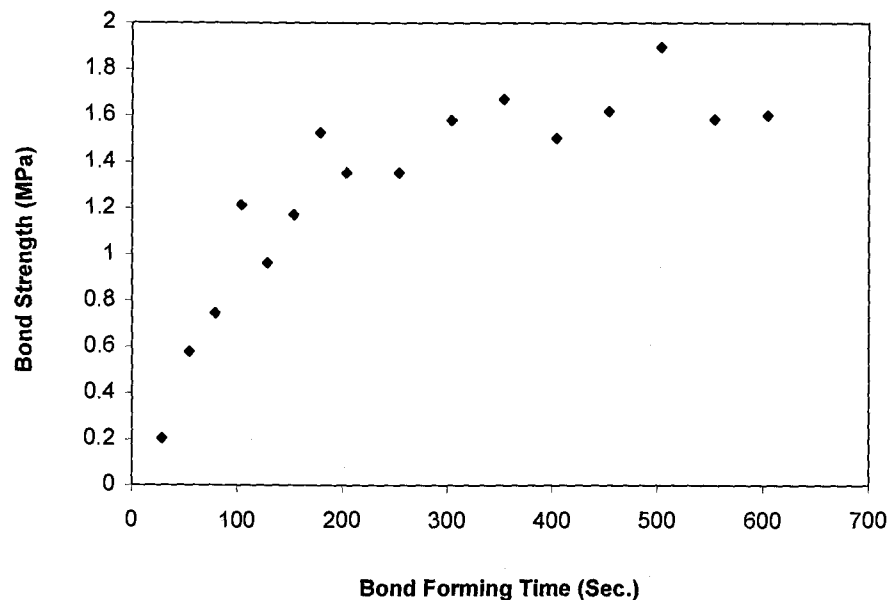


Figure 5.12 A typical set of bond strength development data at room temperature (in this case for PF adhesive-to-maple bonds).

Figure 5.13 represents the accumulated shear strength values for bonds formed at room temperature, at various bond forming times and with various combinations of chemical treatments. The trend of the different series of data in the figure clearly indicates the following points:



- I. The bond strength developed by PF + MeF, and PF + NH<sub>3</sub> + MeF were much higher than the bond strength developed by only PF and PF + NH<sub>3</sub>.
- II. The differences of the bond strength between only PF and PF + NH<sub>3</sub> is not noticeable though the PF + NH<sub>3</sub> series shows slightly higher values.

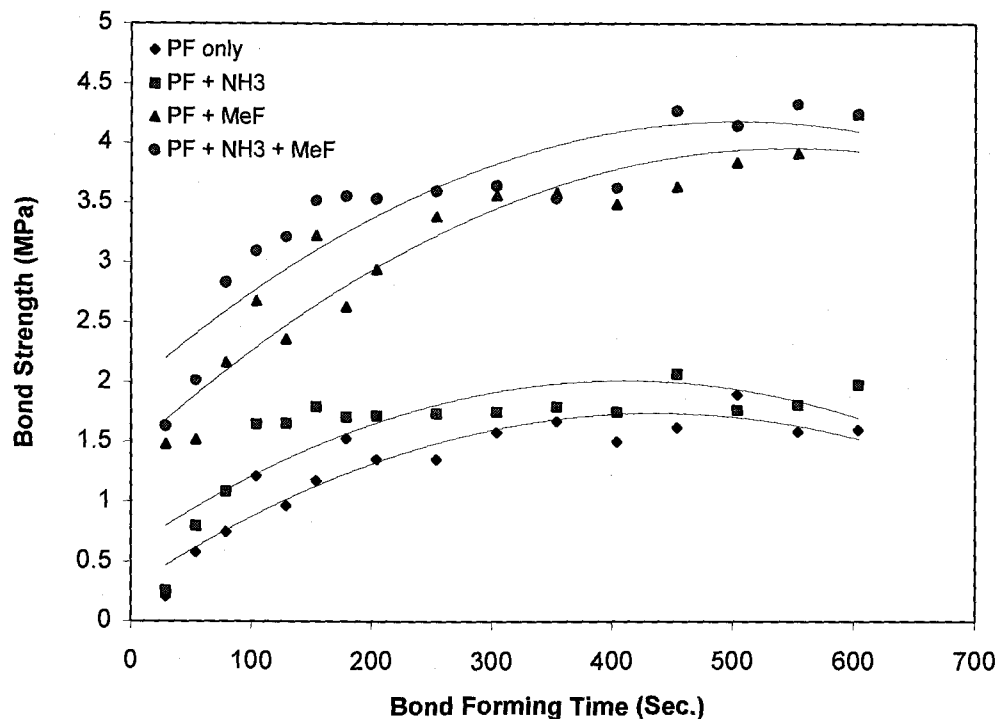


Figure 5.13 Accumulated shear strength values for bonds formed at room temperature, at various bond forming times and with various chemical treatments.

- III. Similarly, the differences of the bond strengths between PF + MeF and PF + NH<sub>3</sub> + MeF is also not noticeable though the latter type of series shows slightly higher values.

Also to describe the effect of different chemicals on the bond strength statistically, five bonds of each treatment type were formed at 308 seconds of pressing time. Analysis shows that there is a significant difference in bond strength between:

- Only PF and PF + MeF (P value =  $7.28 \times 10^{-7}$ ),
- Only PF and PF + NH<sub>3</sub> + MeF (P value =  $1.47 \times 10^{-8}$ ),
- PF + NH<sub>3</sub> and PF + MeF (P value =  $9.66 \times 10^{-7}$ ), and
- PF + NH<sub>3</sub> and PF + NH<sub>3</sub> + MeF (P value =  $1.75 \times 10^{-8}$ ).

However, the difference between PF and PF + NH<sub>3</sub> was not significant (P value = 0.31) and also the difference between PF + MeF and PF + NH<sub>3</sub> + MeF was not significant (P value = 0.36).

From the above discussion it is clear that the influence of ammonia on bond strength development of PF adhesive at room temperature is small or negligible. However, the influence of methyl formate on bond strength development of PF adhesive even at room temperature is significant. As described earlier in this thesis, the probable reasons for significant positive influences of methyl formate may be:

- the presence of the equivalent of another tri-functional reagent (compared to the difunctionality of formaldehyde instance),
- a phenolic nucleus on which a methylol group is already present coming from a trifunctional to at least a tetra-functional reagent, and
- the higher concentration of reagents (the ester here being a proper reagent and not a catalyst).

To examine the action of methyl formate following partial pressing of bonds, methyl formate was injected to the bonds after 400 seconds of pressing (i.e. delayed injection of methyl formate) and the results of that experiment are presented in Figure 5.14. This figure indicates that delayed injection of methyl formate to the bond has a similar positive influence on the bond strength

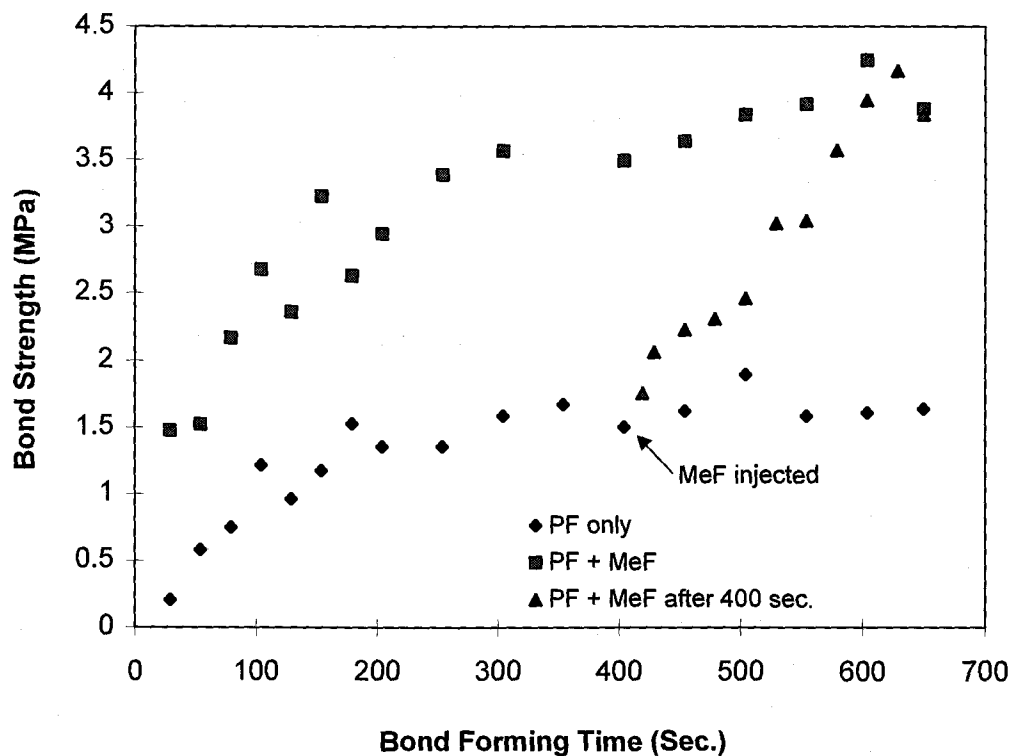


Figure 5.14 Bond strength in delayed (after 400 seconds) injection of methyl formate.

development. The findings will also be helpful for industrial application of methyl formate for low temperature curing of PF resin in wood-based composite manufacturing.

#### **5.4. Characterization of trial fiber disks**

In this part of the research, a trial was made to form some samples by using the newly developed sealed pressing system by treating the fiber-PF-resin-mix mats, first with ammonia for softening and then with methyl formate to cure the glue at near ambient temperature (about 40<sup>0</sup>C). Some samples were also formed by treating the fiber-PF-resin-mix mats only with ammonia and only with methyl formate. Samples pressed with PF adhesive alone at 40<sup>0</sup>C did not hold together, and strength properties of this category are shown as zero in the results below.

##### **5.4.1. Thickness swelling**

Figure 5.15 shows the rate of thickness swelling of the different types of samples as a result of water soaking. The thickness swelling of the NH<sub>3</sub> + MeF treated (GAM) samples (both HD and LD) are greatly reduced compared to the conventionally hot pressed (HP) (HD and LD) samples. The rate of thickness swelling of MeF treated (GM) samples are also less than HP samples. However, the rate of thickness swelling of NH<sub>3</sub> treated samples are much higher than the

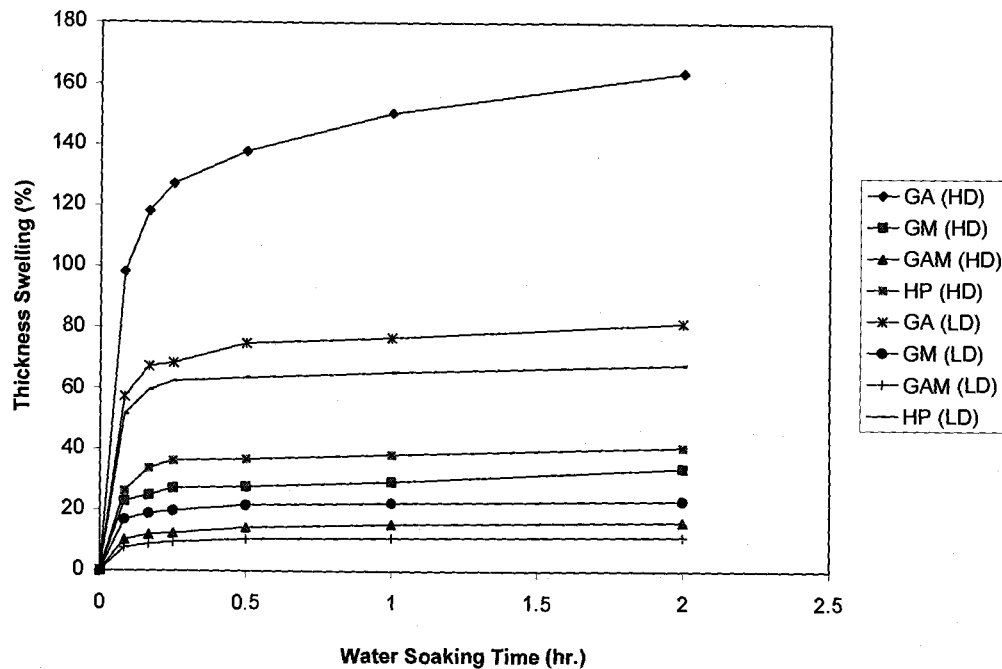


Figure 5.15 Thickness swelling of the different types of samples as a result of water soaking.

HP samples. Swelling rates are especially important when the composites are used in fluctuating humidity conditions. In this experiment  $\text{NH}_3 + \text{MeF}$  treatment produced dramatic reductions in the rate of swelling.

Figure 5.16 shows the average extent of thickness swelling of the different samples after 24 hours of water soaking. Hot pressed (HP) samples (HD) had swollen 45.62% (SD 8.12) in thickness, whereas GAM samples (HD) swelled only 18.71% (SD 2.16). This reduction of thickness swelling may be due to the reduction of irreversible swelling by the ammonia's softening action. The thickness swelling of  $\text{NH}_3$  treated samples (HD) was very high (more than 4 times that of

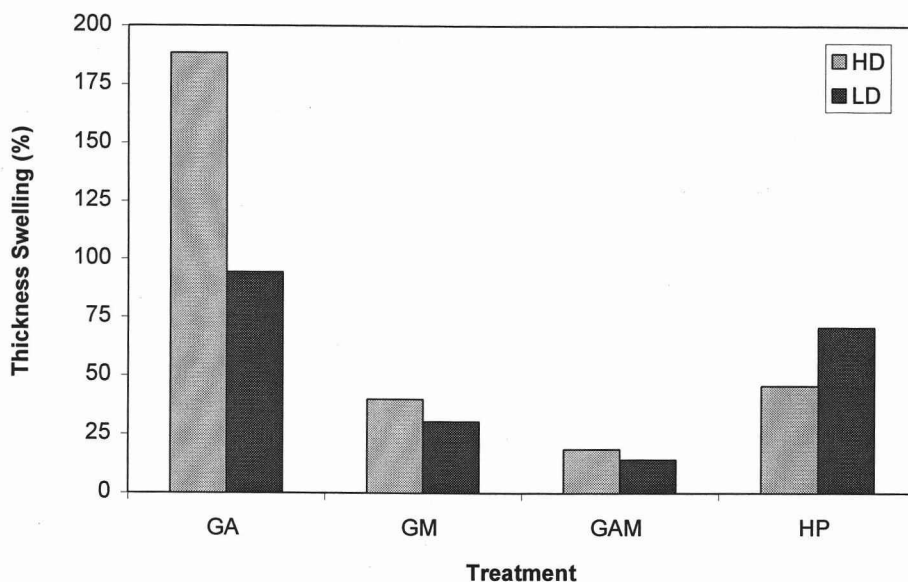


Figure 5.16 Thickness swelling of different types of samples after 24 hours water soaking.

HP (HD) samples. This high thickness swelling indicates that there may be no or very little adhesive bonding in the samples treated with  $\text{NH}_3$  alone which clearly indicates that the influence of ammonia on PF adhesive curing at  $40^\circ\text{C}$  is small or negligible.

#### 5.4.2. Tensile strength

Figure 5.17 illustrates the average value of the tensile strength (TS) found for the samples produced by the different types of treatment. As shown in the figure, HP (HD) samples had the highest Tensile strength. The tensile strength of

GAM (HD) samples formed at 40<sup>0</sup>C was more than 77% that of the HP (HD) samples which were formed at 160<sup>0</sup>C. However hot pressed (LD) samples had lower tensile strengths (about 67.4%) than GAM (LD) samples.

This finding, together with results of the swelling experiments, shows great promise for the use of NH<sub>3</sub> + MeF in natural fiber composites formation. More research will, however, be necessary to explore the optimum conditions under which to produce high quality products and products with properties tailored to specific applications. In this research, only one set of pressing conditions were used in order to demonstrate the approach.

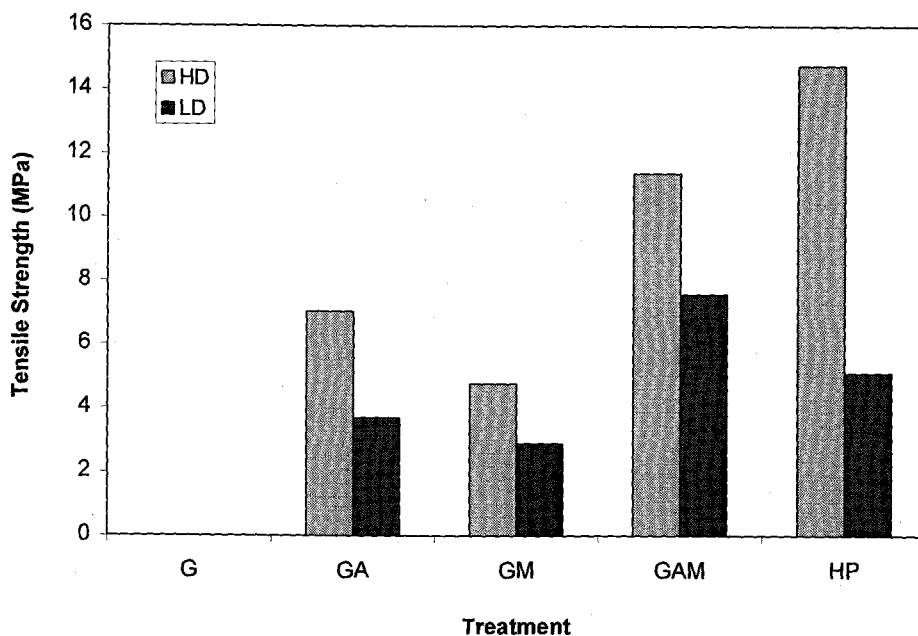


Figure 5.17 Tensile strength of the different types of samples.

Samples treated with methyl formate alone (GM) also gained some strength, but it is likely that, in the absence of a softening agent, residual internal stress upon press opening was high. Such high stress could have broken bonds between fibers and likely also led to the relatively high swelling of the sample. The methyl formate almost certainly did, however, lead to adhesive cure. The absence of ammonia softening could also have led to a lower degree of inter-fiber contact. Bonding area within the micro-structure could also, therefore have been less than with ammonia softened systems.

Samples treated with ammonia alone (GA) also had tensile strengths which were higher than methyl formate treated (GM) samples, but their strength was much lower than fully treated (GAM) samples. The possible reason for the strength of GA samples may be due to ammonia softening which could have led to a higher degree of inter-fiber contact and thus fibers formed some hydrogen bonding.

#### 5.4.3. Bending strength

Figures 5.18 and 5.19 show average values of the modulus of rupture (MOR) and modulus of elasticity (MOE) respectively for range of sample types. Trends for elasticity follow those of tensile strength on most regards. The modulus of rupture of GAM (HD) samples formed at 40<sup>0</sup>C was more than 43%, that of the HP (HD) samples which were formed at 160<sup>0</sup>C and the modulus of elasticity of GAM (HD) samples was more than 45%, that of the HP (HD) samples. However,



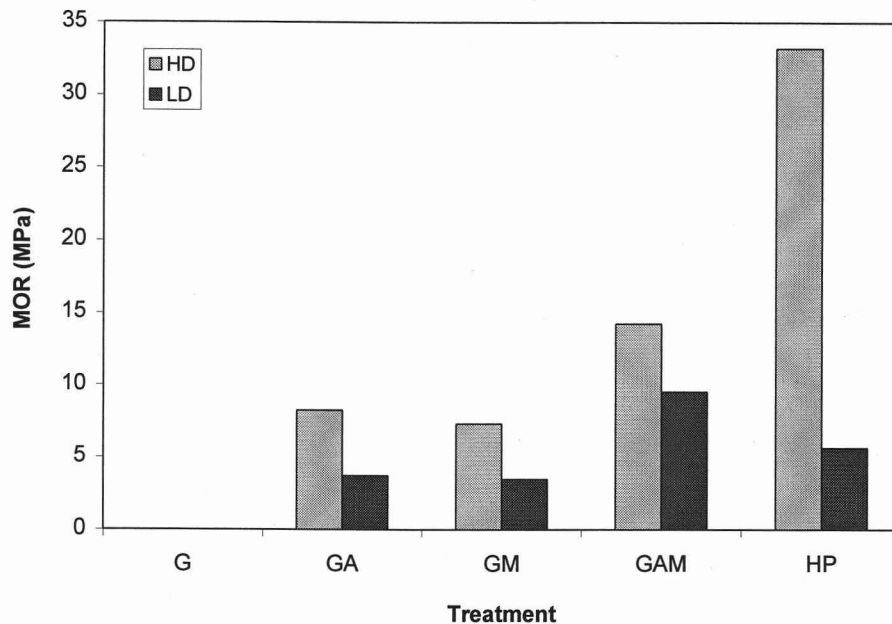


Figure 5.18 Modulus of rupture (MOR) of the different types of samples.

hot pressed (LD) samples had lower MOR and MOE values than GAM (LD) samples.

The physical and mechanical properties of the trial fiber disks presented here are very encouraging. However, only one set of pressing conditions were used in the fiber disks formation trials. More research will be required over a large range of chemical, thermal and mechanical conditions to find out the optimum conditions to synthesize useful material.

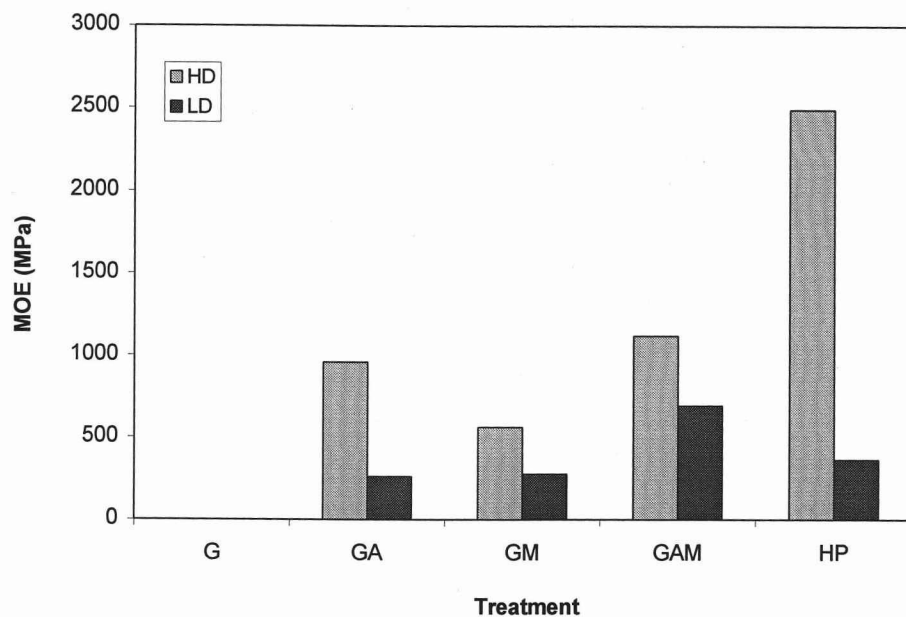


Figure 5.19 Modulus of elasticity (MOE) of the different types of samples.

## CHAPTER 6. CONCLUSIONS AND POSSIBLE FUTURE RESEARCH

### 6.1. Conclusions of the current research

The following are the principal conclusions of the current work:

- This research has developed and used an automated system and technique for sealed pressing of pre-formed natural fiber networks under highly controlled (dynamic) chemical, thermal and mechanical (stress) conditions. This system has provision for chemical (vapor phase) injection and removal, which was used for chemical treatment and consolidation of natural fiber networks in situ. It was also used for characterization of the softening action of ammonia on natural fiber networks.
- The softening action of gaseous ammonia on natural fiber networks has been investigated in terms of treatment time (10 sec to 900 seconds, 19<sup>0</sup>C, 0.62 MPa ammonia vapor pressure, and moisture content of mats 10%), treatment temperature (20<sup>0</sup>C to 100<sup>0</sup>C, at 11% relative vapor pressure of ammonia, and moisture content of mats 10%), and treatment vapor pressure of ammonia (0.0345 MPa to 0.7444 MPa, 19<sup>0</sup>C, time 60 seconds, and moisture content of mats 10%). Results showed that moderate vapor pressures of ammonia can rapidly penetrate and soften the fiber networks at room temperature.
- This study investigated the effect of gaseous ammonia, methyl formate (liquid) and both of them on the shear strength development kinetics of phenol-formaldehyde (PF) resin-to-wood bonds by using a specially modified

Automated Bond Evaluation System (ABES) operated at ambient temperature. Bonding studies showed that methyl formate has a significant positive influence in PF curing, even at room temperature. The influence of ammonia is small or negligible. This information helped in the scheduling of the sequential treatment of ammonia and methyl formate during formation trials of fiber disks.

- Sample formation trials have been conducted by treating a natural fiber-PF-resin mix first with ammonia and then curing the resin by injecting methyl formate vapor at 40<sup>0</sup>C (above the boiling point of methyl formate). These sample formation studies indicated that there is potential to create good products by using ammonia and methyl formate in the sealed pressing system, and to do this rapidly at near-ambient temperatures. Further, since the system is sealed, noxious chemical treatments are possible.

## **6.2. Possible future research**

- The refinement and improvement of the experimental techniques that have been developed for chemical treatment and sealed pressing in situ may lead to its use industrially to improve present manufacturing processes and products. Considerable further development is, however, needed before this potential may be realized.
- The technique could be used to investigate the rheological phenomena that occur during the consolidation of natural fiber networks in composites manufacturing process which include chemical additives.

- A range of important furnish material properties (in addition to rheological ones) may be measured with the sealed pressing system. These include: thermal conductivity as functions of consolidation and chemical modification, and gas permeability as functions of consolidation.
- More research will be required over a large range of chemical, thermal and mechanical conditions to find optimum conditions to synthesize high performance natural fiber composites by treating the natural fiber-PF-resin mix mat with ammonia and methyl formate.
- Internal structure distribution within the formed samples also should be investigated and it could be related to internal property distribution.
- Some other chemical treatment/ modification methods such as treatment with diisocyanate, acrylonitrile, formaldehyde could be investigated in the sealed pressing system.
- Another possible investigation would be the epoxide treatment of fiber-PF (novolak)-resin mix and then curing the resin by injecting formaldehyde from some source.

## BIBLIOGRAPHY

- Agarwal, S. C., K. Kohli, N. K. Shukla and S. Kumar. 1985. Mechanical properties of wood with thioacetic acid. *Journal of the Indian Academy of Wood Science* 16(2):61-67.
- Akitsu, H., M. Norimoto, and T. Morooka. 1991. Vibrational properties of chemically modified wood. *Mokuzai Gakkaishi* 37 (7):590-597.
- Akitsu, H., M. Norimoto, T. Morooka and R. M. Rowell. 1993. Effect of humidity on vibrational properties of chemically modified wood. *Wood and Fiber Science* 25(3):250-260.
- Alder, E. 1977. Lignin chemistry - past, present and future. *Wood Science and Technology* 11:169-218.
- American Society for Testing and Materials. 1989. Standard methods of evaluating the properties of wood-based fiber and particle panel materials. ASTM D 1037. American Society for Testing and Materials, Philadelphia, PA.
- Anon. 1970. Indian Forest Utilization. Vol 1, Forest Research Institute & college, Dehra Dun, India. pp 329-347.
- Baechler, R. H. 1959. Improving wood's durability through chemical modification. *Forest Products Journal* 9:166-171.
- Baird, B. R. 1969. Dimensional stabilization of wood by vapor phase chemical treatments. *Wood Fiber* 1:54-63.
- Banks, W. B. 1990. Derivatization of wood. In *Cellulose sources and exploitation, industrial utilization, biotechnology and physico-chemical properties*, ed. J. F. Kennedy, G. O. Phillips, P. A. William, 221-234. Ellis Horwood, New York.
- Bariska, M. 1975. Collapse phenomena in beechwood during and after NH<sub>3</sub>-impregnation. *Wood Science and Technology* 9:293-306.
- Bariska, M. and C. Schuerch. 1977. Wood softening and forming with ammonia. In *Wood technology: chemical aspects*, ed. I.S. Goldstein, 326-347. American Chemical Society Symposium Series 43. American Chemical Society, Washington, D.C.

- Bariska, M., C. Skaar and R. W. Davidson. 1969. Studies of the wood-anhydrous ammonia system. *Wood Science* 2(2):65-72.
- Barnes, H. M., E. T. Choong, and R. C. McIlhenny. 1969. Several vapor phase chemical treatments for dimensional stabilization of wood. *Forest Products Journal* 19(3):35-39.
- Barry, A. J., F. C. Peterson and A. J. King. 1936. X-ray studies of reactions of cellulose in non-aqueous systems I. Interaction of cellulose and liquid ammonia. *Journal of the American Chemical Society* 55:333.
- Barth, B. P. 1977. Chapter 23 in *Handbook of Adhesives*, 2<sup>nd</sup> Ed., ed. I. Skeist, Van Nostrand Reinhold, New York.
- Biermann, C. J. 1993. *Essentials of pulping and papermaking*. Academic Press, Inc. Harcourt Brace Jovanovich, Publishers, New York. pp 36.
- Bolton, A. J. and P. E. Humphrey. 1989a. The hot pressing of dry-formed wood-based composites Part III. Predicted vapour pressure and temperature variation with time, compared with experimental data for laboratory boards. *Holzforchung* 43(4):265-274.
- Bolton, A. J. and P. E. Humphrey. 1989b. The hot pressing of dry-formed wood-based composites Part IV. Predicted variation of mattress moisture content with time. *Holzforchung* 43(5):345-349.
- Clemons, C., Young, R. A. and Rowell, R. M. 1992. Moisture sorption properties of composite boards from esterified aspen fiber. *Wood and Fiber Science* 24(3):353-363.
- Clermont, L. P. and F. Bender. 1957. The effect of swelling agents and catalysts on acetylation of wood. *Forest Products Journal* 7(5):167-170.
- Chowdhury, M. J. A. and P. E. Humphrey. 1999. The effect of acetylation on the shear strength development kinetics of phenolic resin-to-wood bonds. *Wood and Fiber Science* 31(3):293-299.
- Codd, P., W. B. Banks, J. A. Cornfield and G. R. Williams. 1992. The biological effectiveness of wood modified with heptadecenylsuccinic anhydride against to brown rot fungi: *coniofora puteana* and *Gloeophyllum trabeum*. International Research Group on Wood Preservation. Doc. No. IRG/WP 3705.

- Croon, I. and T. E. Timell. 1960. Distribution of substituents in a partially methylated 4-O-methylglucuronoxylan. *Canadian Journal of Chemistry* 38:720.
- Davidson, R. W. 1968. Plasticizing wood with anhydrous ammonia. Brochure prepared by New York State University, College of Forestry at Syracuse University, Syracuse, New York.
- Davidson, R. W. and W. G. Baumgardt. 1970. Plasticizing wood with ammonia – a progress report. *Forest Products Journal* 20(3):19-25.
- Davis, G. 1997. The performance of adhesive systems for structural timbers. *International Journal of Adhesion and Adhesives* 17(3):247-255.
- Ellis, W. D. and Rowell, R. M. 1984. Reaction of isocyanates with southern pine wood to improve dimensional stability and decay resistance. *Wood and Fiber Science* 16(3):349-356.
- Erinsh, P. and P. Odintsov. 1967. Changes in submicroscopic structure of wood at its plastification by ammonia water solutions. In *Modifikatsiya drevesing*, ed. T.A. Darzinsh, 15-21. Academy of Sciences of the Latvian SSR Institute of the Chemistry of Wood, Izdatelstvo "Zinatne" Riga, Russian.
- Fengel, D. 1971. Ideas on the ultrastructural organization of the cell wall components. *Journal of Polymer Science Part C* 36:383-392.
- Fujimoto, H. 1992. Weathering behaviour of chemically modified wood with a maleic acid-glycerol (MG) mixture. In *Chemical modification of lignocellulosics*, ed. D.V. Plackett and E.A. Dunningham, 87-96. FRI Bulletin No. 176, New Zealand Forest Research Institute, Rotorua, New Zealand.
- Fujimoto, H., T. Anazawa, Y. Ohmiya and K. Yamagishi. 1991. Dimensional stability of a maleic acid-glycerol (MG) treated particleboard: effect of MG contents and hot-press temperature. *Mokuzai Gakkaishi* 37(5):456-461.
- Fujimoto, H., T. Anazawa and K. Yamagishi. 1989. The production of dimensionally stable particleboard - chemical treatment with maleic acid and glycerol mixture. *Proceeding of the 23th international particleboard/ composite materials symposium*, 23:95-114. Pullman, Washington, USA.
- Gierer, J. 1982. The chemistry of delignification I. *Holzforshung* 36:43-51.
- Gierer, J. 1982. The chemistry of delignification II. *Holzforshung* 36:55-65.



Goldstein, I. S., W. A. Dreher, and E. B. Jeroski. 1959. Wood processing inhibition against swelling and decay. *Industrial and Engineering Chemistry* 51(10):1313-1317.

Goldstein, I. S., E. B. Jeroski, A. E. Lund, J. F. Nielson, J.M. Weater. 1961. Acetylation of wood in lumber thickness. *Forest Products Journal* 11:363-370.

Goring, D. A. I. 1971. Polymer properties of lignin and lignin derivatives. In: *Lignins: occurrence, formation, structure and reactions*, ed. K.V. Sarkanen and C.H. Ludwig. 695-768. Wiley-Interscience, New York.

Goring, D. A. I., T. E. Timell, 1962. Molecular weight of native celluloses. *Tappi* 45(6):454-460.

Graf, V. G., H. Koch, R. Schiene und E. Schuster. 1971. Herstellung und festigkeit von platten aus ammoniakplastifizierten fasern (I). *Holztechnologie* 12:235-238.

Graf, V. G., H. Koch, R. Schiene und E. Schuster. 1972. Herstellung und festigkeit von platten aus ammoniakplastifizierten fasern (II). *Holztechnologie* 13:152-155.

Guevara, R. and A. A. Moslemi. 1984. The effect of alkylene oxides, furan resin and vinylpyrrolidinone on wood dimensional stability. *Wood Science and Technology* 18:225-240.

Hadi, Y. S. 1992. Acetylated flakeboard properties. In *Chemical modification of lignocellulosics*, ed. D.V. Plackett and E.A. Dunningham, 9-15. FRI Bulletin No. 176. New Zealand Forest Research Institute, Rotorua, New Zealand.

Haselein, C. R. 1998. Numerical simulation of pressing wood-fiber composites, Ph.D. thesis, Department of Forest Products, Oregon State University, Corvallis, Oregon, USA.

Haselein, C. R. and P. E. Humphrey. 1999. A technique to evaluate the permeability of fiber networks as a function of their consolidation. In review.

Haygreen, J. G. and J. L. Bowyer. 1989. *Forest Products and Wood Science An Introduction*, 2<sup>nd</sup> ed. Iowa State University Press, AMES, USA. pp 412-417.

Hons, D. N. -S. and N. Ou. 1989. Thermoplasticization of wood I. Benzylolation of wood. *Journal of Polymer Science: Polymer Chemistry Ed.* 27:2457-2482.

Hons, D. N. -S. and J. M. San Luis. 1989. Thermoplasticization of wood II. Cyanoethylation. *Journal of Polymer Science: Polymer Chemistry Ed.* 27:4143.

- Howsmon, J. A. and W. A. Sisson. 1954. Submicroscopic structure. In *Cellulose and cellulose derivatives*, ed. E. Ott, H.M. Spurlin and M.W. Grafflin. 231-346. Interscience Publishers, Inc., New York.
- Humphrey, P. E. 1993. A device to test adhesive bonds. US Patent No. 5,176,028. U.S. Patent Office, Washington, DC.
- Humphrey, P. E. 1994. Engineering composites from orientated network fibres: a strategy. *Second Pacific Rim Bio-Based Composites Symposium Proceedings*. Vancouver, Canada, November 6-9. pp. 2-8.
- Humphrey, P. E. 1996. Thermoplastic characteristics of partially cured thermosetting adhesive-to-wood bonds: the significance for wood-based composites manufacture. In *Towards the new generation of bio-based composite products*, ed. H. Kajita and K. Tsunoda, 366-373. *Proceedings from the third Pacific Rim Bio-Based Composites Symposium*, December 2-5, Kyoto, Japan.
- Humphrey, P. E. 1999. Bonding speed of adhesives used in wood-based composites – an automated evaluation system. Paper presented in the 33<sup>rd</sup> International Particleboard Composite Materials Symposium, April 13-15, Washington State University, Pullman, Washington, USA.
- Humphrey, P. E. and D. Zavala. 1989. A technique to evaluate the bonding reactivity of thermosetting adhesives. *Journal of Testing and Evaluation* 17(6):323-328.
- Imamura, Y., K. Nishimoto, Y. Yoshida, S. Kawai, T. Sato and M. Nakaje. 1986. Production technology for acetylated low-density particleboard (II) decay and termite resistance. *Wood Research* 73:35-43.
- Imamura, Y., B. Subiyanto, R. M. Rowell, T. Nilsson. 1989. Dimensional stability and biological resistance of particleboard from acetylated albizzi wood particles. *Wood Research* 76:49-58.
- Kalninch, A. I., V. N. Sergeeva and Z. N. Kreitsberg. 1967. Effect of 25% aqueous solution of ammonia on wood. In *Modifikatsiya drevering*, ed. T. A. Darzinsh, 7-13. Academy of Sciences of the Latvian SSR Institute of the Chemistry of Wood. Izdatelstvo "Zinatne", Riga, Russian.
- Kenaga, D. L., R. C. Sproull. 1951. Further experiments on dimensional stabilization by allylation. *Journal of the Forest Products Research Society* 1:28-32.

- Kiguchi, M. 1990a. Chemical modification of wood surfaces by etherification I. Manufacture of surface hot-melted wood by etherification. *Mokuzai Gakkaishi* 36(8):651-658.
- Kiguchi, M. 1990b. Chemical modification of wood surfaces by etherification II. Weathering ability of hot-melted wood surfaces and manufacture of self hot-melt bonded particleboard. *Mokuzai Gakkaishi* 36(10):867-875.
- Kiguchi, M. 1993. Chemical modification of wood surfaces by etherification IV. Benzoylation with solvent-dilution and vapor-phase methods. *Mokuzai Gakkaishi* 39(1):80-85.
- Kiguchi, M. and K. Yamamoto. 1992. Chemical modification of wood surfaces by etherification III. Some properties of self-bonded benzoylated particleboard. *Mokuzai Gakkaishi* 38(2):150-158.
- Kumar, S. and S. C. Agarwal. 1982. Chemical modification of wood with thioacetic acid. In *Graft copolymerization of lignocellulosic fibers*, ed. D. N. S. Hons, 303-320. American Chemical Society Symposium Series 187, Washington, D.C.
- Kumar, S., and Morrell, J. J. 1993. Improved composites from chemically modified particles. In *Protection of wood-based composite products*, ed. A. F. Preston, 33-37. Forest Products Society, Madison, WI 53705-2295.
- Lemon, P. H. R. B. 1990. An improved sand binder for steel castings. *International Journal of Materials and Product Technology* 5:1, 25-54.
- Mahdalik, M., J. Rajcan, M. Mlcousek and O. Labsky. 1971. Changes of some physical, mechanical, chemical properties of wood treated with liquid ammonia. *Journal of Polymer science: Part C* 36:251-263.
- Maloney, T. M. 1977. *Modern particleboard and dry-process fiberboard manufacturing*, Miller Freeman Publications, 367-412.
- Marra, A. A. 1992. *Technology of wood bonding principles in practice*, Van Nostrand Reinhold, New York.
- Martins, V. A. and W. B. Banks. 1991. Sorptive properties of chemically modified wood. *Wood Protection* 1(2):69-75.
- Marutzky, R. 1989. Release of formaldehyde by wood products. In *Wood adhesives chemistry and technology vol. 2*, ed. A. Pizzi, 307-388. Marcel Dekker, Inc. New York.

Matsuda, H., M. Ueda. 1985a. Preparation and utilization of esterified woods bearing carboxyl groups III. Heat and moisture stability of esterified woods. *Mokuzai Gakkaishi* 31:103-108.

Matsuda, H., and M. Ueda, 1985b. Preparation and utilization of esterified woods bearing carboxyl groups IV. Plasticization of esterified woods. *Mokuzai Gakkaishi* 31(3):215-221.

Matsuda, H., M. Ueda, 1985c. Preparation and utilization of esterified woods bearing carboxylic groups V. Addition reaction of esterified woods with epoxide and oligoesterification of the adducts obtained. *Mokuzai Gakkaishi* 31:267-273.

Matsuda, H., M. Ueda, 1985d. Preparation and utilization of esterified woods bearing carboxyl groups VI. Stepwise alternately adding esterification reaction of esterified woods with epoxides and dicarboxylic acid anhydrides. *Mokuzai Gakkaishi* 31: 468-474.

Matsuda, H., M. Ueda, 1985e. Preparation and utilization of esterified woods bearing carboxyl groups VII. Plasticity of epoxide-adducted esterified woods and oligoesterified wood derived from esterified woods. *Mokuzai Gakkaishi* 31:579-586.

Matsuda, H., M. Ueda, M. Hara. 1984a. Preparation and utilization of esterified woods bearing carboxyl groups I. Esterification of wood with dicarboxylic acid anhydrides in the presence of a solvent. *Mokuzai Gakkaishi* 30:735-741.

Matsuda, H., M. Ueda, and H. Mori. 1988a. Preparation and crosslinking of oligoesterified woods based on phthalic anhydride and glycidyl methacrylate. *Wood Science and Technology* 22(4):335-344.

Matsuda, H., M. Ueda, and H. Mori. 1988b. Preparation and crosslinking of oligoesterified woods based on maleic anhydride and allyl glycidyl ether. *Wood Science and Technology* 22:21-32.

Matsuda, H., M. Ueda, K. Murakami. 1984b. Preparation and utilization of esterified woods bearing carboxylic acid groups II. Esterification of wood with dicarboxylic acid anhydrides in the absence of solvent. *Mokuzai Gakkaishi* 30: 1003-1010.

Matsuda, H., M. Ueda, and K. Murakami. 1988c. Oligoesterified woods based on anhydride and epoxide I. Preparation and dimensional stability of oligoesterified woods by stepwise addition reactions. *Mokuzai Gakkaishi* 34(2):140.

- Matsuda, H., M. Ueda, and K. Murakami. 1988d. Oligoesterified wood based on anhydride and epoxide II. Preparation and dimensional stability of oligoesterified wood by heating wood immersed in anhydride-epoxide solution. *Mokuzai Gakkaishi* 34(7):587-603.
- McMillin, C. W. 1963. Dimensional stabilization with polymerizable vapor of ethylene oxide. *Forest Products Journal* 13(2):56-61.
- Meyer, B. 1979. Urea-formaldehyde resins, Addison-Wesley Publishing Company, Inc. Massachusetts, 166.
- Militz, H. 1993. Treatment of timber with water soluble dimethylol resins to improve thier dimensional stability and durability. *Wood Science and Technology* 27:347-355.
- Minato, K., N. Kubo, M. Norimoto, H. Sasaki, M. Sawada and T. Yamamoto. 1992. Dimensional stabilization of medium-density fiberboard by formaldehyde treatment. *Mokuzai Gakkaishi* 38(1):67-72.
- Minato, K. and H. Yano. 1990. Improvement of dimensional stability and acoustic properties of wood for musical instruments by sulfur dioxide catalyzed formalization. *Mokuzai Gakkaishi* 36:362.
- Minato, K. and R. Yasuda. 1992. Improvement of acoustic and hygroscopic properties of wood by some non-formaldehyde cross-linking agents. In *Chemical modification of lignocellulosics*, ed. D. V. Plackett and E. A. Dunningham, 97-106. FRL Bulletin No. 176. New Zealand Forest Research Institute, Rotorua, New Zealand.
- Morita, M. and I. Sakata. 1986. Chemical conversion of wood to thermoplastic material. *Journal of Applied Polymer Science* 31:831-840.
- Murakami, K., H. Matsuda. 1990a. Oligoesterified woods based on anhydride and epoxide VIII. Resistances of oligoesterified woods against weathering and biodeterioration. *Mokuzai Gakkaishi* 36:538-544.
- Murakami, K., H. Matsuda. 1990b. Oligoesterified woods based on anhydride and epoxide VII. Dynamic mechanical properties of oligoesterified woods. *Mokuzai Gakkaishi* 36(1):49-56.
- Murakami, K., H. Matsuda, and M. Ueda. 1989. Oligoesterified woods based on anhydride and epoxide V. Properties of oligoesterified woods obtained by heating-

suction of wood impregnated with reactant solution. *Mokuzai Gakkaishi* 35(4):328-335.

Narayanamurthi, D. and B. K. Handa. 1953. Acetylated Woods. *Das Papier* 7:87-92.

Nicholas, D. D. and A. D. Williams. 1987. Dimensional stabilization of wood with dimethylol compounds. International Research Group on wood Preservation Doc. No. IRG/WP/3412.

Norimoto, M., J. Gril, K. Minato, K. Okamura, J. Mukudai, and R. M. Rowell. 1987. Suppression of creep of wood under humidity changes through chemical modification. *Moku Kogyo* 42:504-508.

Ohkoshi, M. 1990. Bonding of wood by thermoplasticizing the surfaces I. Effect of allylation and hot press conditions. *Mokuzai Gakkaishi* 36(1):57-63.

Ozo-insh, A. P. and A. D. Yukna. 1967. Effect of ammonia on certain properties of birch wood. In *Modifikatsiya drevesing*, ed. T. A. Darzinsh, 113-120. Academy of Sciences of the Latvian SSR Institute of the Chemistry of Wood. Izdatelstvo "Zinatne", Riga, Russian.

Philipp, B., W. Knecht, I. Nehls and M. Schnabelrauch. 1989. New routes to anionic cellulose esters by homogeneous acylation in non aqueous system. In *Cellulose: structure and fundamental aspects*, ed. J. F. Kennedy, G. O. Philipps and P. A. Williams, 173-179. Ellis Horwood, Chichester, UK.

Pizzi, A. 1983. *Wood adhesives: chemistry and technology*. Marcel Dekker, Inc. New York.

Pizzi, A. and A. Stephanou. 1993. On the chemistry, behavior, and cure acceleration of phenol-formaldehyde resins under very alkaline conditions. *Journal of Applied Polymer Science* 49:2157-2170.

Pizzi, A. and A. Stephanou. 1994a. Phenol-formaldehyde wood adhesives under very alkaline conditions Part I: Behaviour and proposed mechanism. *Holzforchung* 48:35-40.

Pizzi, A. and A. Stephanou. 1994b. Phenol-formaldehyde wood adhesives under very alkaline conditions Part II: Esters curing acceleration, its mechanism and applied results. *Holzforchung* 48:150-156.

- Plackett, D. V., E. A. Dunningham, and A. P. Singh. 1992. Weathering of chemically modified wood: Accelerated weathering of acetylated radiata pine. *Holz Roh-Werkst* 50(4):135-140.
- Ren, S. 1992. Thermo-hygro rheological behavior of materials used in the manufacture of wood-based composites. Ph.D. thesis, Department of Forest Products, Oregon State University, Corvallis, Oregon.
- Ren, S. and P. E. Humphrey. 1999. Technique to measure the hygro-thermo-viscoelastic properties of natural fiber networks. In preparation.
- Risi, J., D. F. Arseneau. 1957. Dimensional stabilization of wood part IV. Allylation. *Forest Products Journal* 7:293-95.
- Rowell, R. M. 1975. Chemical modification of wood: advantages and disadvantages. *Proc. Amer. Wood Preservation Association* 71:41-51.
- Rowell, R. M. 1980. Distribution of reacted chemicals in southern pine modified with methyl isocyanate. *Wood Science* 13(2):102-110.
- Rowell, R. M. 1983. Chemical modification of wood. *Forest Products Abstract*, 6:363-382.
- Rowell, R. M., W. D. Ellis. 1979. Chemical modification of wood: reaction of methyl isocyanate with southern pine. *Wood Science* 12(1):52-58.
- Rowell, R. M., G. R. Esenther, D.D. Nicholas and T. Nilsson. 1987. Biological resistance of southern pine and aspen flakeboard made from acetylated flakes. *Journal of Wood Chemistry and Technology* 7(3):427-440.
- Rowell, R. M., D. I. Gutzmer, 1975. Chemical modification of wood: reactions of alkylene oxide with southern yellow pine. *Wood Science* 7(3):240-246.
- Rowell, R. M., D. I. Gutzmer, I. B. Sachs, R. E. Kinney. 1976. Effects of alkylene oxide treatments on dimensional stability of wood. *Wood Science* 9(1):51-54.
- Rowell, R. M. and F. M. Keany. 1991. Fiberboards made from acetylated bagasse fiber. *Wood and Fiber Science* 23(1):15-22.
- Rowell, R. M., R. Moisuk, J. A. Meyer. 1982. Wood-polymer composites: cell wall grafting with alkylene oxides and lumen treatments with methyl methacrylate. *Wood Science* 15(2):90-96.

- Rowell, R. M., A. Tillman, R. Simonsen. 1986(a). A simplified procedure for the acetylation of hardwood and softwood flakes for flakeboard production. *Journal of Wood Chemistry and Technology* 6(3):427-448.
- Rowell, R. M., A. M. Tillman and L. Zhengtian. 1986(b). Dimensional stabilization of flakeboard by chemical modification. *Wood Science and Technology* 20:83-95.
- Rudkin, A. W. 1950. The role of hydroxyl group in the gluing of wood. *Australian Journal of Applied Science* 1:270-283.
- Schuerch, C. 1952. The solvent properties of liquids and their relation to the solubility, swelling, isolation and fractionation of lignin. *Journal of the American Chemical Society* 54:5061.
- Schuerch, C. 1963. Plasticizing wood with liquid ammonia. *Industrial and Engineering Chemistry* 55:39.
- Schuerch, C. 1964. Principles and potential .... wood plasticization. *Forest Products Journal* 14(9):377-381.
- Schuerch, C. and R. W. Davidson. 1971. Plasticizing wood with ammonia – control of color change. *Journal of Polymer Science Part C* 36:231-239.
- Shaines, A. 1970. Process for paper overlay. US Patent no. 3, 514, 353. May 26.
- Sheen, A. D. 1992. The preparation of acetylated wood fibre on a commercial scale. In *Chemical modification of lignocellulosics*, ed. D. V. Plackett. & E. A. Dunningham, 1-8. FRI Bulletin 176, New Zealand Forest Research Institute, Rotorua, New Zealand.
- Shen, K. C. 1973. Steam-press process for curing phenolic-bonded particleboard. *Forest Products Journal* 23(3):21-29.
- Shen, K.C. 1975. Method and apparatus for pressing particleboard. US Patent No. 3,891,738. June 24.
- Singh, S. P., I. Dev and S. Kumar. 1981. Chemical modification of wood II. Vapor phase acetylation with acetylchloride. *International Journal of Wood Preservation* 1(4):169-171.
- Singh, S. P., I. Dev and Satish Kumar. 1979. Chemical modification of wood: vapor phase acetylation with thioacetic acid. *Wood Science* 11(4):268-270.



- Sjostrom, E. 1981. Wood chemistry, fundamentals and applications. Academic Press, New York. 169.
- Skeist, I. 1990. Handbook of Adhesives. 3<sup>rd</sup> ed. Van Nostrand Reinhold, New York. 603.
- Stamm, A.J. 1955. Swelling of wood and fiberboards in liquid ammonia. Forest Products Journal 5(6):413-416.
- Stamm, A.J. 1959. Dimensional stabilization of wood by thermal reactions and formaldehyde cross-linking. Tappi 42(1):39-44.
- Stamm, A. J. and R. H. Baechler. 1960. Decay resistance and dimensional stability of five modified woods. Forest Products Journal 10(1):22-26.
- Stamm, A. J. and H. Tarkow. 1947. Acetylation of wood and boards. U.S. Patent No. 2,417,995.
- Tarkow, H. and A. J. Stamm. 1953. Effect of formaldehyde treatment upon the dimensional of wood. Journal of the Forest Products Research Society 3(2):33-37.
- Tarkow, H.; A. J. Stamm, E. C. O. Erickson. 1950. Acetylated wood. USDA Forest Service, Forest Products Lab Report No.1593, 29 pp.
- Thoemen, H. and P. E. Humphrey. 1999. The continuous pressing process for wood-based panels: an analytical simulation model. Paper prepared for 3<sup>rd</sup> European Panel Products Symposium, October 6-8, Llandudno, UK.
- Thoman, B. J. and R. G. Pearson. 1976. Properties of steam-pressed particleboard. Forest Products Journal 26(11):46-50.
- Timell, T. E. 1964. Wood hemicelluloses, Part I. Advance Carbohydrate Chemistry 19:247-302.
- Timell, T.E. 1965. Wood hemicelluloses, Part II. Advance Carbohydrate Chemistry 20:409-483.
- Wakeling, A. N., D. V. Plackett, and D. R. Cronshaw. 1992. The susceptibility of acetylated *Pinus radiata* to mould and stain fungi. International Research Group on Wood Preservation, Doc. No. IRG/WP 1548.
- West, H. 1988. Kinetics and mechanism of wood-isocyanate reactions. Ph.D. thesis, University of Wales, Bangor, UK.

West, H., and W. B. Banks. 1986. Topochemistry of the wood-isocyanate reaction: an analysis of reaction profiles. *Journal of Wood Chemistry and Technology* 6(3):411-425.

Yamawaki, T., M. Morita and I. Sakata. 1991. Production of thermally auto-adhered medium density fiberboard from cyanoethylated wood fibers. *Mokuzai Gakkaishi* 37:449.

Yan, M. M. and C. B. Purves. 1956. Extraction of a lignin fraction from maple wood by liquid ammonia. *Canadian Journal of Chemistry* 34:1747.

Yano, H., J. Makudai, and N. Norimoto. 1988. Improvements in the piano pin-blocks. *Mokuzai Gakkaishi* 34(2):94-99.

Youngquist, J. A., R. M. Rowell, and A. Krzysik. 1986. Mechanical properties and dimensional stability of acetylated aspen flakeboard. *Holz als Roh-und Werkstoff* 44(12):453-457.

Zavala, D. and P. E. Humphrey. 1996. Hot pressing of veneer-based products: The interaction of physical processes. *Forest Products Journal* 46(1):69-77.

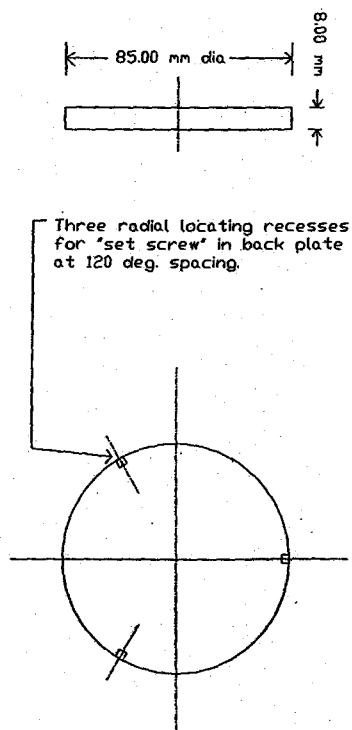
Zhao, G. J., M. Norimoto, F. Tanaka, T. Yamada, and R. M. Rowell. 1989. Structure and properties of acetylated wood: I. Changes in the degree of crystallinity and dielectric properties by acetylation. *Mokuzai Gakkaishi* 33(2):136-142.

APPENDICES

## APPENDIX A

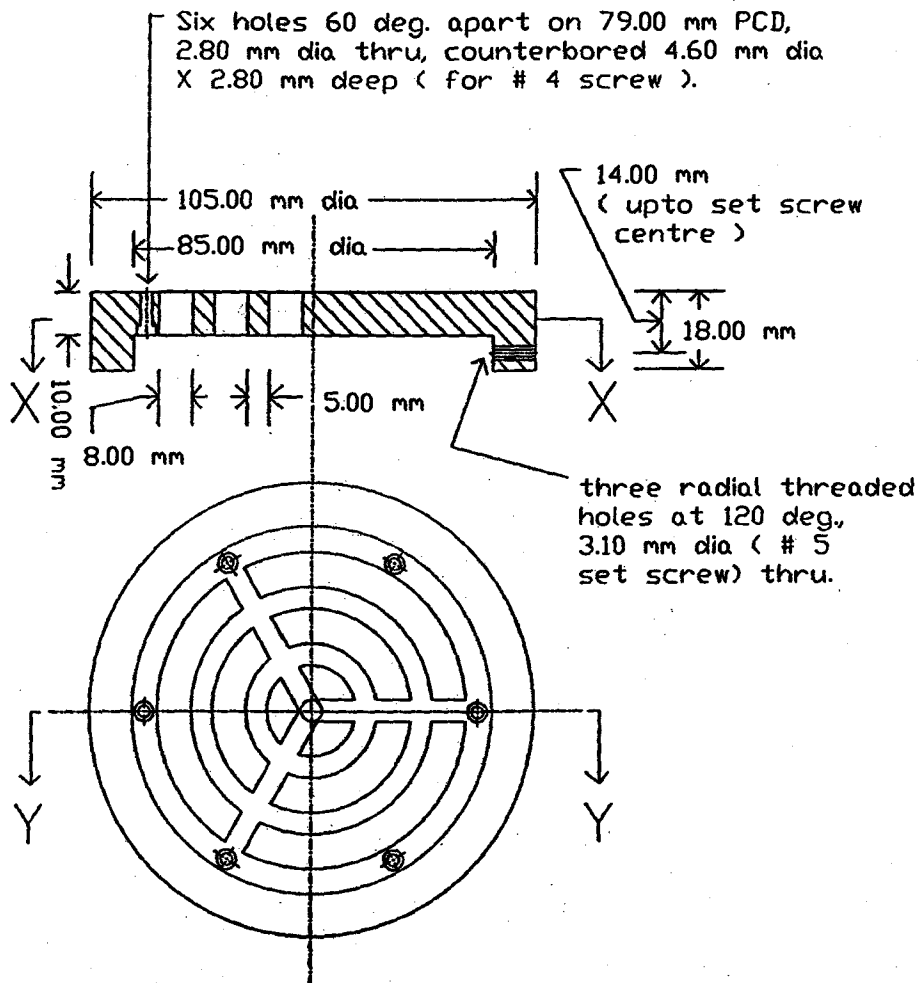
Engineering drawing of each part of the upper/lower portion of the sealed pressing device

The upper and lower portions of the sealed pressing device are identical. Each portion consists of six different parts: porous plate, back plate, gas supply block, heating block, thermal barrier and connecting column. Besides these, the collar that provides peripheral sealing of the pressing system and the safety stop are also important parts of the pressing system. Engineering drawings of all these parts are provided below.



Material: Porous graphite.

Figure A1 Porous plate.



Material: Stainless steel.

Figure A2 Back plate.

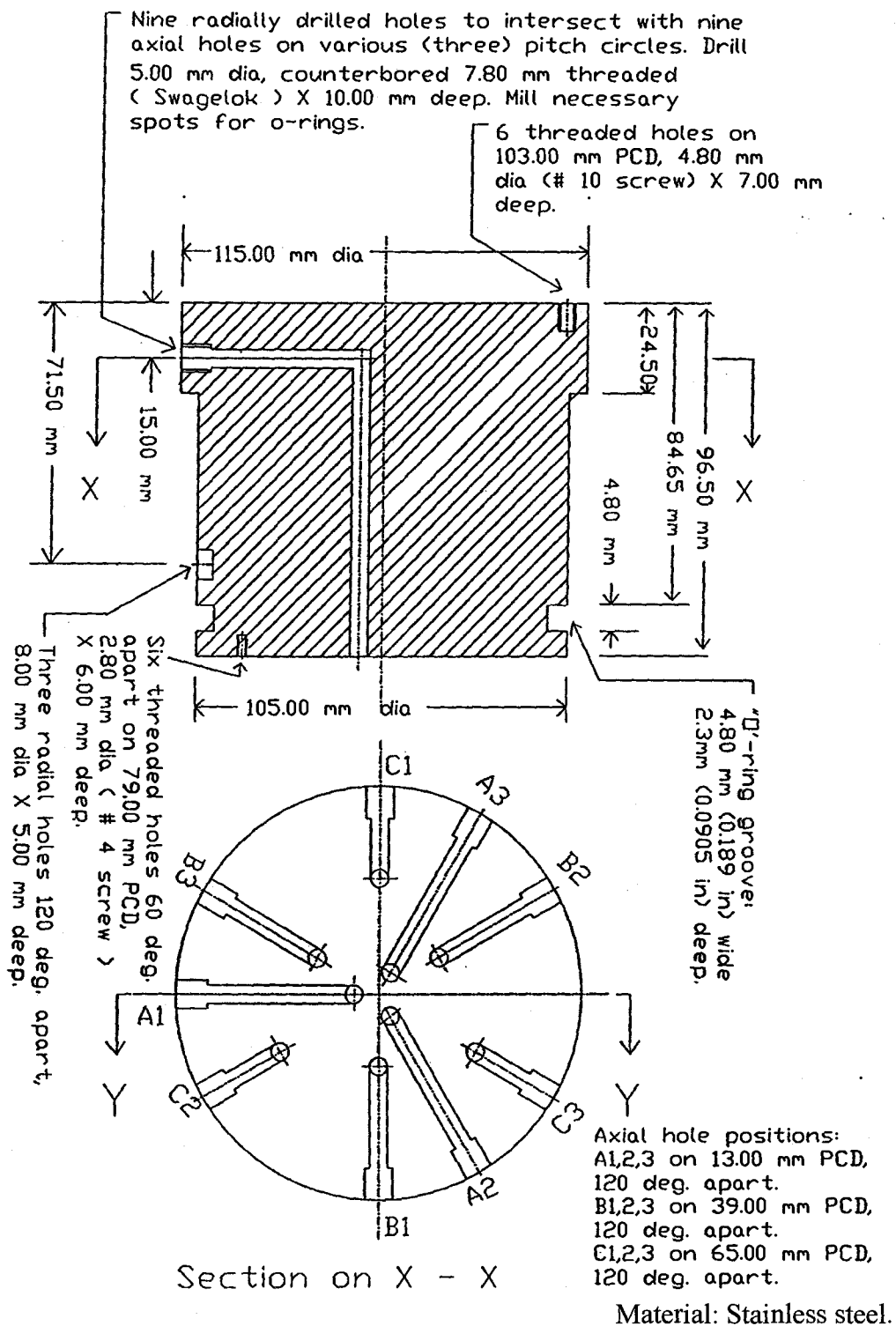
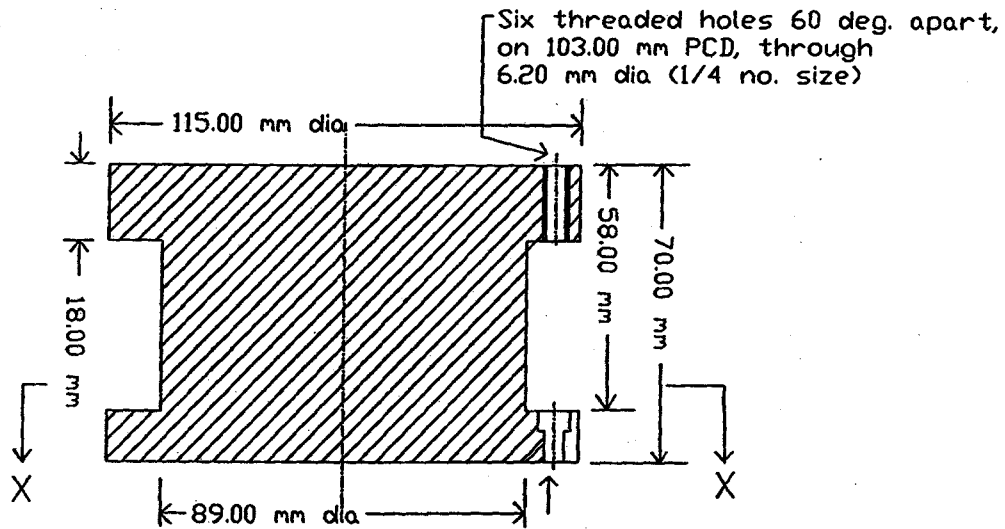
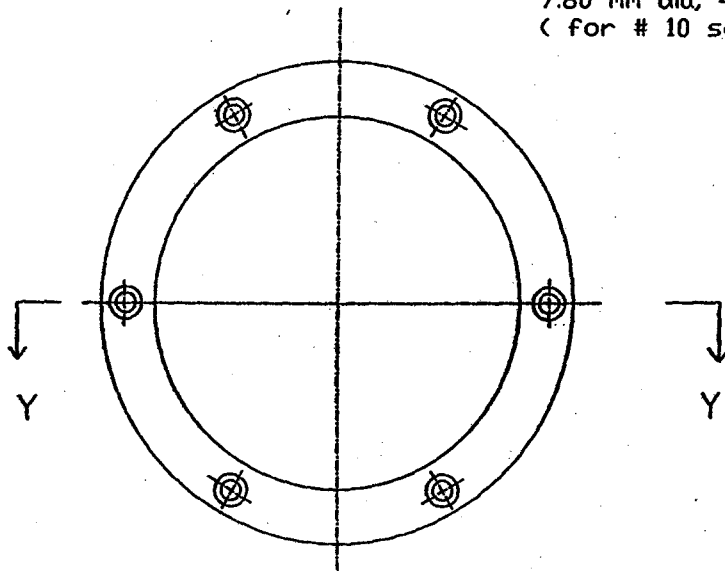


Figure A3 Gas supply block.



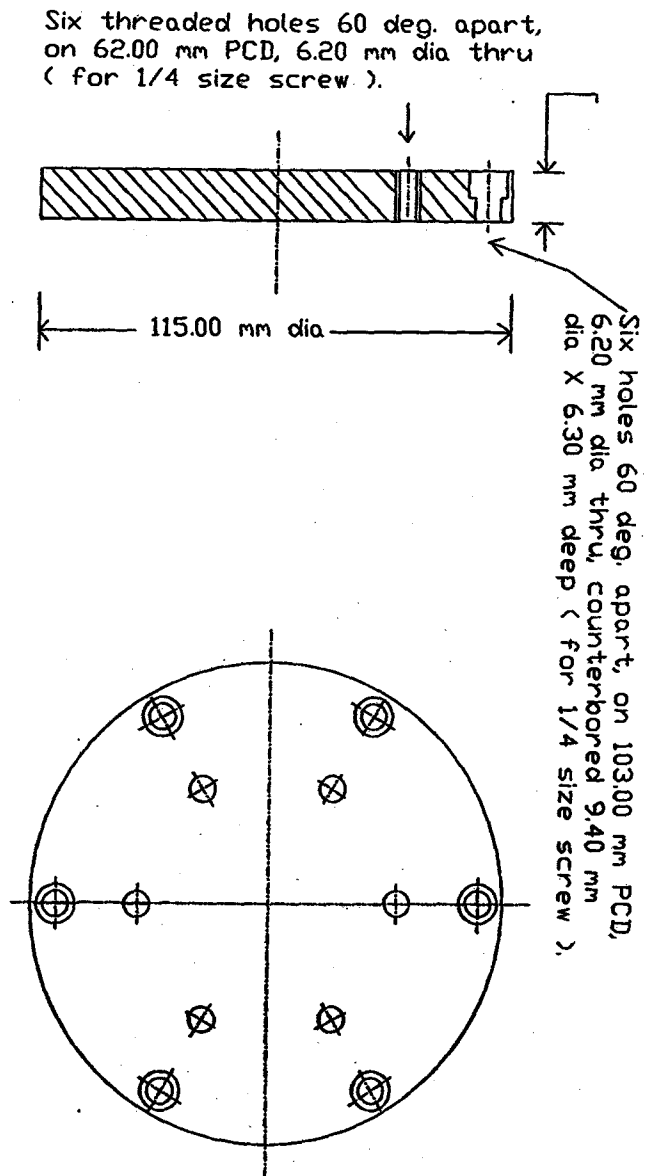
Six holes 60 deg. apart on 103.00 mm PCD, 4.80 mm dia through, counterbored 7.80 mm dia, 4.80 mm deep ( for # 10 screw ).



Section on X - X

Material: 60-61 Aluminum alloy.

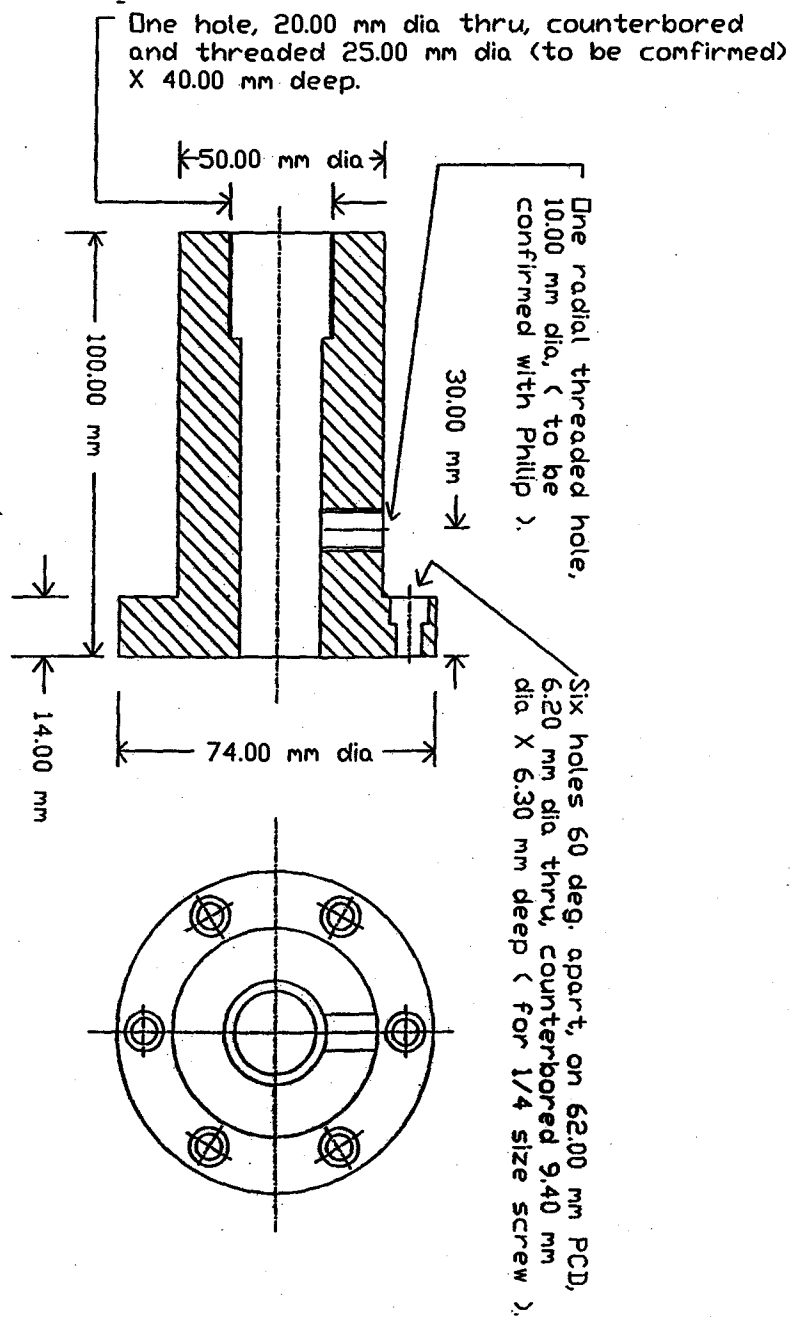
Figure A4 Heating block.



Material: Glass-epoxy composite.

Figure A5 Thermal barrier.





Material: Stainless steel.

Figure A6 Connecting column.

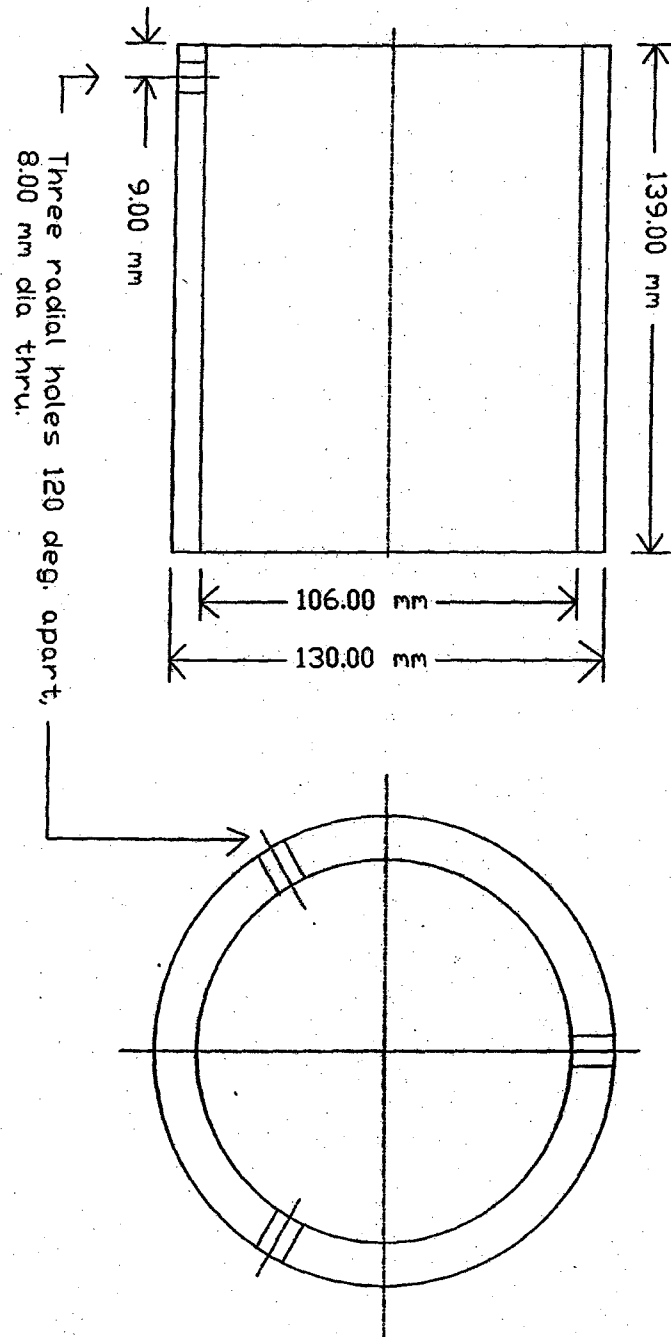
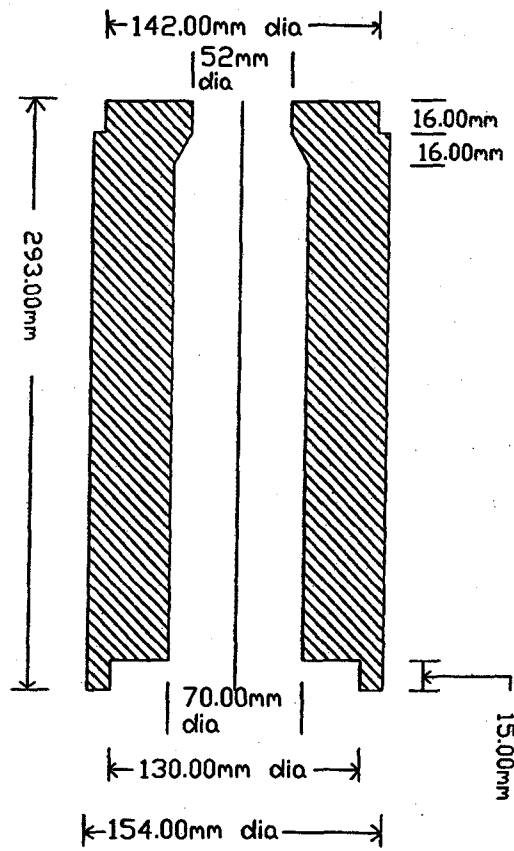
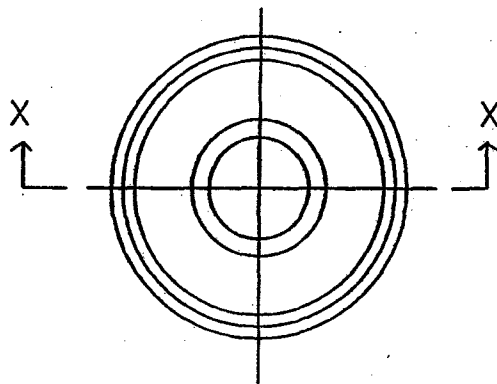


Figure A7 Collar.



Section on X-X



Plan View

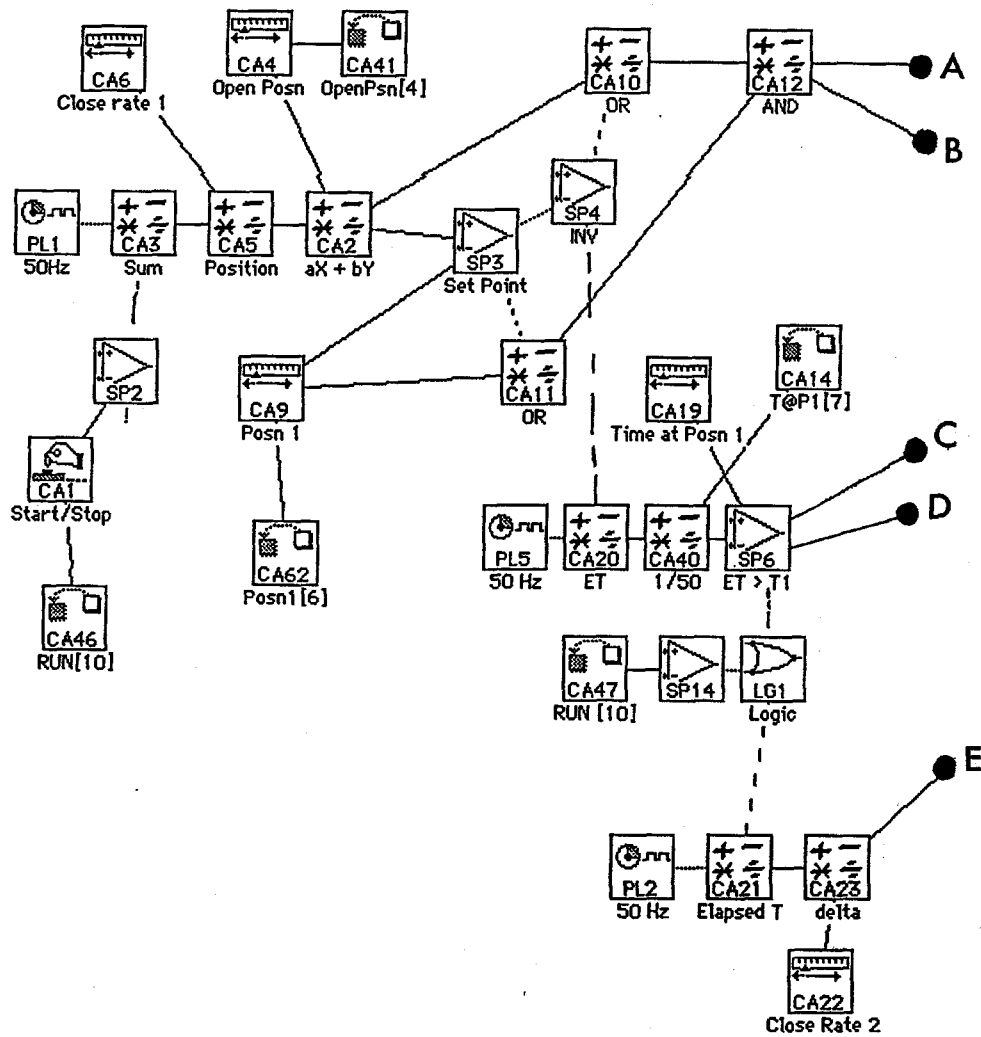
Material: Stainless steel.

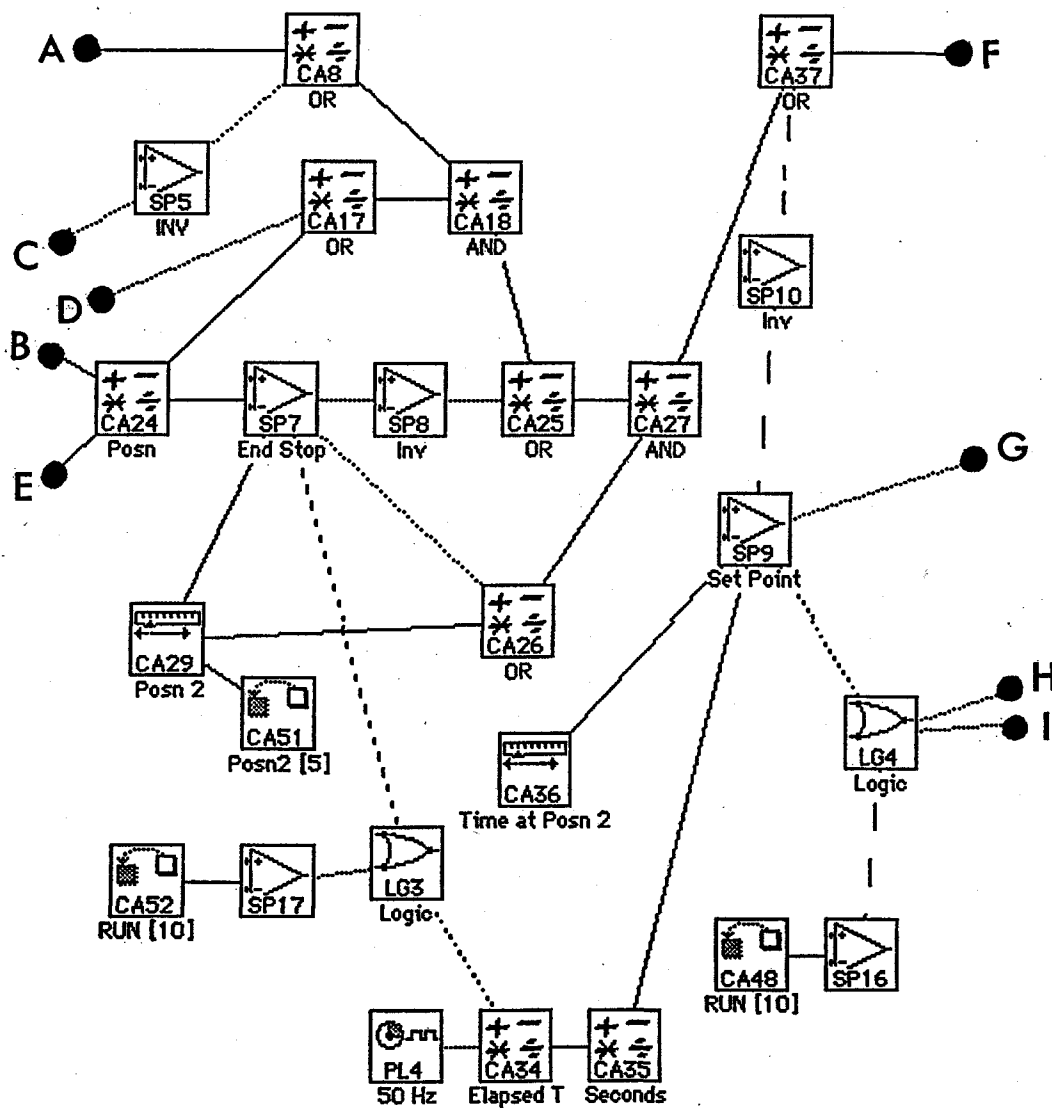
Figure A8 Safety stop.

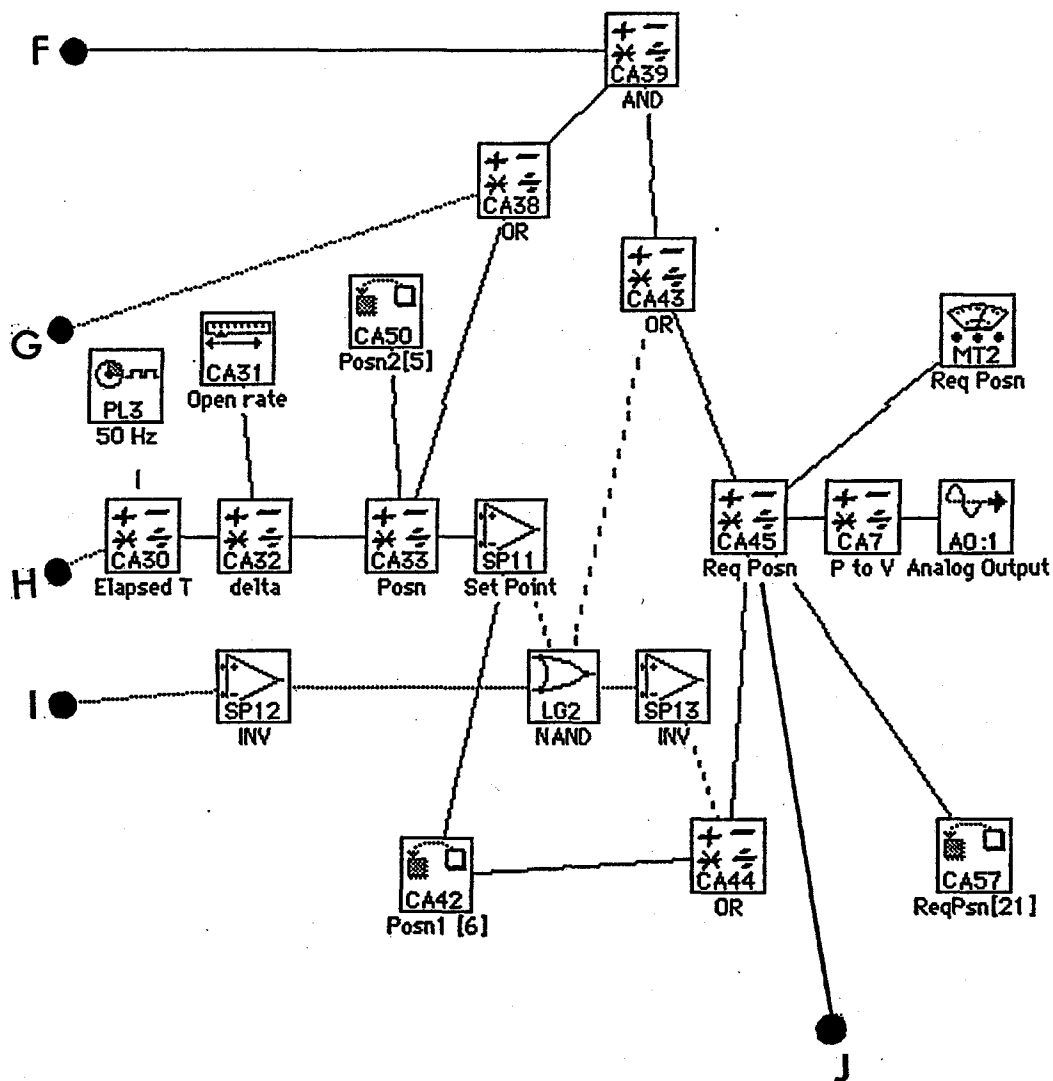
APPENDIX B

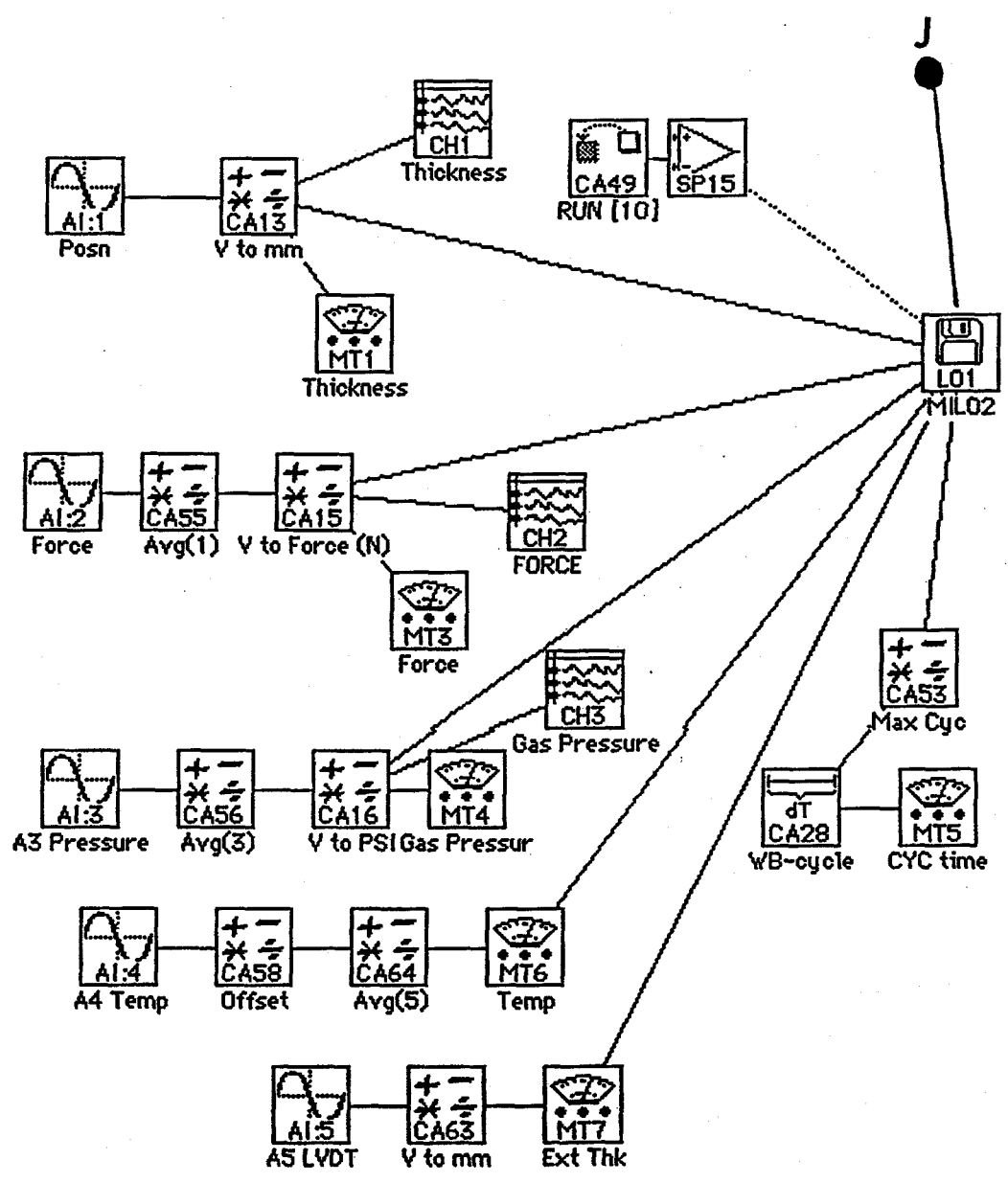
Strawberry Tree® Program

A Strawberry Tree® Program was used to sequentially control head position of the pressing system is provided below. Peripheral letters indicate links to subsequent pages.









## APPENDIX C

## Fluid pressure at the center of trial samples during pressing

Gas pressures at the core layer of samples (mats) during pressing were measured (where ammonia treatment was followed by methyl formate injection). This was done by inserting a small diameter stainless steel tube at the geometric center of the mat prior to its consolidation and connecting this tube to a pressure transducer. This probe was used to explore the magnitude of fluid pressure gradient within the sample (at a density of  $750 \text{ Kg/m}^3$ ) when external conditions were altered. An example is shown in Figure C1.

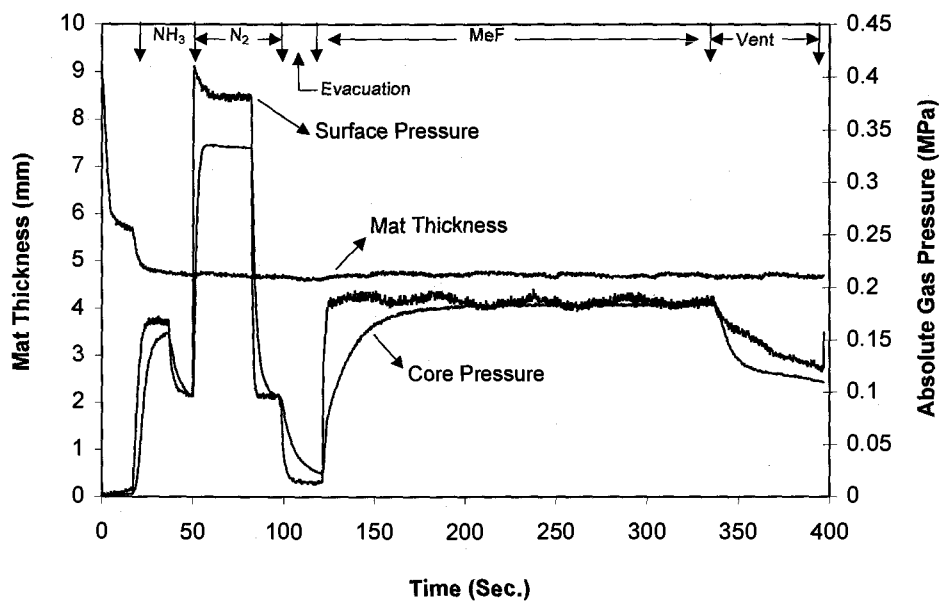


Figure C1 Fluid pressures at the center of trial sample during pressing.



In this experiment, the sample was pre-pressed to 9.00 mm thickness and the treatment chamber was evacuated. The press was then closed to affect a mat thickness of 5.00 mm. After press closure,  $\text{NH}_3$  gas (0.17 MPa) was passed into the chamber for 20-22 seconds and was subsequently vented from the system. The mat was then washed with  $\text{N}_2$  gas (0.38-0.4 MPa) for 32-35 seconds. After venting the  $\text{N}_2$  gas, the system was re-evacuated and the MeF vapor (0.18 MPa) was passed. MeF was held there for the remainder of the pressing period. At the end of the cycle, the residual MeF was purged from the press. During the pressing cycle, time (s), mat thickness (mm), and gas pressures at the surface and at the center of the mat were recorded digitally.

The figure C1 shows that rapid changes in external gas pressure did rapidly change the gas pressure at the core of the sample. However, the gas pressure at the core required a little time to closely track with external gas pressure when external conditions were altered. The results indicate that the penetration of gaseous ammonia and methyl formate vapor into compressed fiber networks is very fast which is an important factor in terms of processing efficiency.